

**ASSESSMENT OF GROUND WATER QUALITY AT ACTIVE WASTE
DUMP SITES IN HAZARIBAGH USING NON-DESTRUCTIVE TEST**

B. S. PUSHPENDUE BISWAS

MASTER OF SCIENCE IN CIVIL ENGINEERING (ENVIRONMENTAL)



**DEPARTMENT OF CIVIL ENGINEERING
BANGLADESH UNIVERSITY OF ENGINEERING AND TECHNOLOGY**

SEPTEMBER, 2019

Assessment of Ground Water Quality at Active Waste Dump Sites in Hazaribagh Using Non-Destructive Test

by

B. S. Pushpendue Biswas
Student No. 1014042104

In partial fulfilment of the requirements for the Degree of
MASTER OF SCIENCE IN CIVIL ENGINEERING (ENVIRONMENTAL)

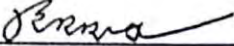


Department of Civil Engineering
BANGLADESH UNIVERSITY OF ENGINEERING AND TECHNOLOGY

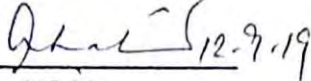
September, 2019

This thesis titled "Assessment of Ground Water Quality at Active Waste Dump Sites in Hazaribagh Using Non-Destructive Test", submitted by B.S. Pushpendue Biswas, Roll No. 1014042104, Session: October 2014, has been accepted as satisfactory for the partial fulfillment of the requirement for the degree of **Master of Science in Civil Engineering (Environmental)** on 12th September, 2019.


BOARD OF EXAMINERS


Dr. Muhammad Ashraf Ali
Professor
Department of Civil Engineering,
BUET, Dhaka-1000

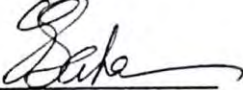
Chairman
(Supervisor)


Dr. Ahsanul Kabir
Professor and Head
Department of Civil Engineering,
BUET, Dhaka-1000

Member
(Ex-officio)


Dr. Tanvir Ahmed
Professor
Department of Civil Engineering,
BUET, Dhaka-1000

Member


Dr. Ganesh Chandra Saha
Professor
Department of Civil Engineering,
DUET, Gazipur-1700

Member
(External)

DECLARATION

It is hereby declared that this thesis or any part of it has not been submitted elsewhere for the award of any degree or diploma.

B.S. PUSHPENDUE BISWAS

B.S. Pushpendue Biswas
Student ID: 1014042104

Dedicated to

My Teachers

ACKNOWLEDGEMENT

I wish to express my profound gratitude and sincere appreciation to my supervisor Dr. Muhammad Ashraf Ali, Professor, Department of Civil Engineering, BUET for his constant support, guidance, encouragement, suggestions during designing and carrying out this study.

I wish to express my gratitude and sincere appreciation to my respected Board of Examiners for their valuable advice and comments.

I am indebted to Dr. Mehedi Ahmed Ansary, Professor, Department of Civil Engineering, BUET for his valuable support during the course of this study. I would like to thank to the members of the Environmental Engineering Laboratory for their support and cordial cooperation during this research work. Special thanks to Dr. Md. Ehosan Habib for his sincere support during carrying out laboratory works.

ABSTRACT

Dhaka city has been experiencing rapid growth of urban population over the past 50 years and it is expected to continue in the near future. Solid waste management in the city is poor and there are many formal and informal waste dump sites in the city. Groundwater contamination from leachates underneath these dump sites is a major concern. The primary objective of this study was to assess the probable groundwater contamination using Electrical Resistivity Tomography (ERT), which is a non-destructive test. Three different locations at waste dump sites in Hazaribagh, Dhaka were selected as the study area.

Three ERT tests were carried out in Hazaribagh, where 32 electrodes were used in each test employing the “Wenner– Schlumberger array”; measurements were carried out with electrodes positioned on the surface. The ERT test data were processed through a 2-D inverse method, using the program RES2DINV. The data were processed by creating a pseudo-section of the apparent resistivity values using RES2DINV software. Computer iterations were then carried out and two dimensional (2-D) resistivity contour maps were created. The resistivity model was used to identify possible groundwater pollution through comparison with reference resistivity values of materials. Subsurface soil profiles have been assessed by both ERT and Microtremor measurement. Microtremor data were processed by using GeSIG Soft software. The resistivity model of a test site was also compared with electrical conductivity (EC) of ground water samples collected from the site, in order to assess the validity of the ERT method for identification of ground water contamination.

From the analyzed resistivity models, it has been found that the subsurface below the dumpsites is characterized by low resistivity, possibly due to leaching of salts and contaminants from the dumps. For example, the maximum depth penetrated by the current during the acquisition of data at one test site (ERT-1) was 14m, and for this test site the resistivity values of subsurface layers were found to be mostly below 5 Ω m, except few cases of high resistivity in the top layer and isolated high resistivity at depth. The resistivity of water contaminated with high concentration of dissolved solids is usually less 10 Ω m. The resistivity-depth model at ERT-1 site suggests infiltration of leachate containing high concentration of dissolved solids to the subsurface environment. The contamination scenarios of two other test sites (ERT-2 and ERT-3) have been found to be similar to ERT-1. These results suggest that the groundwater in and around the dump sites at Hazaribagh has become contaminated up to a depth of about 15 m with leachate containing high concentration of dissolved salts. The soil profiles developed by the resistivity model and Microtremor analysis have been found to be similar, suggesting applicability of the ERT method. Good agreement of resistivity model and the measured EC values of ground water at a dump site also supports the applicability of the non-destructive ERT method for identification of ground water contamination. Results from this study suggest that the non-destructive Electrical Resistivity Tomography (ERT) could be a useful tool for quick and easy identification of shallow groundwater contamination at waste dump sites.

TABLE OF CONTENTS

ACKNOWLEDGEMENT	vi
ABSTRACT	vii
TABLE OF CONTENTS	viii
LIST OF FIGURES	x
LIST OF TABLES	xii
LIST OF ABBREVIATION	xiii
Chapter 1 INTRODUCTION	
1.1 Background	1
1.2 Objectives of the Research	2
1.3 Outline of Methodology	2
1.4 Organization of the Thesis	3
Chapter 2 LITERATURE REVIEW	
2.1 Background	4
2.2 The Electrical Resistivity Tomography: Overview	5
2.2.1 Electrical Properties of Sediments and Sedimentary Rocks	7
2.2.2 Electrical Properties of Metamorphic and Igneous Rocks	7
2.2.3 Electrical Properties of Mineral Ores	7
2.2.4 Types of Surveys	8
2.2.5 Electrode Arrays of ERT	9
2.2.6 Types of Surveys and Models	14
2.2.7 The Software RES2DINV	15
2.2.8 Inversion	16
2.3 Application of ERT in Environmental Engineering	19
2.4 Characterization of Soil Profile Using Microtremor	23
Chapter 3 METHODOLOGY	
3.1 Introduction	25
3.2 Study Area	25
3.3 Data Collection Using Electrical Resistivity Tomography imaging (ERT)	26
3.4 Data Collection Using Microtremor	28
3.5 Installation of Boreholes and Collection of Water Samples	30
3.6 Data processing and analysis	31
3.6.1 The Electrical Resistivity Tomography (ERT) Data	31
3.6.2 Microtremor Data Processing and Analysis:	32
3.6.3 Analysis of Borehole Water Samples	32
Chapter 4 RESULTS AND DISCUSSION	
4.1 Introduction	34
4.2 Data and Model Set Up of ERT	34
4.2.1 Reference Resistivity	34
4.2.2 Data File Operations and Data Format	34
4.2.3 Editing the Data	35
	viii

4.2.4	Changing the Program Settings	37
4.2.5	Inversion options	43
4.2.6	Displaying Inversion Results	49
4.3	Analysis of ERT Data	50
4.4	Comparison of Soil Profile from ERT Analysis with Microtremor Analysis	60
4.5	Comparison between ERT1 Model and EC of Ground Water Samples	65
Chapter 5 CONCLUSIONS		
5.1	Introduction	67
5.2	Conclusions	67
5.3	Recommendation for Future Work	67
REFERENCES		69

LIST OF FIGURES

Figure 2.1: Typical ERT electrode combination	6
Figure 2.2: Reference resistivity values table of various materials (Loke, 2004)	8
Figure 2.3: 2-D electrical imaging survey	9
Figure 2.4: Types of model	9
Figure 2.5: Types of electrode arrays	10
Figure 2.6: Wenner-Schlumberger array	12
Figure 2.7: Dipole-dipole array	12
Figure 2.8: Pole-dipole array	12
Figure 2.9: Multiple gradient array	13
Figure 2.10: Sequence of measurements to build up a pseudo-section using a computer controlle multi-electrode survey setup	14
Figure 2.11: Scheme of data acquisition and configuration of the type Wenner reconstruction of the reltive apparent resistivity pseudosections	14
Figure 2.12: Comparison between the arrangement of electrodes and related pseudosections for Wenner and Schlumberger (Loke, 2004)	15
Figure 2.13: Example of a typical 1-D inversion	16
Figure 2.14: Arrangement of model blocks and apparent resistivity datum points	17
Figure 2.15: Example of a typical inversion	17
Figure 2.16: The finite-difference and finite-element methods	19
Figure 3.1: Study Area in Hazaribagh, Dhaka (Source: Google Maps)	26
Figure 3.2: Open waste dumping sites as at the time of data collection	27
Figure 3.3: Microtremor testing equipment.	29
Figure 3.4: Percussion drilling of the borehole where the tests were carried out as at the time of ground water sample collection.	31
Figure 3.5: Laboratory test of water samples with Multiline P4 (WTW)	33
Figure 4.1: RES2DINV software interface for data file operation and data format.	35
Figure 4.2: RES2DINV software interface for editing data	35
Figure 4.3: Example of ERT1 data set with a few bad data points. The data is displayed using the "Exterminate bad data points" option.	36
Figure 4.4: RES2DINV software interface for change settings	37
Figure 4.5: RES2DINV software interface for limit range of resistivity values.	39
Figure 4.6: RES2DINV software interface for mesh parameters under change settings menu.	40
Figure 4.7: RES2DINV software interface of inversion progress settings under change settings menu.	41
Figure 4.8: RES2DINV software interface of data/display selection under change settings menu.	42
Figure 4.9: RES2DINV software interface of Inversion in the menu bar.	43

Figure 4.10: RES2DINV software interface of inversion methods and settings under the inversion menu	44
Figure 4.11: RES2DINV software interface of type of optimization method under the inversion methods and settings	46
Figure 4.12: RES2DINV software interface of model discretization under the inversion menu	47
Figure 4.13: RES2DINV software interface of model refinement	48
Figure 4.14: RES2DINV software interface of model sensitivity options.	49
Figure 4.15: Display section window interface of RES2DINV	50
Figure 4.16: Raw resistivity model of ERT1 generated by the program RES2DINV.	51
Figure 4.17: Analyzed results of ERT-1 test showing location of contaminated groundwater as well as pure groundwater zones.	54
Figure 4.18: Raw resistivity model of ERT2 generated by using the program RES2DINV.	55
Figure 4.19: Analyzed result of ERT2 test showing location of contaminated groundwater as well as pure groundwater zones	56
Figure 4.20: Raw resistivity model of ERT3 generated by the program RES2DINV.	58
Figure 4.21: Analyzed result of ERT3 test showing location of contaminated groundwater as well as pure groundwater zones	59
Figure 4.22: Raw resistivity model of ERT1 generated by the program RES2DINV	60
Figure 4.23: Analysis of microtremor data to investigate the subsurface of test point-01	61
Figure 4.24: Raw resistivity model of ERT2 generated by the program RES2DINV	62
Figure 4.25: Analysis of microtremor data to investigate the subsurface of test point-02	63
Figure 4.26: Raw resistivity model of ERT3 generated by the program RES2DINV	64
Figure 4.27: Analysis of microtremor data to investigate the subsurface of test point-03	64
Figure 4.28: Analyzed results of ERT-1 test showing location of contaminated groundwater as well as pure groundwater zones.	65

LIST OF TABLES

Table 3.1: Geographic coordinates of the study area.	26
Table 3.2: Reference resistivity values table of various materials (Loke, 2004)	31
Table 3.3: Reference resistivity values table of various materials (Roger et al., 2004)	32
Table 4.1: Soil profile of the Test Point-01 (ERT1) based on reference resistivity	61
Table 4.2: The soil profile types according to Shear Velocity (Vs)	61
Table 4.3: Soil profile of the Test Point-02 (ERT2) based on reference resistivity	62
Table 4.4: Soil profile of the Test Point-02 (ERT2) based on reference resistivity	63
Table 4.5: Electrical Conductivity (EC) Values of Analyzed Water Samples	65

LIST OF ABBREVIATIONS

ERT	Electrical Resistivity Tomography
EC	Electrical Conductivity
ET	Evapotranspiration
RI	Resistivity Imaging
HVSR	Horizontal-to-Vertical Spectral Ratio
MASW	Multichannel Analysis of Surface Wave
BWDB	Bangladesh Water Development Board

Chapter 1

INTRODUCTION

1.1 Background

Dhaka city has been experiencing a rapid growth of urban population over the past 50 years and it will likely to continue in the future due to several unavoidable reasons. Apart from Dhaka, many other cities are also witnessing a rapid population growth. Along with population, solid wastes are also being generated in increasing amounts in these urban centers. However, poor management of solid wastes, as well as other wastes, is becoming a major environmental and public health concern. In most cities and towns, crude dumping of solid waste is practiced by the city/town authorities. As a result, open waste dump sites have been growing and many such sites are active over decades. The environmental and health hazards associated with open dumping of waste are well known. Groundwater pollution from leachate in uncontrolled dump sites is a major concern in many major urban centers of Bangladesh.

In urban centers of Bangladesh, solid wastes from diverse sources, both domestic and industrial, are typically disposed in unlined low-lying areas, that could be characterized as crude dumping. This practice is posing a high risk to the underground water resources, environment, and public health. Most waste dumping sites, particularly the older sites, are unlined and lack artificial barriers to prevent movement of leachate. Solid wastes deposited in landfill/dumping sites undergo changes through chemical and biochemical reactions and produce leachates containing high concentrations of diverse contaminants. Production of leachate is particularly high during the rainy season, when rainwater percolates through the dumped solid wastes. In unlined landfills/dumping sites, the leachates could contaminate groundwater, particularly shallow groundwater. This is a major concern because groundwater is the primary source of potable water in most cities and towns of Bangladesh.

Being unregulated, the exact location, structure, and contents of many such landfills/dump-sites are either unknown or poorly documented. One of the most frequent demands in metropolitan areas is to determine the landfill's geological and geotechnical structure shape and extent, together with the excavation and dumping history (Allen et al., 1997; Mather, 1995; Georgaki et al., 2008). Details on the contents of a landfill may be difficult to acquire but are essential for evaluating the level of risk and hazards associated with leaking pollutants. In such context, the integrated use of geophysical methods provides an essential tool in the characterization and evaluation of contaminants generated by urban residues (domestic and/or industrial) (Green et al., 1999; Heitfeld and Heitfeld, 1997; Marinos et al., 1997; Lanz, 1994; Orlando and Marchesi, 2001; Saltas et al., 2005). Among those geophysical methods, Electrical Resistivity Tomography (ERT) has been found to be suitable for such characterization, due to the conductive nature of most contaminants. The use of electrical resistivity tomography applied to environmental studies is well documented

(Bernstone et al., 2000, Aristodemou and Thomas-Betts, 2000; Dawson et al., 2002; Bengtsson et al., 1994). Generally, geophysical methods provide economic and nondestructive means to investigate contaminant plumes from landfills (Cahyna, 1990; Carpenter et al., 1990; Ross, 1990). In particular, when the leachate which includes many anions causes an increase in dissolved salts in the ground, the consequent increase in its conductivity may be detected by electrical survey. Resistivity surveys are also used to map fracture zones in hard rock terrain (Barker et al., 1992, Carruthers and Smith, 1992) because high resistivity contrasts usually occur between solid rocks and saturated fractures. Seismic refraction method has been commonly used in groundwater and contaminated site investigation because of its relative simplicity and adaptability for shallow zone investigation. Due to the dependence of seismic velocity on the elasticity and density of the material through which the energy is passing, seismic tomography data is used to detect and map fracture and fault zones which could provide pathways for the contaminant plumes. This study focuses on the assessment of groundwater quality at an active solid waste dump site in Dhaka through a non-destructive geophysical method, Electrical Resistivity Tomography (ERT).

1.2 Objectives of the Research

The main objective of the present study was to assess the probable groundwater contamination at a waste dump site in Hazaribagh, Dhaka using Electrical Resistivity Tomography (ERT). The specific objectives were as follows-

- I. To detect the ground water sources in and around the dump site areas at Hazaribagh using Electrical Resistivity Tomography (ERT).
- II. To compare/cross-check soil profile from ERT analysis with Microtremor analyzed soil profile.
- III. To detect groundwater contamination (if any) by Resistivity Model using the software RES2DINV.
- IV. To assess validity of the ERT method by comparing the resistivity models with Electrical Conductivity of groundwater collected from the study site.

The research was aimed at assessing the suitability of using Electrical Resistivity Tomography (ERT) as a non-destructive testing tool for groundwater contamination at waste dump sites.

1.3 Outline of Methodology

The objective of this study was to assess groundwater quality at active waste dump sites in Hazaribagh, Dhaka using a non-destructive test – the Electrical Resistivity Tomography (ERT). The study involved ERT tests at three sites in Hazaribagh that are used for dumping of municipal and industrial solid wastes. The ERT tests were conducted using a Super Sting PASI 16-G-N multichannel system. Thirty-Two (32) electrodes, with a spacing of 3 m, were used in the ERT tests; the length of each profile was 62 m. This configuration is referred to as “Wenner-Schlumberger array”. The data collected from the survey has been analyzed with the software RES2DINV, which produces a two-dimensional (2-D) resistivity model for the

subsurface from the data obtained from electrical imaging surveys. Soil characteristics have been assessed by both ERT and Microtremor measurement. Microtremor data were processed by using GeoSIG Soft software. From the resistivity model, groundwater quality has been assessed. In addition, three monitoring wells (depth 5 to 15 m) were installed at the field sites in Hazaribagh for collection of water samples; these samples will be analyzed for Electrical Conductivity (EC). The conclusions drawn from the ERT analysis has been cross-checked against the EC values of groundwater samples collected from the field.

1.4 Organization of the Thesis

The thesis has been presented in five chapters. Chapter 1 presents the background of the study and objectives of the research. The other Chapters are organized as follows:

Chapter Two: This Chapter presents a literature review on geophysical methods for analysis of contaminant plume, with particular focus on Electrical Resistivity Tomography (ERT). The background theory of the Electrical Resistivity Tomography (ERT) has been discussed in this chapter.

Chapter Three: This chapter presents the methodology of the study. The study area selection and data collection procedures have been discussed in this chapter.

Chapter Four: This Chapter presents analysis of ERT data with the software RES2DINV, analysis of Microtremor data with GeoSiG Soft software, and laboratory test of collected water samples from the site. Locations of groundwater sources, contamination scenario of groundwater sources and scope of application of ERT at waste dump sites have been discussed in this chapter.

Chapter Five: This Chapter summarizes the major conclusions of the study and presents recommendations for future studies.

Chapter 2 LITERATURE REVIEW

2.1 Background

The purpose of electrical surveys is to determine the subsurface resistivity distribution by making measurements on the ground surface. From these measurements, the true resistivity of the subsurface can be estimated. The ground resistivity is related to various geological parameters such as the mineral and fluid content, porosity and degree of water saturation in the rock. Electrical resistivity surveys have been used for many decades in hydro-geological, mining and geotechnical investigations. More recently, it has been used for environmental surveys. Electrical resistivity is known to be highly variable among other physical properties of rock. In some cases, different in extreme values of a single rock type can differ by a factor approaching several orders of magnitude. Wide range of rock's resistivity parameter has always been the reason that makes it difficult to distinguish subsurface rock type if no information on the geological surroundings of field survey is available. Electrical current flows through the earth material under subsurface through two methods, which are electrolytic and electronic conduction.

Electric current flows in earth materials at shallow depths through two main methods. They are electronic conduction and electrolytic conduction. In electronic conduction, the current flow is via free electrons, such as in metals. In electrolytic conduction, the current flow is via the movement of ions in groundwater. In environmental and engineering surveys, electrolytic conduction is probably the more common mechanism. Electronic conduction is important when conductive minerals are present, such metal sulfides and graphite in mineral surveys. (Loke, 2004).

Electrical geophysical methods have proven to be fairly effective in delineating inorganic contaminants in the subsurface. The mechanism and responses are fairly well understood. Their application for mapping organic contaminants in the subsurface, in particular non-aqueous phase liquids is not as well accepted nor the mechanisms as well understood. Various surveys have reported results conducted over subsurface organic contamination; however, the actual anomaly associated with the organic contamination has been difficult to ascertain over other factors caused by variations in the porosity, degree of saturation, mineralogy, and structure (Pitchford, 1989).

Electronic conduction, which is conduction through the rock's mineral compositions, occurs mainly through metallic ore minerals, providing that these minerals exist in dense enough concentration. However, most conducting minerals rarely exist in sufficient quantity in a rock composition, especially granite, to have considerable effect on the electrical properties of host rock. This conduction is controlled by matrix properties (semi conduction, lattice defects, and

conductive accessories) which often resulted in very high resistivity values (Parkhomenko, 1967).

For 2D resistivity imaging, it is important to have a large set of data recorded along a survey line to effectively map the complex resistivity distribution of subsurface structure. The most practical way to acquire such large amount of data is by using automated multi-electrode data acquisition system. In the interpretation of ground resistivity survey, it is important to differentiate between apparent resistivity and true resistivity. Apparent resistivity can be defined as the volumetric average of a heterogeneous half-space, except that the averaging is not done arithmetically but by a complex weighing function dependent on electrode's configurations (Dahlin, 2001).

In practice, there are a lot of factors that can affect resistivity pseudo section imaging. Apparent resistivity is measured instead of true resistivity due to unknown near surface strata with different resistivity. This affects the conduction of current through earth material and thus affects the resistivity measurement. Most of field resistivity surveys conducted by geophysicist are not always validated by laboratory measurement. The difficulty in obtaining the core sample, where the drilling works should be preceded by resistivity survey has made it difficult for geophysicist to analyze samples in laboratory (Nguyen and Garambois, 2005).

2.2 The Electrical Resistivity Tomography: Overview

The electrical resistivity method allows the calculation of the resistivity present in soil. The calculation of resistivity makes it possible to obtain information about the subsoil nature and structure. Applying a potential difference (ΔV) to the two poles of a conductor, in it will pass a current of intensity (I) which is related to the potential difference from Ohm's law:

$$R = \Delta V / I \quad (2.1)$$

Where,

R= electrical resistance that depends on the nature and geometric characteristics of the conductor.

ΔV = difference of potential measured between M and N [V]

I = current injected into soil [A]

For each acquisition performed in the selected spreading, the following formula is generally applied:

$$\rho = \left(\frac{\Delta V}{I} \right) \cdot K \quad (2.2)$$

Where, ρ = apparent resistivity [Ω m]

ΔV = difference of potential measured between M and N [V]

I = current injected into soil [A]

K = geometric coefficient related to the sounding being used

ρ (spell it „rho“) is known as resistivity, is measured in $\Omega \cdot m$ and provides useful elements for identifying the nature of the rock types investigated. The value of this parameter depends on

the mineralogical composition of soils, the presence of fluid saturation, temperature, porosity and degree of cementation.

In the electrical or resistivity method, the measured resistivity (ρ) applying an electric current (I) through four metal electrodes planted in the ground. A small current (10 to 50 mA) is injected into the ground using two electrodes, A and B (or C_1 and C_2). The resulting voltage difference at two points on the ground surface caused by the current is measured using two potential electrodes, M and N (or P_1 and P_2).

Fields of application of ERT:

- Geology: lithological discontinuities and voids, tectonic lines localization, deposits of gravel and sand, mining plans etc.
- Hydrogeology: aquifers surveys, interface freshwater/salt detection etc...
- Environmental studies: presence of pollutants in the soil, filling areas, leakage from landfills, trace contaminants in leachate and groundwater
- Archaeology: surveys of large buried structures.

Advantages / Disadvantages:

- Difficulty of interpretation in areas morphologically rough or with many underground pipes
- We need open spaces for cables and electrodes array, the electrodes must be planted into the ground (can also be applied in paved areas or asphalt, drilling holes).
- Good vertical and lateral stratigraphic resolution.
- For best accuracy, you need a calibration reference stratigraphy
- Very useful for discrimination of metal, clay / sand and aquifers

Figure 2.1 shows the typical ERT electrode combination.

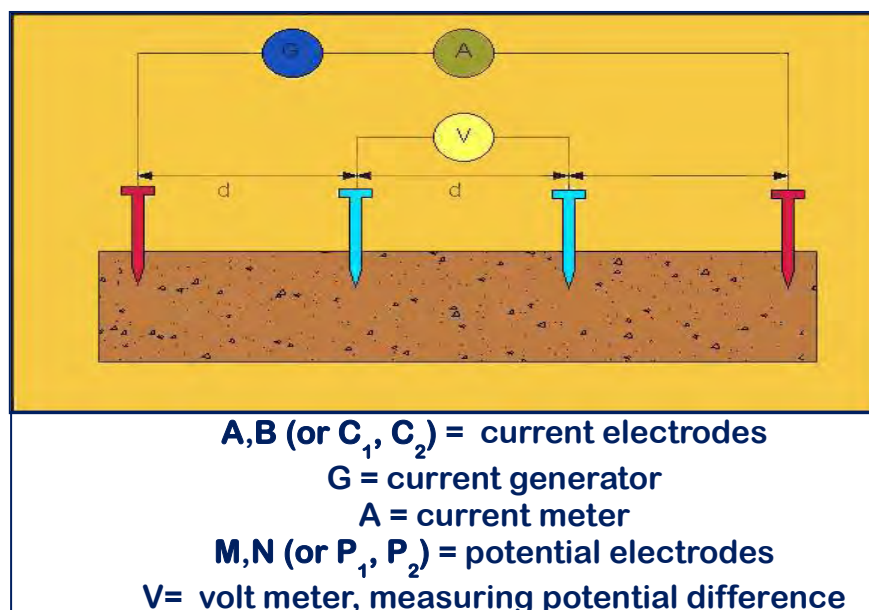


Figure 2.1: Typical ERT electrode combination (<https://www.pasisrl.it/index.php?ln=en>)

2.2.1 Electrical Properties of Sediments and Sedimentary Rocks

The resistivity of sedimentary rocks and sediments/soils depend mainly on the porosity, fluid content and clay content. Most resistivity values range from 10 to 1000 ohm*m. Resistivity decreases with increasing clay content. Most clays have resistivity of 1 to 10 ohm.m. For rocks and sediments with a low clay-content, the electrical conduction is mainly through the fluids filling the pores of the rock.

The relationship between resistivity and porosity is given by Archie's Law:

$$\rho_r = a \rho_w \phi^{-m} \quad (2.3)$$

($a \approx 1$, $m \approx 2$, ρ_r = rock resistivity, ρ_w = fluid resistivity, ϕ = fraction of the rock filled with fluid)

The resistivity of ground water varies from 10 to 100 $\Omega \cdot m$, depending on the concentration of dissolved salts. The resistivity of sea water is about 0.2 $\Omega \cdot m$ due to the relatively high salt content.

2.2.2 Electrical Properties of Metamorphic and Igneous Rocks

Igneous and metamorphic rocks typically have high resistivity values of over 1000 Ωm . The resistivity of these rocks is greatly dependent on the degree of fracturing, and the percentage of the fractures filled with ground water. A given rock type can have a large range of resistivity, from about 1000 to 10 million Ωm , depending on whether it is wet or dry. This characteristic is useful in the detection of fracture zones and other weathering features, such as in engineering and groundwater surveys.

2.2.3 Electrical Properties of Mineral Ores

Metals, such as iron, have extremely low resistivity values. Metallic sulfides (such as pyrrhotite, galena and pyrite) have typically low resistivity values of less than 1 $\Omega.m$. The resistivity value of a particular ore body can differ greatly from the resistivity of the individual crystals. Other factors, such as the nature of the ore body (massive or disseminated) have a significant effect. Graphitic slate has a low resistivity value, similar to the metallic sulfides, which can give rise to problems in mineral surveys. Most oxides, such as hematite, do not have a significantly low resistivity value. One exception is magnetite. Figure 2.2 Reference resistivity values table of various materials.

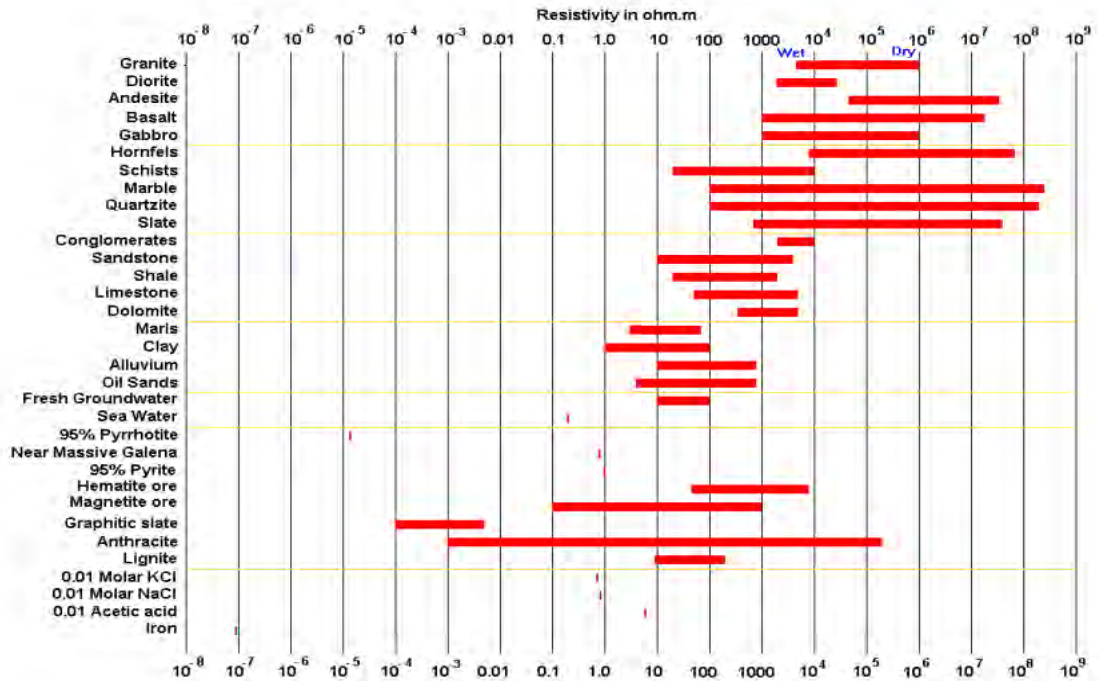


Figure 2.2: Reference resistivity values table of various materials (Loke, 2004)

2.2.4 Types of Surveys

In geophysical inversion, we seek to find a model that gives a response that is similar to the actual measured data. The model is an idealized mathematical representation of a section of the earth (which is always 3-D). The models used can be classified as 1-D, 2-D and 3-D.

1-D: Resistivity only changes in the vertical direction (with depth). Surveys are the simplest to carry out, but interpretation model is too simplistic and not sufficiently accurate in many cases. Traditional 1-D models are probably too inaccurate for most surveys where there are significant lateral variations. Lateral changes might be mistaken for vertical changes in the resistivity. For more complex situations, a 2-D (or even a 3-D) survey and interpretation model is required.

2-D: Resistivity changes in the vertical direction and one horizontal direction (the x-direction). Assume resistivity does not change in y-direction. Probably the best compromise in many situations, particularly over elongated geological structures. A 2-D imaging survey is usually carried out with a computer controlled resistivity meter system connected to a multi-electrode cable system. The control software automatically selects the appropriate four electrodes for each measurement to give a 2-D coverage of the subsurface. A large variety of arrays and survey arrangements can be used with such a system. Figure 2.3 below shows the 2-D electrical imaging survey-

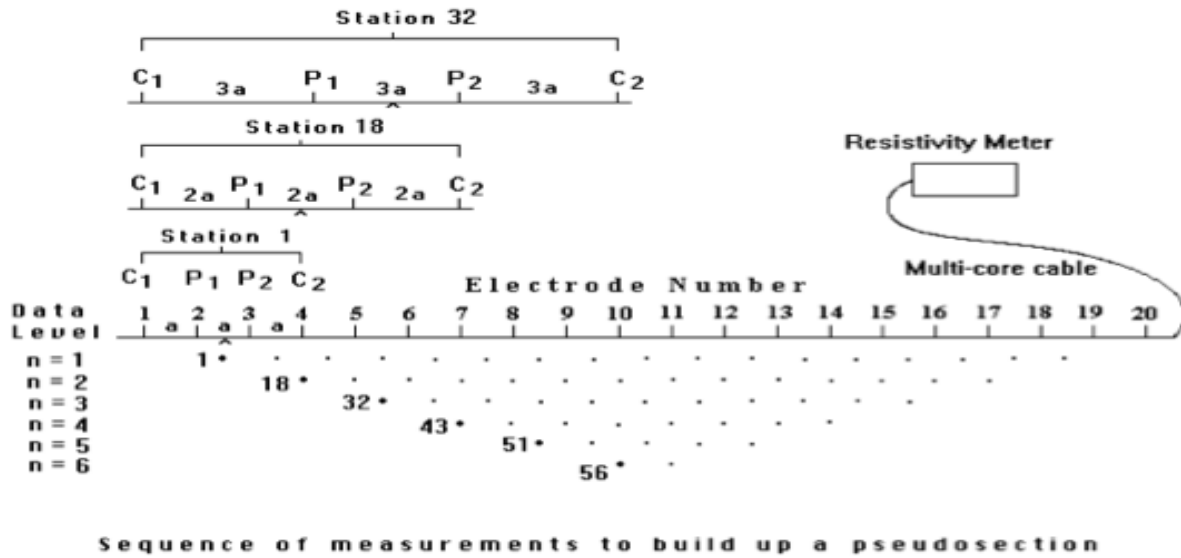


Figure 2.3: 2-D electrical imaging survey (<https://www.pasisrl.it/index.php?ln=en>)

3-D: Resistivity can change in all directions.

Figure 2.4 below shows the different types of models.

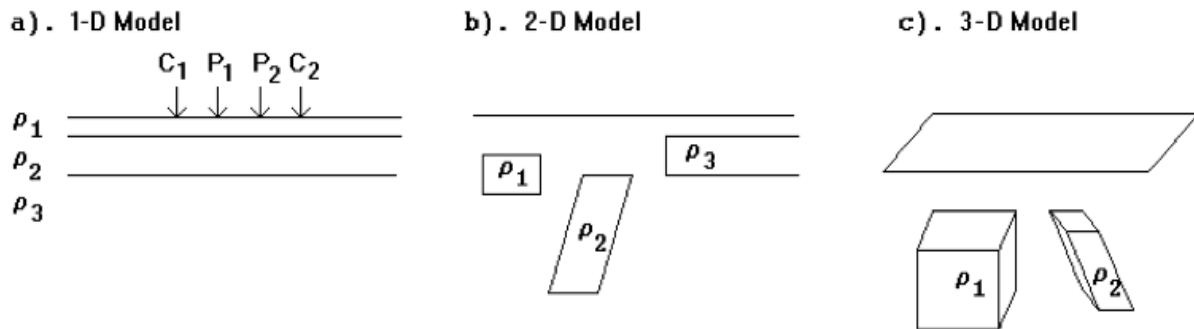


Figure 2.4: Types of model (<https://www.pasisrl.it/index.php?ln=en>)

2.2.5 Electrode Arrays of ERT

Common array types are-

- Wenner array
- Wenner-Schlumberger array
- Dipole-dipole array
- Pole-dipole
- Multiple gradient array

Wenner configuration is, on equal terms, the most robust since it allows a greater ΔV signal and therefore less sensitive to environmental noise. This is due to the geometrical factor K, for Wenner is the smallest possible. Among the characteristics of an array that should be considered are:

- the depth of investigation

- the sensitivity of the array to vertical and horizontal changes in the subsurface resistivity
- the horizontal data coverage
- the signal strength

A new consideration is the efficiency in which it can be implemented for multi-channel systems, i.e. the number of simultaneous readings that can be made with a common pair of current electrodes. The signal strength is an important factor in noisy areas, or when large electrode spacing's are used or for surveys with conductive material. The signal strength is inversely proportional to the geometric factor, so it can be easily estimated. The Wenner (alpha) array has the smallest geometric factor, and thus the highest signal strength. This means surveys with the Wenner alpha array are generally less noisy. The pole-pole array has the same geometric factor but it has higher telluric noise due to the large distance between the potential electrodes. Figure 2.5 below depicts the types of electrode arrays-

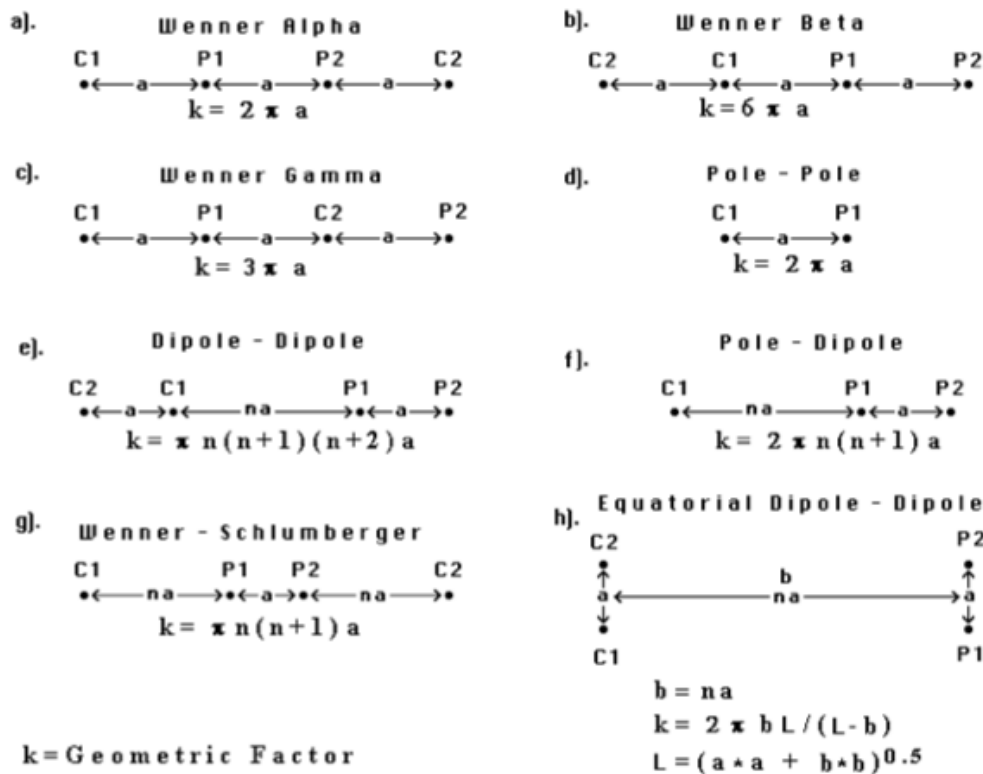


Figure 2.5: Types of electrode arrays (<https://www.pasisrl.it/index.php?ln=en>)

Signal strenght of different arrays are as-

- The geometric factor for the dipole-dipole array is proportional to n^3 , thus dipole-dipole surveys tend to have the noisiest data. As a general rule, the maximum „n“ value should not exceed 6.

- The geometric factors for pole-dipole and Wenner-Schlumberger arrays are proportional to n^2 , thus the signal strength is stronger than the dipole-dipole but weaker than the Wenner.
- The signal strength for the gradient array is between that of the Schlumberger and pole-dipole arrays.

Depth of Investigation of Different Arrays

The "median depth of investigation", z_e , can be easily calculated for different arrays, and the results are listed in the table below. The depths are given as the ratio to the „a“ spacing or the total length „L“ of the array. To calculate the actual depth of investigation, just multiply this ratio by the „a“ spacing or „L“ length used in the field survey.

Array type	z_e/a	z_e/L	Array type	z_e/a	z_e/L
Wenner Alpha	0.519	0.173	Wenner-Schlumberger		
Wenner Beta	0.416	0.139	n = 1	0.519	0.173
Wenner Gamma	0.594	0.198	n = 2	0.925	0.186
			n = 3	1.318	0.189
Dipole-dipole			n = 4	1.706	0.190
n = 1	0.416	0.139	n = 5	2.093	0.190
n = 2	0.697	0.174	n = 6	2.478	0.191
n = 3	0.962	0.192	n = 7	2.863	0.191
n = 4	1.220	0.203	n = 8	3.247	0.191
n = 5	1.476	0.211	n = 9	3.632	0.191
n = 6	1.730	0.216	n = 10	4.015	0.191
n = 7	1.983	0.220			
n = 8	2.236	0.224	Pole-dipole		
			n = 1	0.519	
Equa. dipole-dipole			n = 2	0.925	
n = 1	0.451	0.319	n = 3	1.318	
n = 2	0.809	0.362	n = 4	1.706	
n = 3	1.180	0.373	n = 5	2.093	
n = 4	1.556	0.377	n = 6	2.478	
			n = 7	2.863	
Pole-Pole	0.867		n = 8	3.247	

The depth of investigation of the Wenner alpha array is about half the „a“ spacing between the electrodes. Also note that the pole-pole array has the deepest depth of investigation. The „median depth of investigation“ for the dipole-dipole array is probably an underestimate, due to the extreme form of the shape of the sensitivity function.

The Wenner-Schlumberger Array Arrangement

This is a combination of the Wenner and Schlumberger arrays. The “n” factor for this array is the ratio of the distance between the C1-P1 (or P2-C2) electrodes to the spacing (“a”) between the P1-P2 potential pair. The geometric factor is proportional to n^2 . Figure 2.6 shows the Wenner-Schlumberger array-

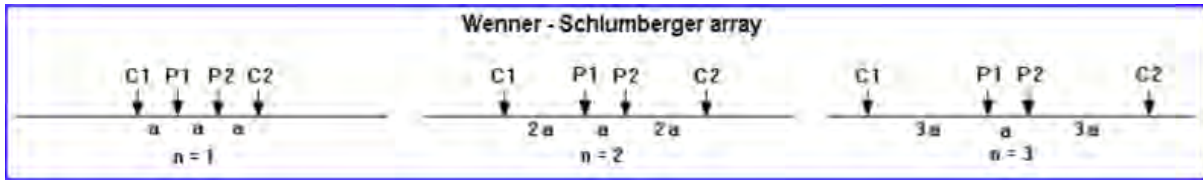


Figure 2.6: Wenner-Schlumberger array (<https://www.pasisrl.it/index.php?ln=en>)

The Dipole-Dipole Array

To use this array, the resistivity meter should have comparatively high sensitivity and very good noise filtering circuitry, and there should be good contact between the electrodes and the ground. A high current output is also desirable. This array has been successfully used in many areas to detect structures such as cavities where the good horizontal resolution of this array is a major advantage. Figure 2.7 shows the Dipole-dipole array-

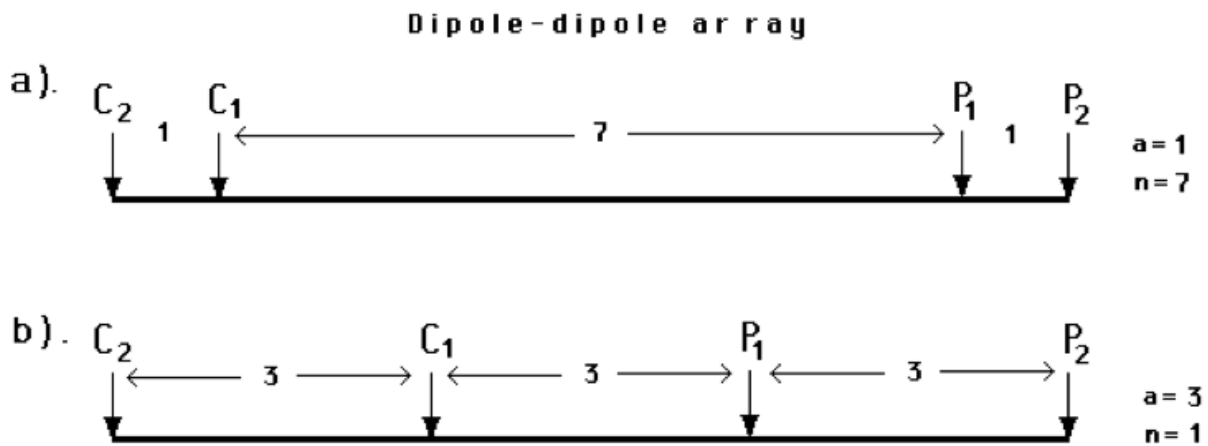


Figure 2.7: Dipole-dipole array (<https://www.pasisrl.it/index.php?ln=en>)

The Pole-Dipole Array Electrode Arrangement

Unlike the other arrays, the pole-dipole array is an asymmetrical array. The pole-dipole array requires a remote electrode, the C2 electrode, which must be placed sufficiently far from the survey line (at least 5 times the maximum C1-P1 distance used). Over symmetrical structures the apparent resistivity anomalies in the pseudosection are asymmetrical. In some situations, the asymmetry in the measured apparent resistivity values could influence the model obtained after inversion. Figure 2.8 shows the Pole-dipole array.

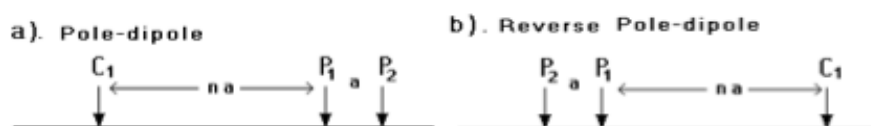


Figure 2.8: Pole-dipole array (<https://www.pasisrl.it/index.php?ln=en>)

One method to eliminate the effect of the asymmetry of this array is to repeat the measurements with the electrodes arranged in the reverse manner. By combining the measurements with the “forward” and “reverse” pole-dipole arrays, any bias in the model due to the asymmetrical nature of this array would be removed. However, this procedure will double the number of data points and consequently the survey time.

The Multiple Gradient Array

This is a relatively new array developed primary for multi-channel resistivity meter systems. In the multiple gradient array, different sets of measurements are made with the potential electrodes at different locations for the same current electrodes. As an example, for a system with 32 electrodes, one set of measurements can be made with the current electrodes at nodes 1 and 32. Next, another series of measurements are made with the current electrodes at nodes 1 and 16, as well as another with the current electrodes at 16 and 32. A similar set of measurements can be made with the C1-C2 electrodes at 1-8, 8-16, 16-24 and 2-32. This can be repeated using smaller distances between the current electrodes. Figure 2.9 illustrates the multiple gradient array.

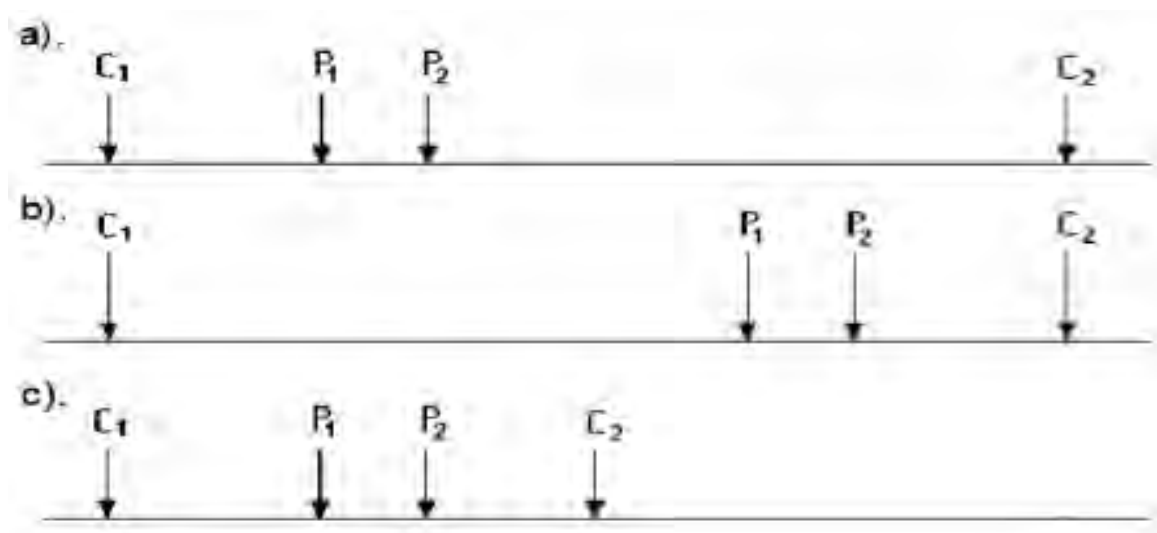


Figure 2.9: Multiple gradient array (<https://www.pasisrl.it/index.php?ln=en>)

The Wenner array is an attractive choice for a survey carried out in a noisy area (due to its high signal strength) and also if good vertical resolution is required. The dipole-dipole array might be a more suitable choice if good horizontal resolution and data coverage is important (assuming the resistivity meter is sufficiently sensitive and there is good ground contact). The Wenner-Schlumberger array (with overlapping data levels) is a reasonable all-round alternative if both good horizontal and vertical resolutions are needed, particularly if good signal strength is also required. If a system has a limited number of electrodes and limited survey line length, the pole-dipole array with measurements in both the forward and reverse directions might be a suitable choice. It is an alternative to the dipole-dipole for IP surveys.

2.2.6 Types of Surveys and Models

Pseudosection data plotting method: To plot the data from a 2-D imaging survey, the pseudosection contouring method is normally used. The horizontal location of the point is placed at the mid-point of the set of electrodes used to make that measurement. The vertical location of the plotting point is placed at a distance that is proportional to the separation between the electrodes. For example, the data point measured by electrodes 1, 2, 3 and 4 are plotted at the mid-point between electrodes 2 and 3 in the diagram below. Figure 2.10 below shows the sequence of measurements to build up a pseudo-section using a computer controlled multi-electrode survey setup

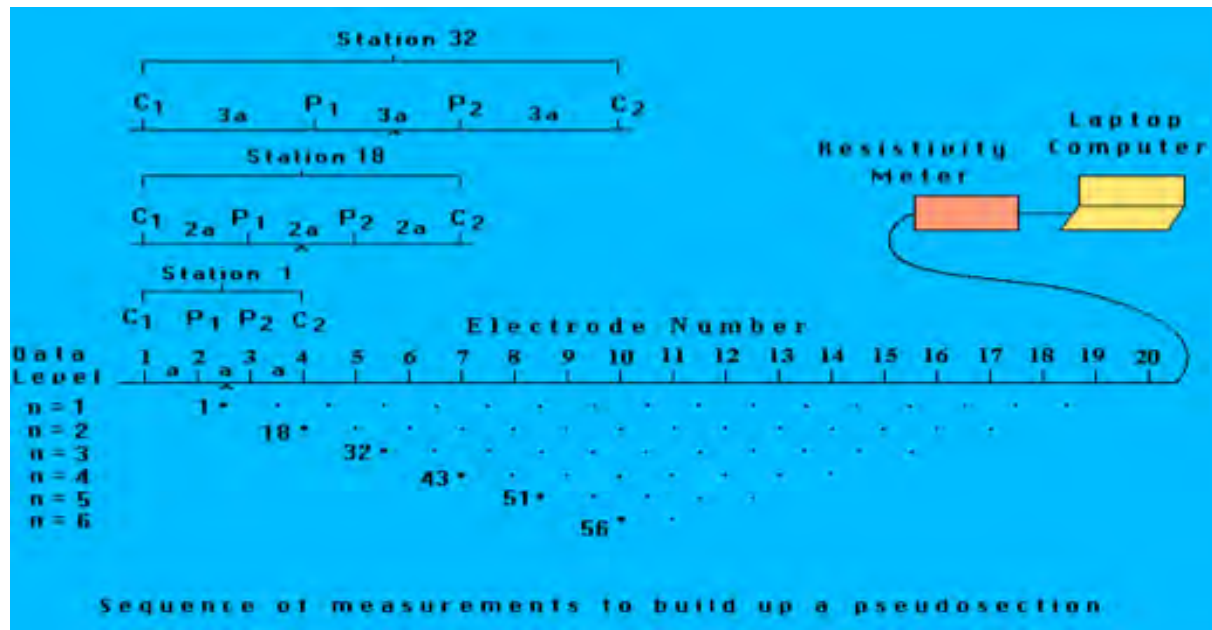


Figure 2.11 shows the scheme of data acquisition and configuration of the type Wenner reconstruction of the relative 2D apparent resistivity pseudosections.

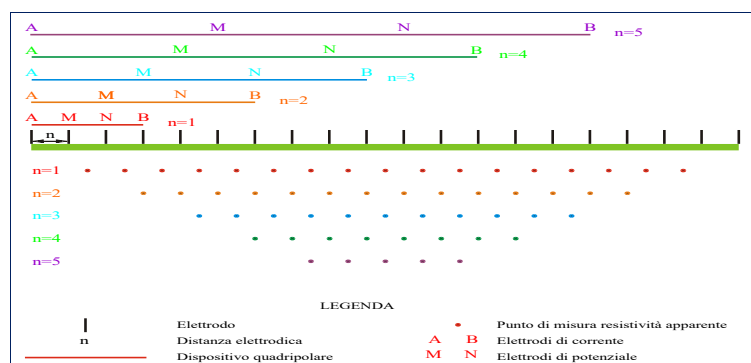


Figure 2.11: Scheme of data acquisition and configuration of the type Wenner reconstruction of the relative apparent resistivity pseudosections

Different arrays allows:

- A "volume under investigation" of different shape, and therefore different resolving power
- A different density "investigation" as a function of depth within the volume predicted

Different arrays implies:

- A different geometrical coefficient, and therefore different signal level (S/N ratio)
- A different economy of execution, processing and interpretation of data (tools, time, results)

Figure 2.12 below illustrates the comparison between the arrangement of electrodes and related pseudosections for Wenner and Schlumberger.

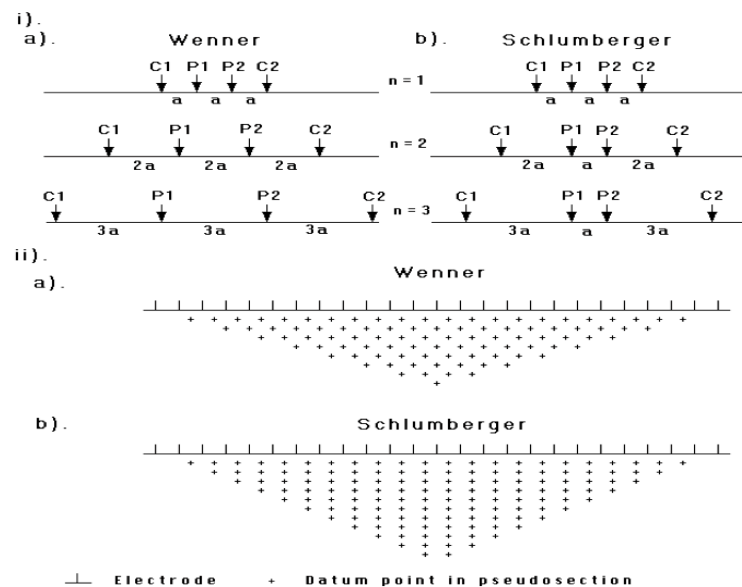


Figure 2.12: Comparison between the arrangement of electrodes and related pseudosections for Wenner and Schlumberger (Loke, 2004)

3-D: Surveys and models are potentially the most accurate, but requires involves higher surveys costs and greater computational resources.

In geophysical inversion, the finding is a model that gives a response that is similar to the actual measured data. The models used can be classified as 1-D, 2-D and 3-D.

2.2.7 The Software RES2DINV

RES2DINV is a computer program that will automatically determine a two-dimensional (2-D) resistivity model for the subsurface for the data obtained from electrical imaging surveys [24]. This program is designed to invert large data sets (with about 200 to 21000 data points) collected with a system with a large number of electrodes (about 25 to 16000 electrodes). The 2-D model used by the inversion program consists of a number of rectangular blocks. A

forward modeling subroutine is used to calculate the apparent resistivity values, and a non-linear least-squares optimization technique is used for the inversion routine [25-26].

2.2.8 Inversion

The purpose of an inversion program is to convert the apparent resistivity values into the true resistivity of the subsurface.

$$\rho_a \rightarrow \rho_{\text{true}}$$

The relationship between the apparent resistivity and the true resistivity is a very complex relationship. It depends on whether the subsurface is assumed to be 1-D, 2-D or 3-D. The below figure 2.13 shows an example of a typical 1-D inversion.

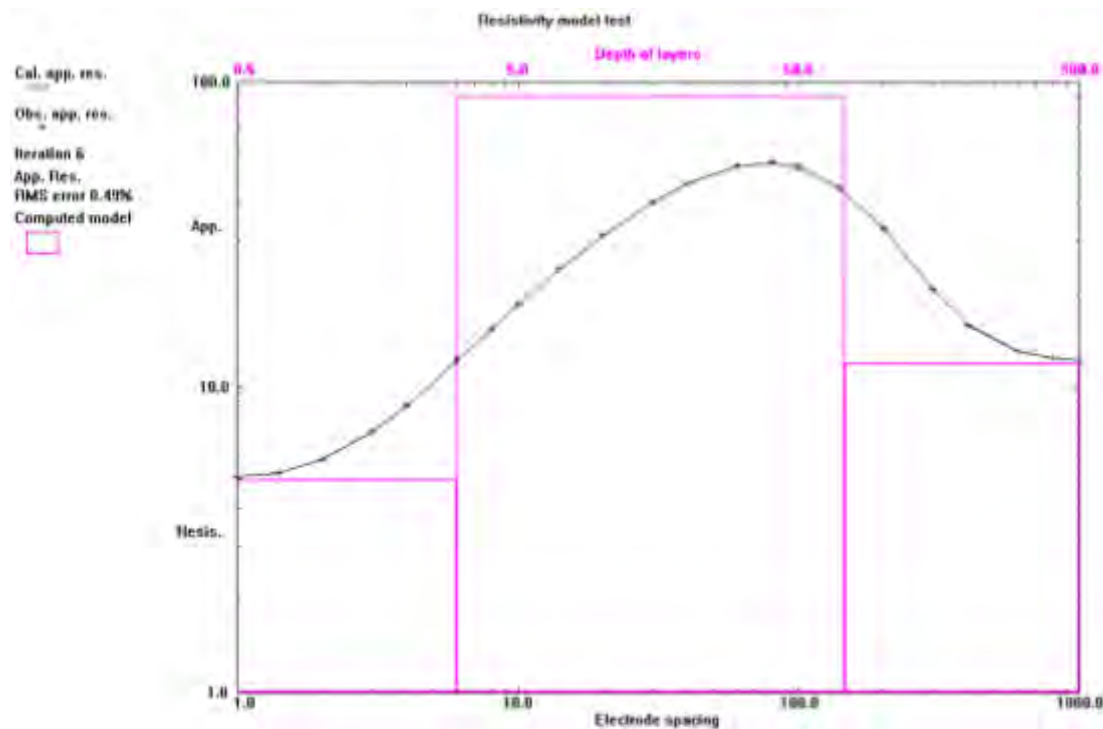


Figure 2.13: Example of a typical 1-D inversion (<https://www.pasisrl.it/index.php?ln=en>)

A 2-D model is used to interpret the data from a 2-D imaging survey. The model usually consists of a large number of rectangular cells. The size and position of each cell is fixed. An inversion program is used to determine the resistivity of the cells from the measured apparent resistivity values. Figure 2.14 below shows the arrangement of model blocks and apparent resistivity datum points.

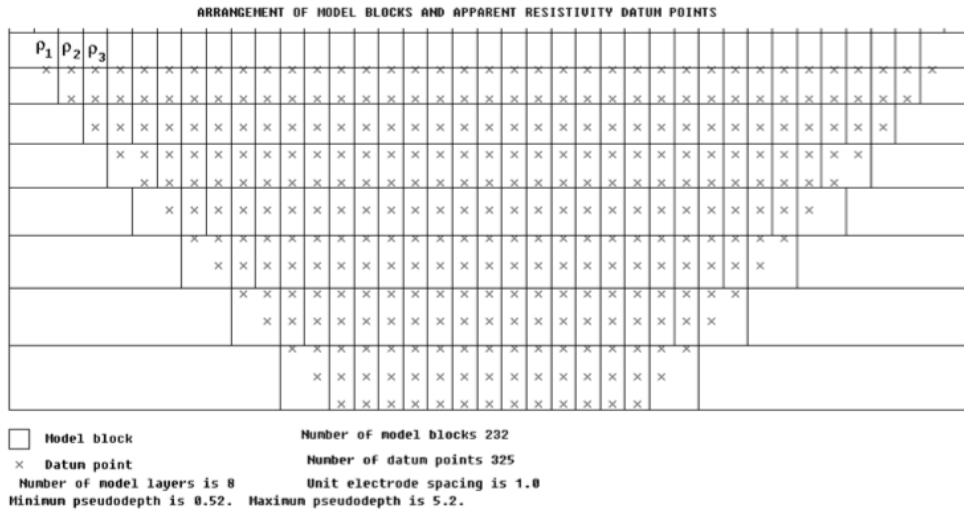


Figure 2.14: Arrangement of model blocks and apparent resistivity datum points (<https://www.pasisrl.it/index.php?ln=en>)

What we have: Observed data (y) - logarithm of measured apparent resistivity values.

What we want: Model parameters (q) - logarithm of model cells resistivity values.

The connection between them: Model response (f) - logarithm of calculated apparent resistivity values

Starting an Inversion

All inversion methods try to determine a model for the subsurface whose response agrees with the measured data subject to certain restrictions. The model parameters are the resistivity values of the model cells, while the data is the measured apparent resistivity values. An initial model (usually a homogenous model) is modified in an iterative manner so that the difference

$$g = y - f \tag{2.4}$$

between the calculated (f) and measured (y) apparent resistivity values is reduced.

Figure 2.15 below shows an example of a typical inversion-

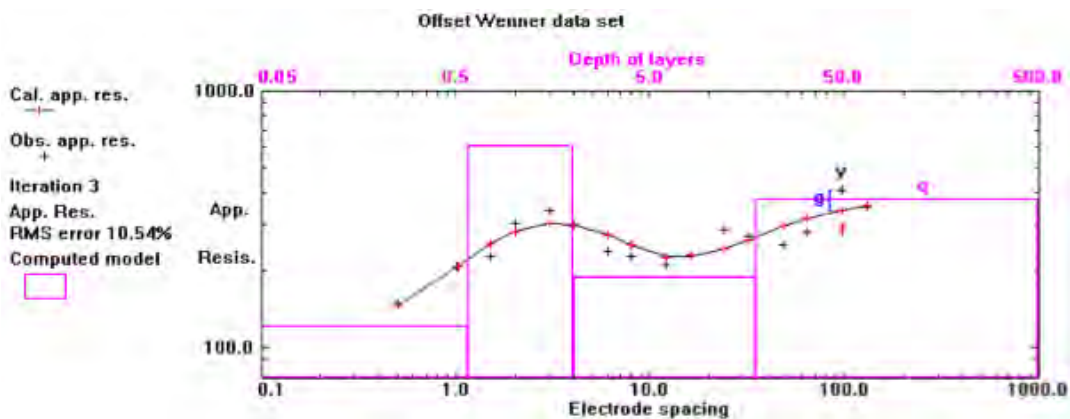


Figure 2.15: Example of a typical inversion (<https://www.pasisrl.it/index.php?ln=en>)

Pseudosection Data Plotting Method

- The pseudosection gives a very approximate picture of the true subsurface resistivity distribution, as the shapes of the contours depend on the type of array used as well as the true subsurface resistivity.
- The pseudosection is useful as a means to present the measured apparent resistivity values in a pictorial form, and as an initial guide for further quantitative interpretation.
- The figure also gives you an idea of the data coverage that can be obtained with different arrays. Note that the pole-pole array gives the widest horizontal coverage, while the coverage obtained by the Wenner array decreases much more rapidly with increasing electrode spacing.
- One useful practical application of the pseudosection plot is for picking out bad apparent resistivity data points, which have unusually high or low values.

In the inversion of a data set it's necessary to calculate the apparent resistivity values for the model used – this is the forward modeling problem. In forward modeling, the subsurface resistivity distribution is specified and the purpose is to calculate the apparent resistivity that would be measured by a survey over such a structure. The 2-D subsurface is divided into many cells, and the finite-difference or finite-element method is used to calculate the apparent resistivity values.

The Finite-Difference and Finite-Element Methods

Both methods are designed to solve the following equation:

$$-\nabla \cdot \left[\frac{1}{\rho(x, y)} \nabla \Phi(x, y, z) \right] = I_c \quad \dots\dots\dots (2.5)$$

I_c is the current and $\Phi(x, y, z)$ is the potential at the nodes that is to be calculated. The subsurface is divided into a large number of cells and each model cell can have a different resistivity value. The finite-difference method is limited to rectangular grids. The finite-element method can have non-rectangular cells and thus is normally used when there is topography. The time taken by both methods depends on the number of nodes (cells). The total number of nodes depends on the number of nodes in the horizontal and vertical directions. Normally 2 or 4 horizontal nodes are used between adjacent electrodes.

Figure 2.16 depicts the finite-difference and finite-element methods –

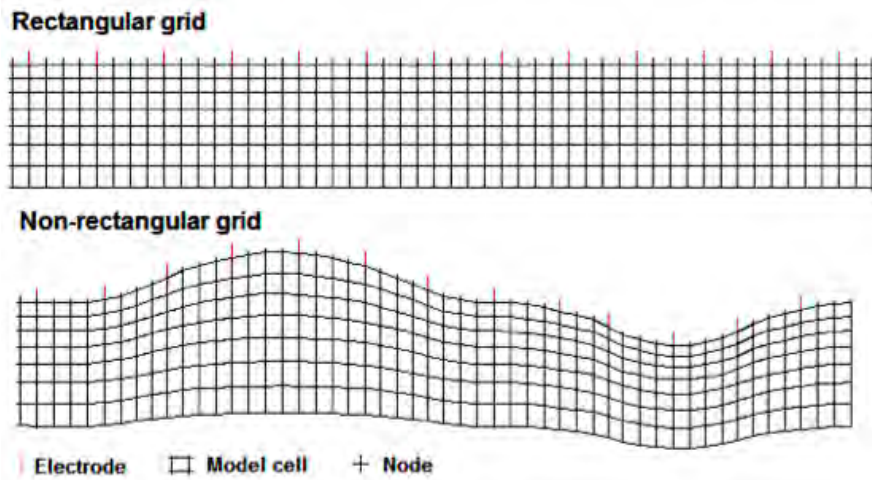


Figure 2.16: The finite-difference and finite-element methods
<https://www.pasisrl.it/index.php?ln=en>

2.3 Application of ERT in Environmental Engineering

Operating landfills as bioreactor landfills is becoming increasingly popular, and it is crucial to understand and monitor the moisture content and its distribution within the landfilled solid waste. Monitoring moisture distribution within the MSW in a bioreactor landfill is essential not only for the design and operation of leachate recirculation systems, but also to identify locations of non-uniform leachate distribution, because this may lead to ponding and seepage of water through side slopes, raising concern for potential slope failure. At present, moisture content of landfilled MSW is determined by collecting MSW samples using soil drilling rigs and then measuring the moisture content gravimetrically in the laboratory.

However, the major limitations of this method are (1) this provides only moisture content of MSW at a certain point, not a general view of moisture distribution within solid waste; (2) for time-dependent moisture variation, samples need to be collected from a site on a regular basis; and (3) this approach may not be cost effective. Several indirect methods such as time domain reflectometry (TDR), neutron probes, partitioning gas tracer, electrical resistance sensor, fiber optic sensors, and electrical resistivity imaging were used in the past [27].

Electrical resistivity imaging (ERI) is a nondestructive geophysical surveying method that has been widely used for environmental and geotechnical investigations. ERI is based on injecting current into the ground via an electrode pair and measuring the potential difference between another electrode pair.

ERI can detect variations in moisture content, because, along with other factors, resistivity varies with moisture content. ERI can produce detailed profiles of the subsurface, showing the spatial distribution of moisture within the landfill. However, these profiles do not give quantitative information about the moisture content of the waste. MSW samples in a landfill can have identical moisture contents, but still have different resistivity values because of different degrees of compaction and different stages of decomposition, as well as different

compositions and differing amounts of mixed-in soil. Therefore, there is a need to study the variation of moisture (Dhalin, 2001, Griffiths and Barker, 1993).

Electrical resistivity is a physical property of the material and is affected by water content, temperature, porosity, particle size, pore fluid composition, and clay content (deGroot-Hedlin and Constable, 1990, Loke and Barker, 1996; Imhoff, 2007; Ward, 2000). Two-dimensional (2D) electrical resistivity methods were first applied to soils, but several authors demonstrated their applicability to MSW in the field. However, very few studies were conducted in the laboratory to understand the factors that affect the electrical resistivity of MSW (Grellier et al., 2005; Grellier et al., 2007; Grellier et al., 2008).

Electrical resistivity and moisture content are commonly related by Archie "s law which for clay-free soil is given by

$$\frac{\rho}{\rho_w} = a \phi^{-m} S^{-n} \quad (2.6)$$

where ρ = bulk resistivity; ρ_w = resistivity of the pore fluid; ϕ = porosity; S = saturation; a is a constant ranging from 0.5 to 2.5; m = cementation factor and falls between 1.3 and 2.5; and n is a constant which is normally equal to 2. Assuming $m = n$, Archie "s law can be written as-

$$\rho = \rho_w a \theta^{-m} \quad (2.7)$$

Resistivity is also affected by temperature. In general, electrical resistivity decreases by about 2% for a temperature increase of 1°C (Archie, 1942; Reynolds, 1997).

Compacted clay soils are widely used to line waste impoundments and to close the waste disposal unit. During construction of bottom liners, stringent quality controls are recommended to ensure low hydraulic conductivity ($K_s \leq 1 \times 10^{-7}$ cm/s). Therefore, it is important to identify the appropriate compaction condition of soils to restrict water intrusion through compacted clay liners. Daniel and Benson (1990) proposed an acceptable zone in the moisture density curve of liner soils, which encompasses low hydraulic conductivity criterion. Although it is important to consider the acceptable zone during compaction of liners, the proposed moisture–density zone can be modified to take into consideration shear strength, shrink-swell criteria, and the construction practices of a given area. Additionally, Benson et al. (1999) performed a study to evaluate the importance of compaction parameters, i.e., molding water content and dry density, to the construction of clay liners. According to the study, an increase in the degree of saturation in the soils caused a reduction in hydraulic conductivity of clay liners, resulting in their being under the acceptable zone of moisture-density curve (Daniel and Benson, 1990).

The evaluation of change in the degree of saturation in vertical and horizontal directions is also important for the effective performance of an evapotranspiration (ET) cover. An increase in saturation emphasizes that the cover system is approaching its storage capacity. Specifically, when the ET cover consists of a capillary barrier, saturated fine soil provides an indication of the potential percolation. Because of time and cost constraints, a detailed

investigation of non-uniform compaction conditions, poor bonding of lifts, and/or variable soil composition in clay liners, final covers, and ET covers is often not possible, using the available in-situ and laboratory methods. Moreover, the applicability of the available methods is restricted, in many instances, when spatial variability of the subsurface is expected (Hakonson, 1997).

Resistivity Imaging (RI) is a geophysical method employed to investigate a large area in a rapid and non-destructive way. This method can provide a continuous image of subsurface in both vertical and horizontal directions. RI method utilizes electrical resistivity responses of soils which are functions of degree of saturation, clay content, pore water, and mineralogical content. Typically, high resistivity of clay liner soils is an indication of a low degree of saturation, high air-filled voids, and poor lift bonding. Kalinski (1992) conducted electrical resistivity tests in compacted liner of Lincoln landfill using Wenner configuration. The liner soil consisted of high plasticity clay (CH), low plasticity clay (CL), and clayey silt (ML–CL). The study results indicated that the resistances of liner soils were in between 4.0 and 5.4 Ohm. Therefore, RI method can be used as a tool for construction quality control in clay liners of landfill. The application of electrical resistivity to evaluate moisture and density is documented in several studies (Kalinski, 1992; Kalinski and Kelly, 1994).

McCarter (1984) evaluated the effect of air-void ratio in soil resistivity on Cheshire and London clays. The results of the study indicated that the degree of saturation is an important factor in resistivity variation. Hassanein et al. (1996) performed a comprehensive study on the effects of molding water content and compactive efforts in soil resistivity. It was observed that the resistivity was high, when soil was compacted at dry optimum, and low, when compacted at wet optimum. Moreover, resistivity was sensitive to molding water content below optimum condition. On the other hand, resistivity was almost independent of molding water content at wet of optimum. In addition, electrical resistivity can provide useful information about moisture distribution, presence of voids, and heterogeneity of the final cover.

Genelle et al. (2011) conducted a study using Resistivity Imaging (RI) and self-potential (SP) methods to determine water recharge in the final cover. The study results indicated that RI was able to map cracks in the final cover. Carpenter et al. (1991) researched the fracture and erosion of landfill covers, using electrical resistivity and seismic refraction. The results showed that the azimuthal resistivity was able to identify deep cover cracks, which required remediation to avoid infiltration of moisture and emission of landfill gases.

The resistivity imaging (RI) test has been a very popular site investigation and characterization tool for different geotechnical and geo-environmental applications over the years (Khan et al., 2012). Different factors affecting the resistivity of the soil and solid waste were studied by several researchers, and it was observed that electrical resistivity varies with the water content, temperature, ion content, particle size, resistivity of the solid phase,

permeability, porosity, clay content, degree of saturation, organic content, and pore water composition present in the materials (Clement et al., 2010).

Recent studies have shown that the problem of environmental contamination and waste management is one of the main concerns of geoscientists and researchers from other related fields of science around the globe. Fast industrial development and the uncontrolled growth of the urban population result in the production of toxic solid wastes. Urban waste materials, mainly domestic garbage, are usually disposed of inadequately in waste disposal sites posing a high risk to the underground water resources, the environmental pollution, and the community health. Moreover, older waste sites often lack reliable geological or artificial barriers, so that leaching of pollutants into the groundwater is a concern. Contamination problems are particularly severe for waste dumped in abandoned gravel pits, many of which extend to below the groundwater table. Being small and unregulated, the exact location, structure, and contents of such landfills are either unknown or poorly documented. The solution to the day-to-day problems of modern urban societies demands fast and effective geophysical methods. One of the most frequent demands in metropolitan areas is to determine the landfill's geological and geotechnical structure shape and extend, together with the excavation and dumping history (Allen et al., 1997; Mather, 1995; Georgaki et al., 2008).

Details on the contents of a landfill may be difficult to acquire but are essential for evaluating the level of risk associated with leaking pollutants. In such context, the integrated use of geophysical methods provides an essential tool in the characterization and evaluation of contaminants generated by urban residues (domestic and/or industrial) (Green et al., 1999; Heitfeld and Heitfeld, 1997; Lanz et al., 1994; Orlando and Marchesi, 2001; Saltas et al., 2005). Among those geophysical methods, electrical resistivity tomography has been found very suitable for such kind of environmental studies, due to the conductive nature of most contaminants. The use of electrical resistivity tomography applied to environmental studies is well documented (Bernstone et al., 2000; Aristodemou and Thomas-Betts, 2000; Dawson et al., 2000).

The management of solid waste landfills has been a major problem of our urban centers in Nigeria and other developing countries as well as the disposal of waste indiscriminately in rivers and landfills and mostly their proximity to the living quarters. The landfill constituents are predominately household waste. Other waste comes from shops, offices, and chemical and manufacturing industries. These wastes may contain toxic substances as they are decomposed or biodegraded, with the preference of infiltrating water, to produce organic liquid known as leachate. Sometimes, especially during the peak of the raining season, the landfills are covered by flood water. These also contributes to the leachate plumes, which contains liquid that permeates into the solid and water system through the landfill. This result pollutant to load on the environment which depends on the quantity and quality of the water that percolates through the dumpsite and penetrates down to the ground water (Bengtsson et al., 1994).

Trochobanogous et al., (1993) said that CO₂ and methane are the principal gases produced from the anaerobic decomposition of the biodegradable organic waste components in municipal solid waste. Because only limited amounts of oxygen are present in a landfill when methane concentrations reach this critical level, there is little danger that the landfill will explode. However, methane mixtures in the explosive range can form if landfill gas migrates offsite and mixes with air.

2.4 Characterization of Soil Profile Using Microtremor

The microtremor array observation method was first advocated by Aki (1957), an alternative method was proposed by Capon (1969), and the development towards utilization was made by Horike (1985) and Okada and Matsushima et al. (1990).

Although there are various ways of finding the soil profile, most of them cannot be conducted in large numbers because they are large-scaled and hence expensive. According to the array observation method, the soil velocity structure, fitted for the obtained dispersion curve of surface wave's phase velocity, can be directly searched through inverse analysis. The H/V spectrum method and the array observation method are economical and good in mobility, and it is extremely important to use the exact application conditions.

On the contrary, a microtremor test is one of the powerful means for inferring the soil profile from the viewpoint of simplicity and cost. Microtremors are often influenced by the environmental vibration sources such as traffic-induced vibrations. It has been pointed out that the spectral shapes of H/V spectra do not change between day and night and are quite stable (Nakamura and Ueno, 1986; Tokimatsu and Miyadera, 1992). In this paper, correlations between the shapes of H/V spectra and the characteristics of existing soil data are examined for Hazaribagh, and the possibility of estimating the soil profile based on microtremors are studied based on the earthquake observation data.

Among other geophysical and geotechnical methods used for microzonation, the seismological microtremor horizontal-to-vertical spectral ratio (HVSR) method has achieved high recognition in the last decade because it provides very important data on the main resonance frequency of soft sediments overlaying stiff geological bedrock. The results of the free field microtremor measurements are thus used in different soil classification standards (Brad, 1999).

The microtremor HVSR method has gained great popularity also because it provides the sediments' resonant frequency without knowing the thickness of sediments and their vertical S-wave velocity profile, the data that are otherwise needed to numerically calculate the frequency. However, these data can be acquired only with relatively expensive geophysical investigations like seismic refraction, MASW methods, or drilling. In contrast, the microtremor method provides results only when there is a relatively strong impedance contrast between sediments and the bedrock. If the knowledge on the sediments and bedrock physical properties is insufficient, the method should be first tested to prove that it is effective

in given geological conditions. This is especially important in case of very heterogeneous geological settings (Ansal, 2004).

The horizontal-to-vertical (H/V) spectrum method is one of the microtremor observation methods used for soil structure surveys. The relevance of the H/V spectrum ratio and underground soil structure has been pointed out and examinations of the applicability of this method to soil structure surveys have been performed by many researchers. Studies have put forth that the multiple reflection of a body wave can explain the formation of H/V spectrum peaks (Nakamura and Ueno, 1986), that a surface wave motion may produce the peaks and that the mode ratio of the surface wave can also explain the generation of the peaks (Arai and Tokimatsu, 2004). Those causes being set aside, the H/V spectrum shows peaks at the predominant frequency, if the contrast of the surface layer to the lower layer is strong, and it has been used successfully as an aid in soil structure investigation.

Chapter 3

METHODOLOGY

3.1 Introduction

The overall objective of this study was to assess the probable groundwater contamination at a waste dump site in Hazaribagh, Dhaka using Electrical Resistivity Tomography (ERT), which is a non-destructive geophysical method. This chapter presents the methodology followed in carrying out this research, including rationale for site selection, installation of monitoring wells, collection and testing (for electrical conductivity) water samples, details of ERT tests carried out in the field ERT data processing using the software RES2DINV, and details of microtremor test carried out and analysis of microtremor data to check the microtremor analyzed soil profile to resistivity soil profile.

3.2 Study Area

To detect the probable contamination in the waste dump site at Hazaribagh Electrical Resistivity Tomography (ERT) was conducted. Three different sites of Hazaribagh of Dhaka city were selected as the study area as shown below in figure 3.1.

These sites were used earlier for disposal of solid wastes. Dumping at the site was indiscriminate and unsorted. Wastes types dumped on the site are mainly domestic and hazardous and non-hazardous industrial wastes. Percolating groundwater provides a medium through which the wastes particularly organics can undergo transport and degradation (of organic components) through biochemical reactions involving dissolution, hydrolysis, oxidation and reduction processes. The percolating liquid forms a complex mixture called leachate. This leachate migrates downward and contaminates the shallow groundwater underneath the dumpsites. Shallow groundwater extracted through shallow tubewells could expose people living in the area to this contamination.



Figure 3.1: Study Area in Hazaribagh, Dhaka (Source: Google Maps)

3.3 Data Collection Using Electrical Resistivity Tomography imaging (ERT)

Three Electrical Resistivity Tomography imaging (ERT) tests, denoted as ERT1, ERT 2, and ERT 3, were performed in three different locations of Hazaribagh of Dhaka City. Electrical Resistivity Tomography imaging (ERT) tests were conducted using a Super Sting PASI 16-G-N multichannel system.

Thirty-Two (32) electrodes, with a spacing of 3 m, were used in the ERT tests; therefore, the length of each profile was 62 m. The configuration used is referred to as “Wenner–Schlumberger array”. According to the literature, Wenner– Schlumberger array has the advantages of low electromagnetic coupling and high sensitivity in response to the variations in both horizontal and vertical direction; therefore, Wenner-Schlumberger array was utilized to conduct the ERT tests. The penetration depth of each electrode was less than 20 cm during the ERT tests to avoid potential intrusion of the compacted soils. Table 3.1 shows the coordinates of the three test sites.

Table 3.1: Geographic coordinates of the study area.

Sl. no	Date	Name of the point of study area	Location		City
			Latitude	Longitude	
ERT1	16/10/04	Hazaribagh	23.729501 N	90.363461 E	Dhaka
ERT2	16/10/04	Hazaribagh	23.73044 N	90.364885E	Dhaka
ERT3	16/12/19	Hazaribagh	23.73077 N	90.365218” E	Dhaka

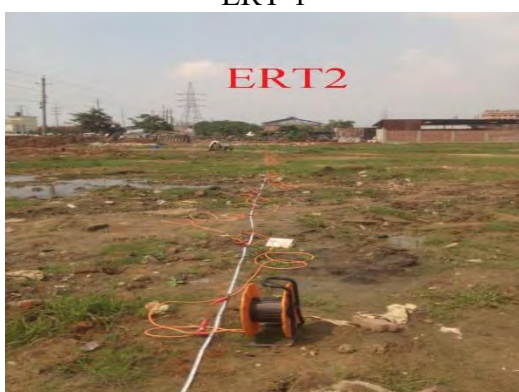
The Electrical Resistivity Tomography (ERT) data have been gathered through electrodes of length 50 cm, partially driven into the ground. The electrodes were then connected through multichannel cables, adopting the Wenner-Schlumberger array configuration. The details of the data collection set up for the three sites are given below. Figure 3.2 shows the three dumping sites where the ERT tests were carried out as at the time of data collection.



ERT-1



ERT-1



ERT-2



ERT-2



ERT-3



ERT-3

Figure 3.2: Open waste dumping sites as at the time of data collection

(A) Test Point-01 (ERT1)

- Low land area which is situated at a distance of about 500m from the Buriganga River.

- Number of Electrodes used = 32
- Electrode spacing = 3m
- Data acquisitions were made @ 3m apart of each electrode.

(B) Test Point-02 (ERT2)

- Low land area which is situated at a distance of about 600m from the Buriganga River.
- Number of electrodes used = 32
- Data acquisitions were made @ 3m apart of each electrode.

(C) Test Point-03 (ERT3)

- Low land area which is situated at a distance of about 700m from the Buriganga River.
- Number of electrodes used = 32
- Data acquisitions were made @ 3m apart of each electrode

3.4 Data Collection Using Microtremor

The purpose of conducting Microtremor measurements is to obtain an estimation of site response for a particular location. Three approaches are commonly used to analyze microtremor data; power spectral densities obtained directly from the Fourier amplitudes, spectral ratios relative to a reference site, and Nakamura's technique, which is defined as the spectral ratio of horizontal components to vertical components recorded at the same site (H/V ratio). It is common to perform tests over a period of time to observe the stability of the measured site response, in order to provide a reliable prediction of the period of potential earthquake motion at that site (Nakamura and Ueno, 1986).

Nakamura's technique describes the microtremors as Rayleigh waves propagating in a single layer over a half-space, and assumes that the microtremor motion is due to local sources such as traffic and human and construction activity nearby. It further assumes that the vertical component of ground motion is not amplified by the soil layer. Hence, the spectral ratio of the horizontal to the vertical components at the surface (H/V ratio) gives an estimate of the period at which it peaks, corresponding to the site period.

The equipment used for the microtremor testing system consists of three velocity transducers; two horizontal and one vertical, an amplifier and a laptop computer used for data acquisition. For the selection of the test location, care is taken to avoid heavy traffic, manholes, foundation sand other underground structures. The sensors are placed so that the two horizontal sensors are orthogonal, preferably facing North and East. The analysis is carried out using Nakamura's method, plotting the H/V spectral ratios that are the result of taking the RMS of the east and North spectral ratios. The most significant peak of the H/V spectral ratio is taken to be the dominant frequency of the site.

Numerous theoretical and practical researches have been carried out on reliability of the microtremor method in micro zoning studies (Nakamura and Ueno, 1986). In this study,

microtremor measurements were performed at three sites of Hazaribagh, Dhaka. Five sensors were placed @ 20m apart on the surface covering a total length of 80 meters. At each site at least 20 minutes noise data collected with generally 100 Hz sampling frequency. The locations were carefully selected to avoid the influence of buildings, industrial facilities, and traffic as much as possible, although this was not always possible in the urban environment. The following procedure is applied to determine resonance frequency (or period) and seismic amplification for the site being analyzed.

- loading microtremor data,
- if necessary, some data correction operations (excluding some noisy parts of data, instrument correction, normalizing, component rotation, data re-sampling) may be applied.

Methods to get geophysical information from the microtremor measurement were 1) obtaining the phase velocity by array observation of microtremor and 2) obtaining H/V spectrum by using 3 component sensors. After obtaining the phase velocity or H/V spectrum, S-wave velocity profiles should be interpreted by applying an inverse analysis.

Soil characteristics can be assessed by Microtremor measurement. Hard soil gives high frequency and soft soil gives low frequency. A structure may experience a vibration period at which it oscillates in the earthquake vibration motion and will tend to respond that. Natural frequency is obtained based on the spectral ratio of horizontal component of the structure to that of ground. Wave propagation mechanism of Microtremor and its relation with ground vibration characteristics were studied from the beginning of Microtremor studies (Aki, 1957).

Confirmation of the soil structure by the H/V spectrum method even at the point where detailed soil velocity structure was acquired by logging survey is recommended. When making a revised soil model, the microtremor array observation serves as an effective method. Figure 3.3 shows the microtremor testing equipment.



Figure 3.3: Microtremor testing equipment.

3.5 Installation of Boreholes and Collection of Water Samples

Boreholes are constructed by drilling. There are different types of methods of drilling. The methods are as follows-

- Cable tool/percussion/standard method
- California stovepipe method
- Jetting method
- Direct rotary method
- Reverse circulation rotary method

For the installation of borehole at Test Point-01 percussion method has been used here.

Percussion drilling: In percussion drilling, a heavy bit is repeatedly lifted and dropped, progressively boring through the earth. In rotary drilling, the drilling results from the continuous scraping of the bit under constant pressure. The hole is cleaned out as the drilling progresses, either with a drilling fluid (mud), with high velocity air or, in auger drilling, by the mechanical lifting of the auger. Percussion drilling is a manual drilling technique in which a chisel faced bit is repeatedly raised and dropped. The bit breaks and pulverizes the materials. A slurry of water and cuttings, which is formed by the drilling action, is periodically removed by a bailer. Water is continually added to the borehole as needed.

Suitable conditions for percussion drilling: Percussion drilling is suitable for unconsolidated and consolidated formations: Sand, silt, stiff clays, sandstone, laterite and gravel layers. Manual percussion drilling is generally used up to depths of 25 meters. Before drilling starts, it is good to analyze where the water might be.

Advantages of percussion drilling:

- Unlike any other drilling method, percussion can remove boulders and break harder formations, effectively and quickly through most types of earth.
- Percussion drilling can in principle deal with most ground conditions.
- Can drill hundreds of feet
- Can drill further into the water table than dug wells, even drilling past one water table to reach another.

Three boreholes at Test Point-01 have been made by percussion drill. Fresh water has been added during the drilling to make the drilled soil slurry. The depth of these boreholes are 5m, 10m and 15m respectively. First a borehole of 5m length has been made. Then steel pipes 4m in length and a 1m strainer has been installed in the borehole. The strainer is fixed at the bottom of the 5m depth. Then the top of the steel pipe of the borehole on the surface is fixed with a readymade steel platform to fix the portable hand pump. After fixing the hand pump properly, water withdrawal started. The ground water sample was collected after 5minutes washout of the water that remained in the borehole during the drilling.

The ground water samples of 10m and 15m were collected by following the same procedure of 5m borehole. Figure 3.4 shows the percussion drilling of the borehole where the tests were carried out as at the time of ground water sample collection.



Figure 3.4: Percussion drilling of the borehole where the tests were carried out as at the time of ground water sample collection.

3.6 Data processing and analysis

3.6.1 The Electrical Resistivity Tomography (ERT) Data

Data collected from the survey have been analyzed with the software RES2DINV. RES2DINV is a computer program that automatically determines a two-dimensional (2-D) resistivity model for the subsurface from the data obtained from electrical imaging surveys (Dhalin, 1996; Loke, 2018). The assessment for ground water pollution will be done by comparing the different resistivity values of the different layers of the models comparing to the standard resistivity values of different contaminants. The standard resistivity values of different materials are shown in Table 3.2.

Table 3.2: Reference resistivity values of various materials (Loke, 2004) [19]

Formation	Typical Resistivity (Ωm)	Usual Limit (Ωm)
Iron	9.074×10^{-8}	9.074×10^{-8}
0.01 M Potassium chloride	0.708	0.5-0.8
0.01 M Sodium chloride	0.843	0.8-1.0
0.01 M acetic acid	6.13	6-7.5
Xylene	6.998×10^{16}	6.998×10^{16}
Sea water	2	0.1-10

Formation	Typical Resistivity (Ωm)	Usual Limit (Ωm)
clay	40	8-70
Ground well and spring water	50	10-150
Clay and sand mixtures	100	4-300
Shale, Slate, Sandstone etc.	120	10-100
Peat, Loam and Mud	150	5-250
Lake and brook water	250	100-400
Sand	2000	200-3000
Moraine gravel	3000	40-10000
Ridge gravel	15000	30-30000
Solid granite	25000	10000-50000
Ice	100000	10000-100000

Table 3.3: Reference resistivity values of various materials (Roger et al., 2004) [57]

Formation	Electrical Resistivity Range
Sea water	0.1–0.3
Salted water	0.3–0.9
Brackish water	0.9–5
Leachate	0.9–5
Scrap Metal	1-12
Garbage	12-30
Fresh water	10–80
Debris and Dump Soil	50-350
Clay	5–30
Wet sand	20–150
Sandstone	30–300
Limestone	100–800
Dry sand	250–4000
Granite	1000–20,000

On the basis of data presented in Table 3.2 and Table 3.3, a comparison between the standard values and modeled values was carried out to detect possible contamination.

3.6.2 Microtremor Data Processing and Analysis:

The analysis was performed using the GeoSiG software for microtremor. Five sensors were fixed on different positions @ 20m each, covering 80m of free field near the surface. After taking the observation with the help of microtremor, the time domain velocity data was converted into to frequency domain data and natural frequency.

3.6.3 Analysis of Borehole Water Samples

Electrical Conductivity (EC) is the opposite of Electrical Resistivity. The main aim of this thesis was to find out the probable ground water contamination by using the ERT. The purpose of collecting ground water samples and analyzing Electrical Conductivity (EC) was

to compare these with ERT results. Very low resistivity values, up to 0 to 10 Ωm , are indicative to ground water contamination. If Electrical Conductivity (EC) values of the water samples fit with the corresponding modeled resistivity values, then it justifies the ERT results.

In this study, ground water samples were collected from depths of 5m, 10m and 15m in boreholes, and were analyzed for EC in the Environmental Engineering Laboratory by using the Multiline P4 (WTW) Multimeter with logger function. Figure 3.5 shows the Multiline P4 Multimeter, and measurement of EC of groundwater samples.



Figure 3.5: Laboratory test of water samples with Multiline P4 (WTW)

Chapter 4

RESULTS AND DISCUSSION

4.1 Introduction

The main objective of this study was to assess the probable groundwater contamination at a waste dump site in Hazaribagh, Dhaka using Electrical Resistivity Tomography (ERT). To achieve this objective, 3 ERT tests were carried out in Hazaribagh. The data obtained from the ERT tests were analyzed using the software RES2DINV. This Chapter presents the analysis of ERT data, analysis of microtremor data, a comparison between the soil profile generated by ERT and microtremor. This Chapter also presents the EC values of groundwater samples collected as a part of this study, and compares the EC values with the ERT data and resistivity model developed using RES2DINV.

4.2 Data and Model Set Up of ERT

4.2.1 Reference Resistivity

After the field measurements, the resistance values obtained from ERT tests were reduced to apparent resistivity values. All commercial multi-electrode systems come with the computer software to carry out this conversion. The assessment for ground water pollution will be done by comparing the different resistivity values of the different layers of the models comparing to the standard resistivity values of different contaminants. Table 3.2 and Table 3.3 in Chapter 3 show the reference resistivity values table of various materials.

4.2.2 Data File Operations and Data Format

The collected data using the PASI-16GN were in text format. To read these data in RES2DINV, the text formatted data was imported as PASI text format. The RES2DINV reads the data in PASI text format. Figure 4.1 shows the RES2DINV software interface for data file operation and data format.

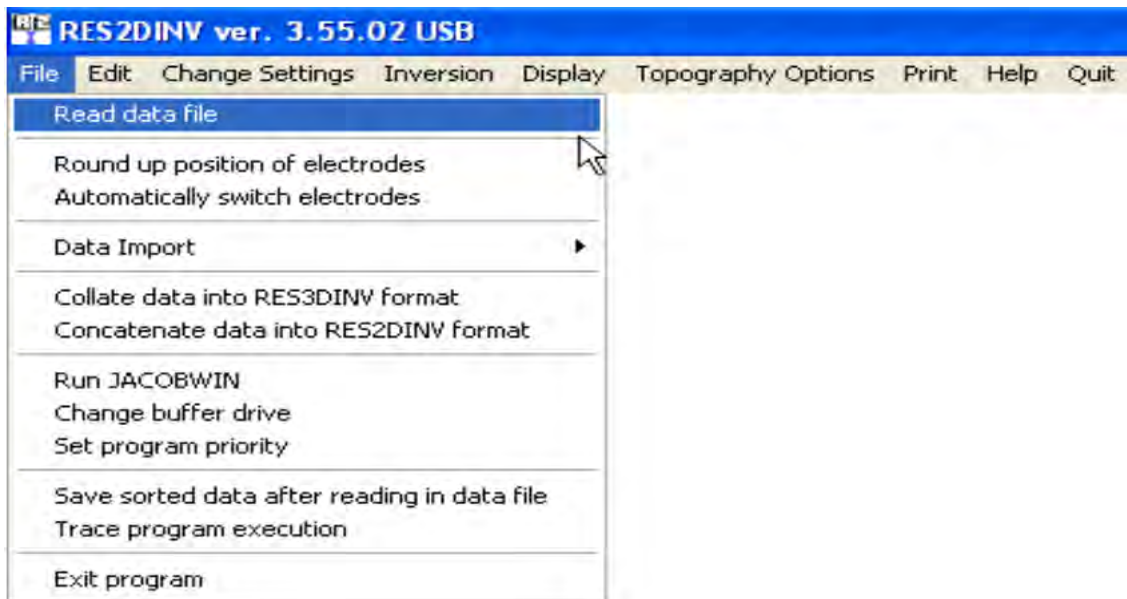


Figure 4.1: RES2DINV software interface for data file operation and data format.

4.2.3 Editing the Data

This option enables to make some changes to the data that have read from the input data file described in Section 4.2.2. It enables to remove bad data points, and to select a portion of the data set to invert for very large data sets. When this option is selected, the following submenu (Figure 4.2) will be displayed as follows:

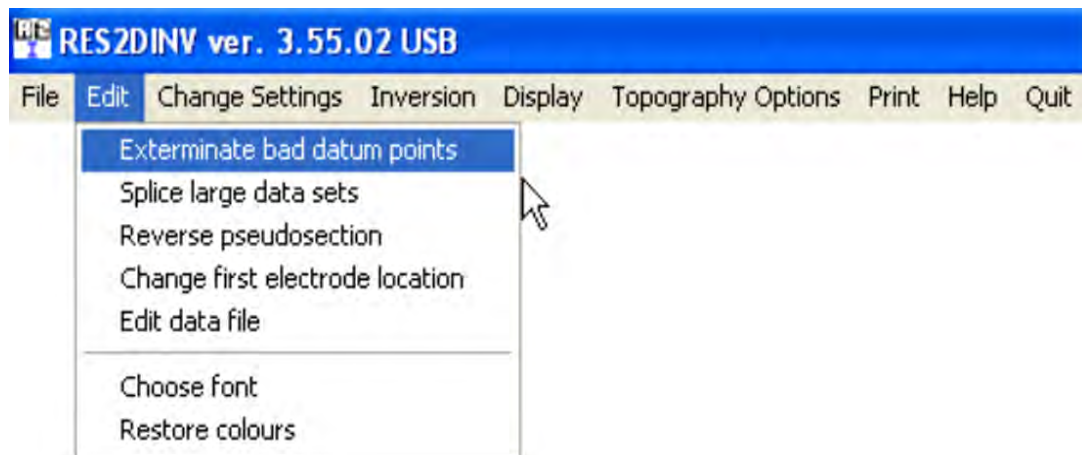


Figure 4.2: RES2DINV software interface for editing data

Exterminate bad datum points: In this option, the apparent resistivity data values are displayed in the form of profiles for each data level. User can use the mouse to remove any bad data point. The main purpose of this option is to remove data points that have resistivity values that are clearly wrong. Such bad data points could be due to the failure of the relays at one of the electrodes, poor electrode ground contact due to dry soil, or shorting across the cables due to very wet ground conditions. These bad data points usually have apparent

resistivity values that are obviously too large or too small compared to the neighboring data points. The best way to handle such bad points is to drop them so that they do not influence the model obtained. Figure 4.3 shows the ERT1 data set with a few bad data points. The bad data points were removed by moving the cross-shaped cursor with the mouse to the data point and left clicking the mouse button. The colour of the data point should change from black to purple. If the user clicks the same data point again, it will not be removed from the data set.

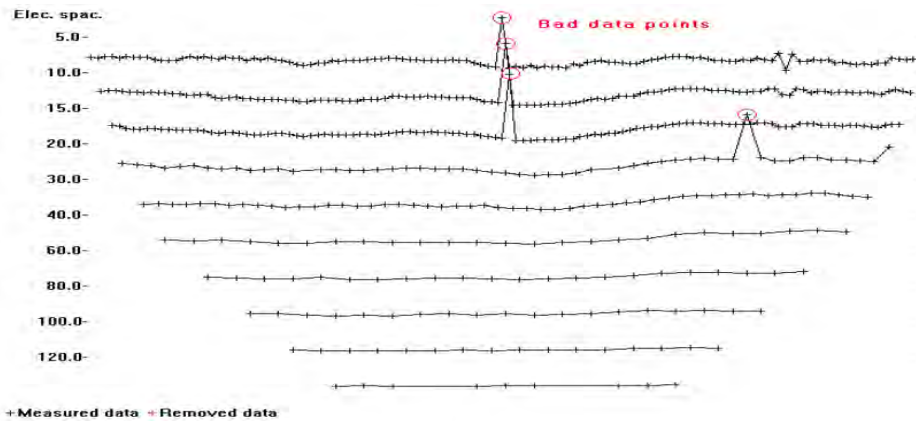


Figure 4.3: Example of ERT1 data set with a few bad data points. The data is displayed using the "Exterminate bad data points" option.

To get a good resistivity model from the ERT test data, the data must be of equally good quality. Bad data points fall into two broad categories, i.e. “systematic” and “random” noise. Systematic noise is usually caused by some sort of failure during the survey such that the reading does not represent a true resistivity measurement. Systematic noise is fairly easy to detect in a data set as it is usually present in limited number of readings, and the bad values usually stick out like sore thumbs. Random noise includes effects such telluric currents that affects all the readings, and the noise can cause the readings to be lower or higher than the equivalent noise-free readings. This noise is usually more common with arrays such as the dipole-dipole and pole-dipole that have very large geometric factors, and thus very small potentials for the same current compared to other arrays such as the Wenner. It is also common with the pole-pole array due to the large distance between the P1 electrode and the remote (and fixed) P2 electrode. This array tends to pick up a large amount of telluric noise due to the large distance between the two potential electrodes.

Splice large data set: This option enables to choose a section of the full data set (which is too large to be processed at a single time) to invert. After choosing this option, the distribution of the data points in a pseudosection will be displayed. One can select a section of the data set to invert by using the arrow keys.

Reverse pseudosection: This option flips the pseudosection horizontally from left to right. This is helpful when you have parallel survey lines but the surveys were started from different ends.

Change location of first electrode: This allows changing the location of the first electrode in the survey line. It is basically intended for plotting purposes, so that overlapping survey lines have the same x-locations for electrodes that coincide.

Edit data file: When selecting this option, the text editor (by default NOTEPAD) will start up. To return to the RES2DINV program, user must first exit from the text editor program.

4.2.4 Changing the Program Settings

The program has a set of predefined settings for the damping factors and other variables that generally give satisfactory results for most data sets. However, in some situations, modification of the parameters that control the inversion process gives the better result. When selecting the "Change Settings" option, the following list of menu options is displayed as follows:

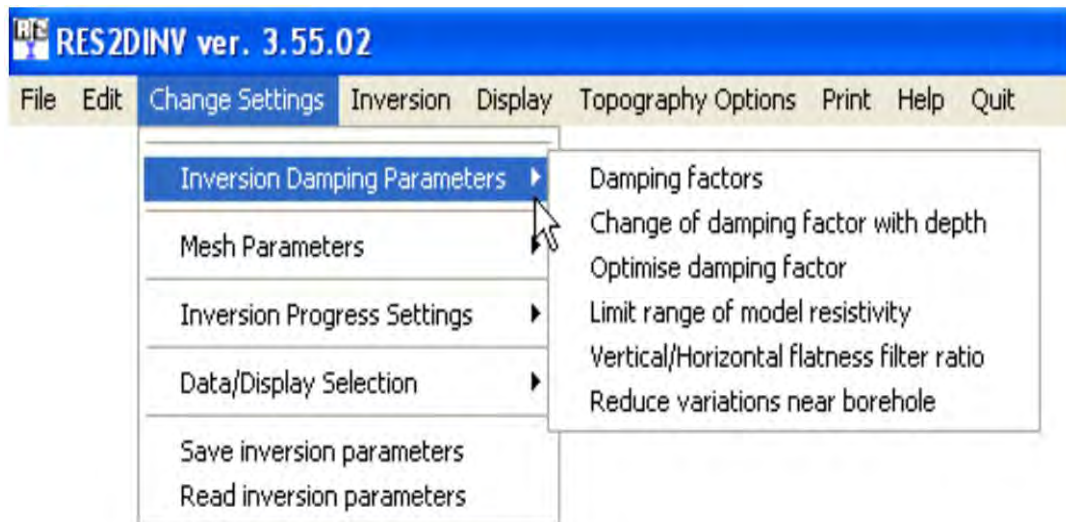


Figure 4.4: RES2DINV software interface for change settings

Inversion Damping Parameters:

The inversion routine used by the program is based on the smoothness-constrained least-squares method (deGroot-Hedlin and Constable, 1990). The smoothness-constrained least-squares method is based on the following equation-

$$(J^T J + uF) d = J^T g \quad (2.8)$$

Where, $F = f_x f_x^T + f_z f_z^T$

f_x = horizontal flatness filter

f_z = vertical flatness filter

J = matrix of partial derivatives

u = damping factor

d = model perturbation vector

g = discrepancy vector

The following options modify the use of the damping factor u in equation (2.8)-

Damping factors: In this option, the initial value for the damping factor in equation (2.8), as well as the minimum damping factor has been set. If the data set is very noisy, a relatively larger damping factor (for example 0.3) should be used. If the data set is less noisy, a smaller initial damping factor (for example 0.1) is convenient. The inversion subroutine will generally reduce the damping factor in equation (2.8) after each iteration. However, a minimum limit for the damping factor must be set to stabilize the inversion process. The minimum value should usually set to about one-fifth the value of the initial damping factor.

Change of damping factor with depth: Since the resolution of the resistivity method decreases exponentially with depth, the damping factor used in the inversion least-squares method is normally also increased with each deeper layer. This is done in order to stabilize the inversion process. Normally, the damping factor is increased by 1.05 times with each deeper layer, but it is changeable based on judgement. A larger value should be used if the model shows unnatural oscillations in the resistivity values in the lower sections. This will help to suppress the oscillations. User can also select the choice to allow the program to determine the value to increase the damping factor with depth automatically. This might be a good choice if the thickness of the layers is much thinner than the default values, for example if the unit electrode spacing is reduced by half in the data file in order to produce a model with smaller model blocks.

Optimize damping factor: the program will attempt to find the optimum damping factor u in equation (2.8) that gives the lowest RMS error in each iteration. By optimizing the damping factor, the number of iterations the program requires to converge can be significantly reduced. However, the time taken per iteration will be increased. For small to medium size data sets, this can significantly reduce the overall computer time needed to invert the data set. For very large data sets with more than 1000 data points, the time taken in each iteration could be significantly increased as it is necessary to solve the least-squares equation more than once per iteration.

Limit range of model resistivity: When selecting this option, the following (Figure 4.5) dialog box opened-

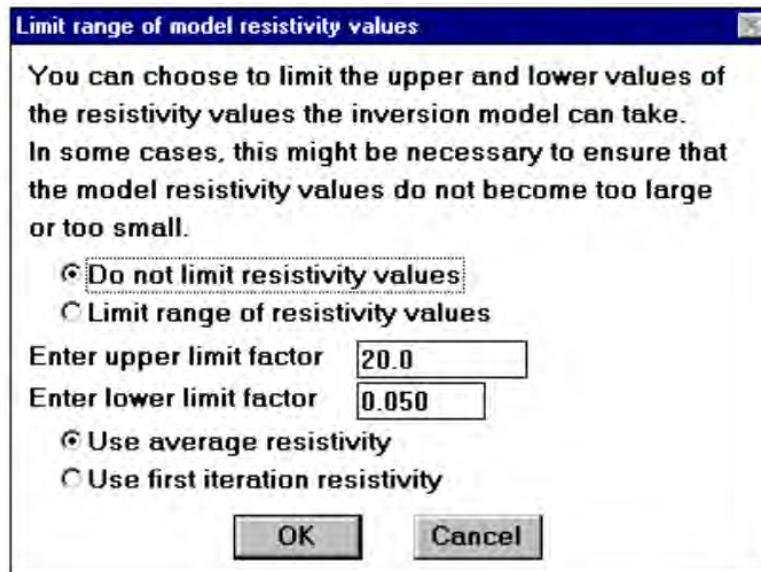


Figure 4.5: RES2DINV software interface for limit range of resistivity values.

This option allows limiting the range of resistivity values that the inversion subroutine will give. In the Figure 4.5, the upper limit for is 20 times the average model resistivity value for the previous iteration while the lower limit is 0.05 times (i.e. 1/20 times). The program uses “soft” limits that allow the actual resistivity model values to exceed the limits to a certain degree. However, this option will avoid extremely small or large model resistivity values that are physically unrealistic.

Vertical to horizontal flatness filter ratio: The ratio of the damping factor has been used for the vertical flatness filter (f_z) to the horizontal flatness filter (f_x). By default, the same damping factor is used for both.

Mesh Parameters

These set of options change the finite-difference or finite-element mesh used in the forward modeling subroutine. Figure 4.6 shows the RES2DINV software interface for mesh parameters under change settings menu.

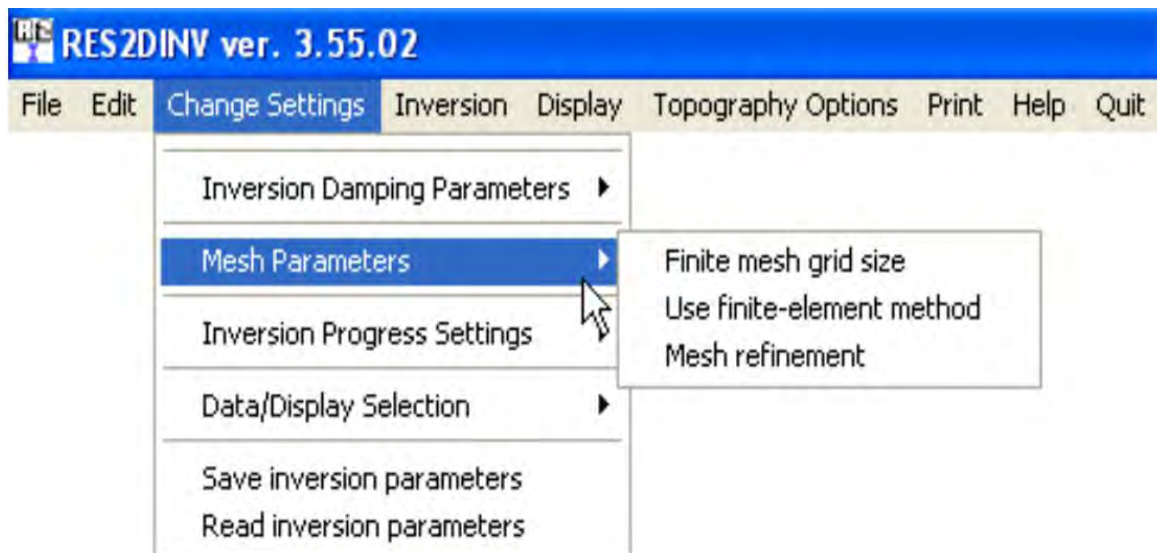


Figure 4.6: RES2DINV software interface for mesh parameters under change settings menu.

Finite mesh grid size: There's an option to choose a mesh grid used by the forward modelling program to have 2 or 4 nodes between adjacent electrodes. With 4 nodes per electrode spacing, the calculated apparent resistivity values would be more accurate (particularly for large resistivity contrasts). By default, the program will use the 2 nodes option if the data set involves more than 90 electrodes.

Use finite-element method: This option allows to use either the finite difference or finite-element method to calculate the apparent resistivity values. By default, the program will use the finite-difference method, which is faster, if the data set does not contain topography. If the data set contains topography, the default choice is the finite-element method. As in this research finite different method has been used.

Mesh refinement: This option allows to use a finer mesh (in the vertical direction) for the finite-difference or finite-element method. The apparent resistivity values calculated by either method will be more accurate with a finer mesh. The use of a finer mesh can give better results for cases where subsurface resistivity contrasts of greater than 20:1 is expected. This is particularly useful in areas where a low resistivity layer lies below a high resistivity layer.

Inversion Progress Settings

The following set of options (Figure 4.7) control the path the inversion subroutine takes during the inversion of a data set.

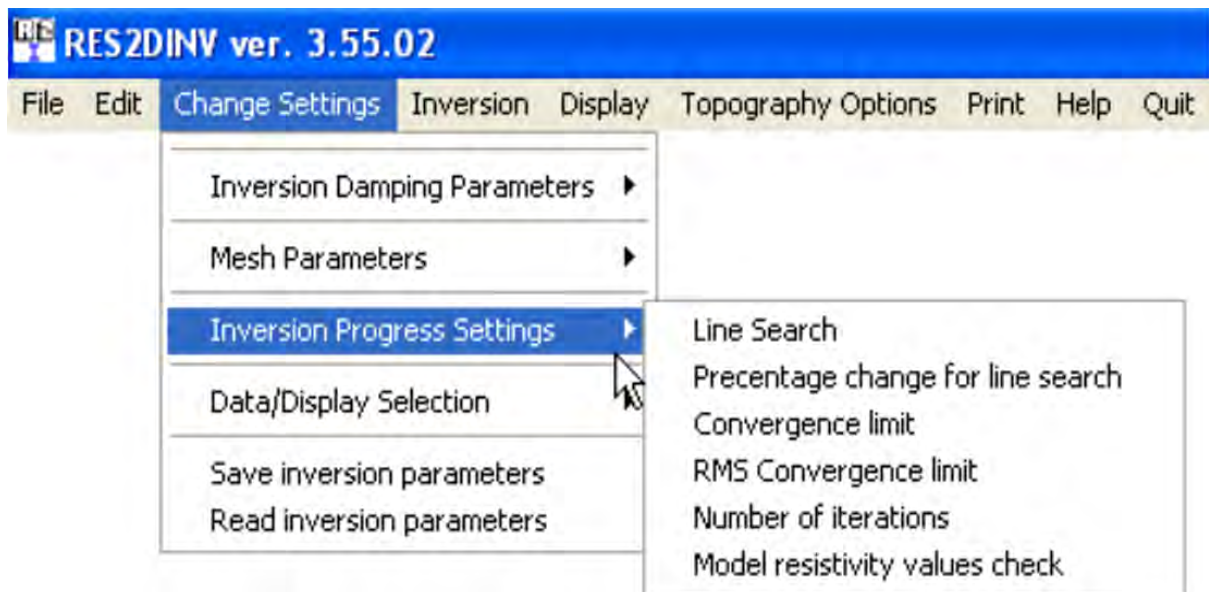


Figure 4.7: RES2DINV software interface of inversion progress settings under change settings menu.

Line search: The inversion routine determines the change in the model parameters by solving equation (2.8). Normally the parameter change vector d will result in a model with a lower RMS error. In the event that the RMS error increases, there's two options. One option is to perform a line search using quartic interpolation to find the optimum step size for the change in the resistivity of the model blocks. The program will attempt to reduce the RMS error, but it can also be trapped in a local minimum. The alternative is to ignore the increase in the RMS error, and hope that the next iteration will lead to a smaller RMS error. This might enable to jump out of a local minimum, but it could also lead a further increase in the RMS error. A third alternative is to perform a line search at each iteration. This will usually give the optimum step size, but will require at least one forward computation per iteration. In some cases, the extra forward computations could be worthwhile if it reduces the number of iterations needed to bring the RMS error down to an acceptable level. For the first two iterations, where the largest changes in the RMS error usually occurs, the program will always carry out a line search to find the optimum step size to further reduce the RMS error.

Percentage change for line search: The line search method used can estimate the expected change in the apparent resistivity RMS error. If the expected change in the RMS error is too small, it might not be worthwhile to proceed with the line search to determine the optimum step size for the model parameter change vector. A value between 0.1 and 1.0 % has been used for the ERT analysis of this thesis.

Convergence limit: This sets the lower limit for the relative change in the RMS error between 2 iterations. By default, a value of 5% is used. In this program the relative change in

the RMS error, rather than an absolute RMS value, is used to accommodate different data sets with different degrees of noise present.

RMS convergence limit: This sets the percentage RMS error in the inversion of the apparent resistivity data where the program will stop after the model produce has an RMS error less than this limit. Normally a value of between 5% and 10% should be used, depending on the quality of the data.

Number of iterations: This allows setting the maximum number of iterations for the inversion routine. By default, the maximum number of iterations is set to 5. There's also option to change the iteration number.

Model resistivity values check: The program will display a warning if after an iteration in the inversion of the data set, a model resistivity value becomes too large (more than 20 times the maximum apparent resistivity value) or too small (less than 1/20 the minimum apparent resistivity value). This option allows disabling the warning.

Data/Display Selection

This section has minor options for pre-processing of data files and display of the sections during the inversion. Figure 4.8 shows the data/display option under the change settings menu.

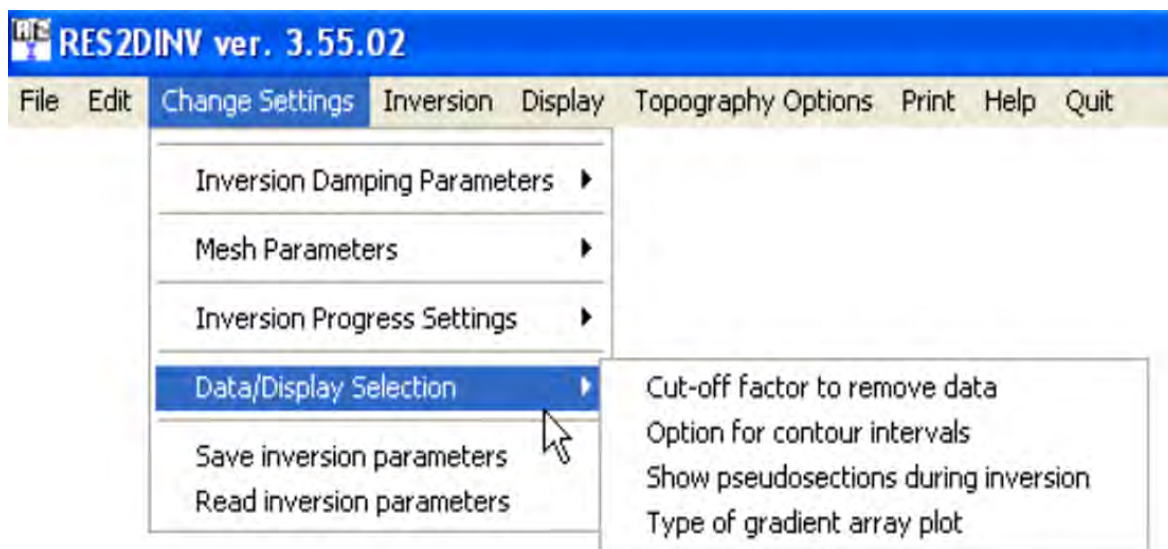


Figure 4.8: RES2DINV software interface of data/display selection under change settings menu.

Cutoff limit for borehole resistance readings: In cross-borehole measurements, certain combinations of the current and potential electrodes could result in extremely low potential values. This could result in readings with very low signal to noise ratios. To filter out such

potentially noisy readings, the program estimates the potential per a unit input current that would be measured by each electrode configuration used in the data set. If the estimated potential falls below a certain limit, compared with the combination that gives the maximum potential, the reading is rejected. For example, if the user chooses a value of 0.001, this means configurations that will result in potential values that are a thousand times smaller than the maximum potential measured will be rejected. Normally a value of between 0.008 and 0.0007 is used. The program also allows entering the measurements as resistance values, and carrying out the inversion with the resistance (rather than apparent resistivity) values. In this case, the cutoff limit option is not used.

Option for contour intervals: By default, the program has used logarithmic contour intervals for the pseudo-sections and model sections when displaying the results in the “Inversion” option in the Main Menu. This is usually the best choice for most data sets. However, there’s option to choose to use the linear or the user defined contour intervals.

Show pseudo-sections during inversion: There’s option to choose between to display the pseudo-sections during the data inversion, or just display the model RMS values.

Save inversion parameters: This option saves the inversion parameters into a file RES2DINV.IVP.

Read inversion parameters: This option reads back the parameters stored in the RES2DINV.IVP files and uses them in the program. RES2DINV_NEW.IVP is an example file that contains more inversion parameters.

4.2.5 Inversion options

This option enables to carry out the inversion of the data set that had read in using the "File" option. It also displays the arrangement of the blocks used by the inversion model, as well as to change some of the parameters that control the inversion process. On selecting this option, the following menu (Figure 4.9) will be displayed.

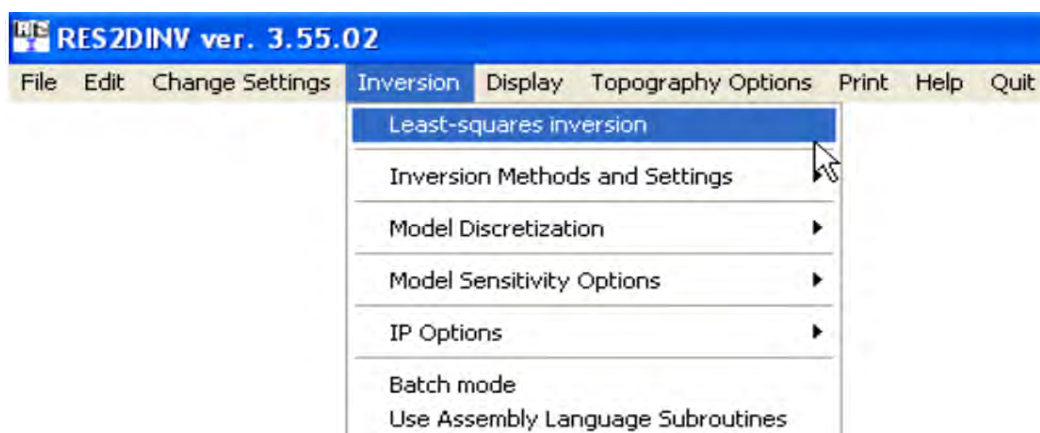


Figure 4.9: RES2DINV software interface of Inversion in the menu bar.

Least-squares inversion

This option will start the least-squares inversion routine. It will be asked for the name of the output data file in which to store the results, and the contour intervals for the pseudo-sections if the user had chosen the user defined option for the contour intervals.

Inversion Methods and Settings

These set of options (Figure 4.10) allow selecting the type of regularized inversion method to use.

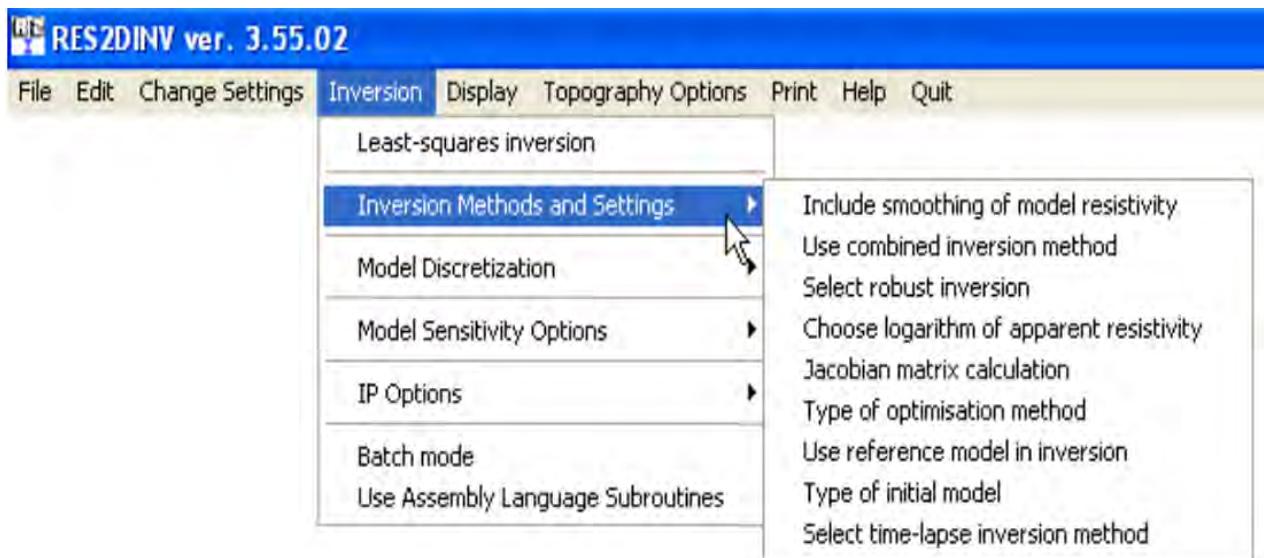


Figure 4.10: RES2DINV software interface of inversion methods and settings under the inversion menu

Include smoothing of model resistivity values: The least-squares formulation used in equation (2.8) applies a smoothness constraint on the model perturbation vector d only, and not directly on the model resistivity values. In most cases, it will produce a model with a reasonably smooth variation in the resistivity values. In some cases, particularly for very noisy data sets, better results might be obtained by applying a smoothness constraint on the model resistivity values as well. The resulting least-squares equation is given by-

$$(J^T J + uF) d = J^T g - uFr \quad (2.9)$$

where r is a vector containing the logarithm of the model resistivity values. While for the same damping factors this will usually produce a model with a larger apparent resistivity RMS error, this modification will ensure that the resulting model shows a smooth variation in the resistivity values.

Use combined inversion method: This option is intended for use in unusual situations where the data sensitivity values of the model blocks are significantly distorted by large resistivity variations. In some situations, such as a survey over a very low resistivity body, the current

paths could be distorted such that parts of the subsurface are not well mapped and have very low data sensitivity values in the inversion model. This could lead to large distortions just below the low resistivity body. By combining the ridge regression and smoothness-constrained inversion methods, the distortions in some cases might be reduced. This option should be used as a last resort if everything else fails! However, it has been found that this method is unstable when the data contains noise if a model with a relatively large number of model parameters is used.

Select robust inversion: This allows selecting the robust or blocky inversion method. It should be used when sharp boundaries are expected to be present.

Choose logarithm of apparent resistivity: By default, the program used the logarithm of the apparent resistivity values as the data parameter when carrying out the inversion. For most cases, this gives the best results. In some cases, for example with negative or zero apparent resistivity, this is not possible. This option enables the apparent resistivity value by itself to be used for such situations.

Jacobian matrix calculation: In this program there's three options in the calculation of the Jacobian Matrix J in equation (2.8). The fastest method is to use the quasi-Newton method to estimate the Jacobian matrix. A third alternative is to recalculate the Jacobian matrix for the first 2 iterations only, and use the quasi-Newton updating method for subsequent iterations. The largest changes in the Jacobian matrix usually occur in the first few iterations. So in many cases, a limited recalculation of the Jacobian matrix gives the best compromise between speed and accuracy. By default, the program will choose the limited recalculation option for the Jacobian matrix.

Type of optimization method: This option allows choosing two different methods to solve the least-squares equation (2.8). On selecting this menu option, the following dialog box (Figure 4.11) is shown.

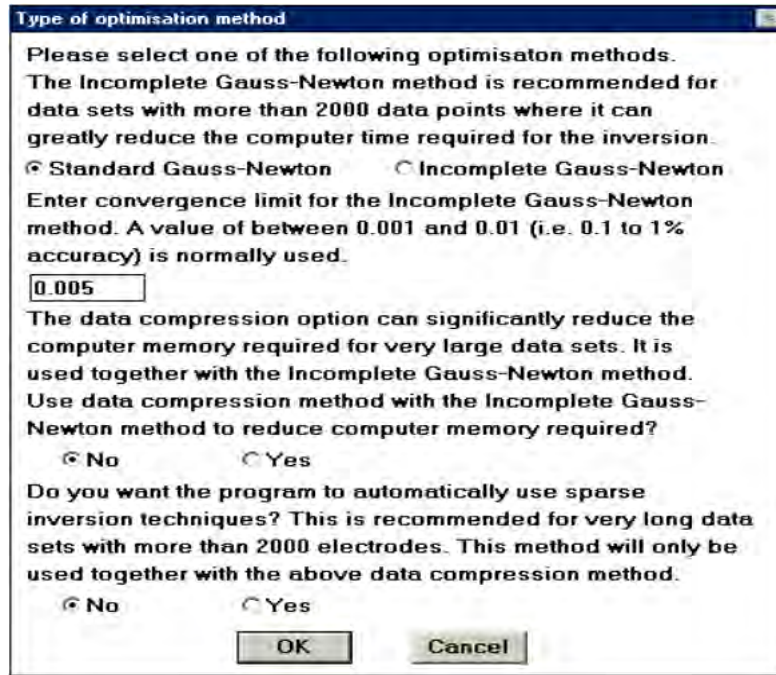


Figure 4.11: RES2DINV software interface of type of optimization method under the inversion methods and settings

By default, the program uses the „Standard Gauss-Newton“ least-squares method, particularly if the number of data points and/or model cells is small (less than a few thousand), where an exact solution of the least-squares equation is calculated. If the number of data points and/or model cells is large (more than 2000), the time taken to solve the least-squares equation could be the most time-consuming part of the inversion process. To reduce the inversion time, an alternative method that calculates an approximate solution of the least squares equation using the „Incomplete Gauss-Newton“ method can be used. The user can set the accuracy of the solution. For most data sets, an accuracy of about 0.5% (i.e. a convergence limit of 0.005 in the above dialog box) seems to provide a solution that is almost the same as that obtained by the „Standard Gauss-Newton“ method.

Model Discretization

These options (Figure 4.12) allow modifying the way the program subdivides the subsurface into cells that is used as the inversion model.

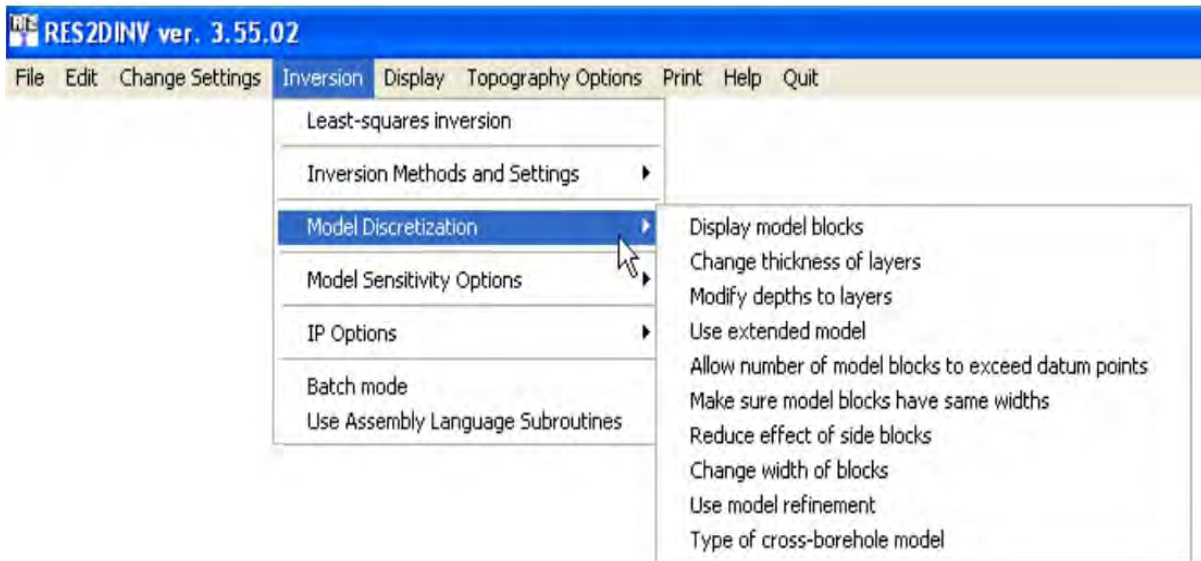


Figure 4.12: RES2DINV software interface of model discretization under the inversion menu

Display model blocks: This option displays the distribution of the model blocks and data points. The data points will be plotted at the median depth of investigation for the array used. The program has a maximum limit of 24 model layers.

Change thickness of layers: In this section there's an option to choose a model where the thickness of the layers increases by 10% or by 25% with each deeper layer. If there are only a small number (8 or less) of data levels, the 10% option fits. If there are a large number of sparse data levels, the 25% option might be better. Within this option, user can also allow the number of model blocks to exceed the number of data points. The program normally uses a model where the depth to the deepest layer does not exceed the maximum pseudo-depth in the data set. To use a model that spans a deeper depth range, the factor should be changed to increase model depth range, for e.g. from 1.0 to 1.30 to increase the model depth range by 30%.

Modify depths to layers: This option allows to change the depth of the layers used by the inversion model. Depths could be adjusted so that some of the boundaries coincide with known depths from borehole and other data.

Use extended model: This option extends the model cells to the edges of the survey line.

Allow number of model blocks to exceed datum points: By default, the program will try to arrange the position and size of the model cells such that they do not exceed the number of data points. This is probably the best option for large and medium size data sets collected with more than about 50 electrodes, particularly where the distribution of the data points with the larger spacing's is sparser. In some cases, the width of the model cells in the lower layers might be larger than those in the upper layers. However, for smaller data sets, it might be useful to relax this constrain, and allow the number of model parameters to exceed the

number of data points. This will produce a model where the interior cells in all layers have a uniform width that is equal to the smallest electrode spacing.

Make sure model blocks have same widths: This option will ensure that all the cells have the same width that is equal to the unit electrode spacing.

Reduce effect of side blocks: This option affects the calculation of the Jacobian matrix values for the model blocks located at the sides and bottom of the model section. Normally, for a block located at the side, the contributions by all the mesh elements associated with the model block are added up right to the edge of the mesh. This gives a greater weight to the side block compared to the interior blocks. In some cases, particularly when the robust inversion option is used, this can result in unusually a high or low resistivity value for the side block. This option leaves out the contribution of the mesh elements outside the limits of the survey line to the Jacobian matrix values for the side blocks.

Change width of blocks: This option allows the user to force the program to use model cells which are wider than one-unit electrode spacing for all the layers.

Model refinement: The RES2DINV program by default uses a model where the width of the interior model cells is the same as the unit electrode spacing. This works well in most cases. In some situations, particularly where there are large resistivity variations near the ground surface, better results can be obtained by using narrower model cells. There are two possible ways to reduce the width of the model cells. The first is by using the “Use model refinement” option on the „Inversion” menu. Clicking this option will show the following dialog box (Figure 4.13). This allows to choose model cells with widths of half the unit electrode spacing. In almost all cases, it gives the optimum results.

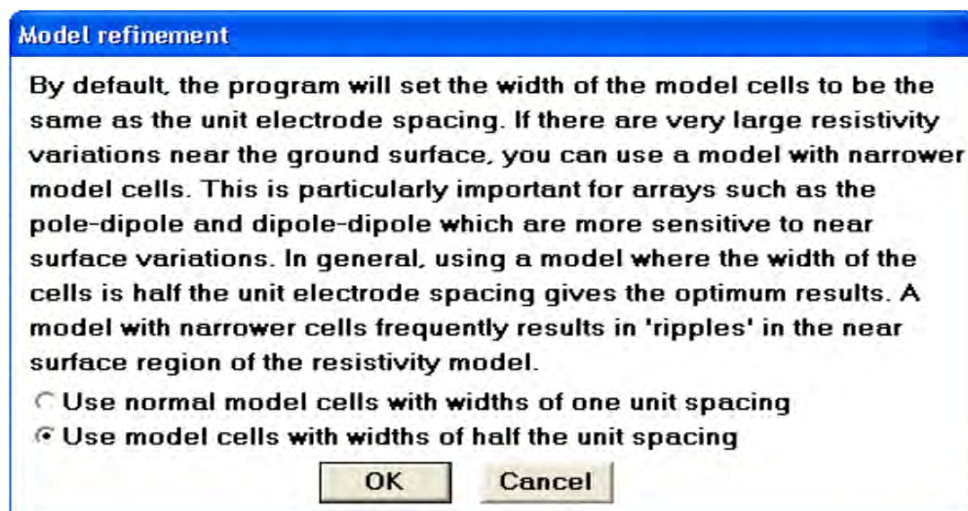


Figure 4.13: RES2DINV software interface of model refinement

Model Sensitivity Options

Figure 4.14 shows the RES2DINV software interface of model sensitivity options.

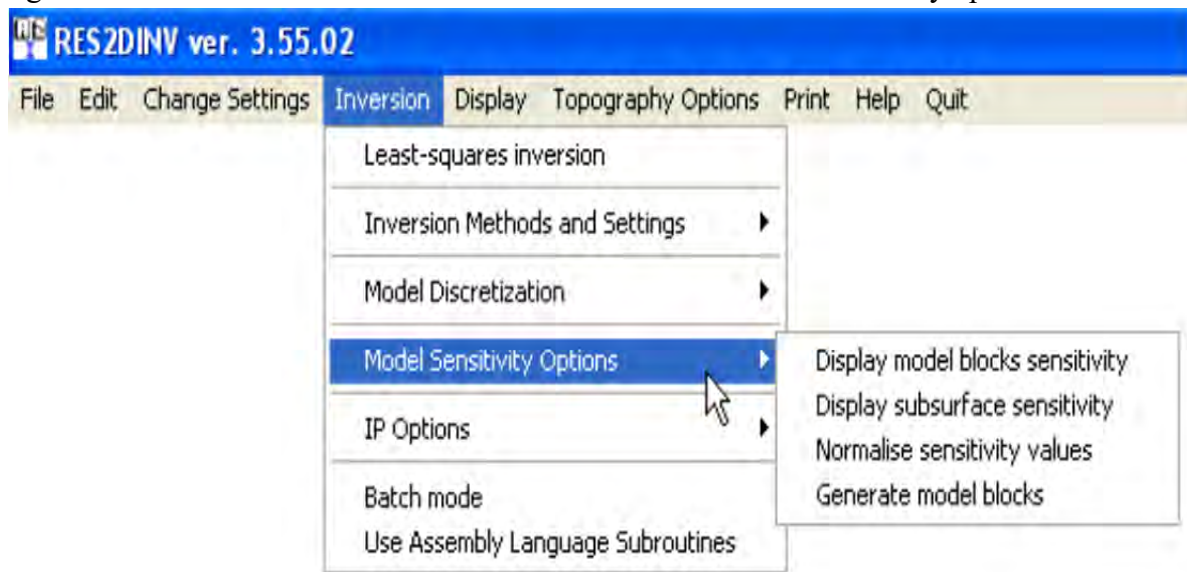


Figure 4.14: RES2DINV software interface of model sensitivity options.

Display blocks sensitivity: It shows a plot of the sensitivity of the blocks used in the inversion model. The sensitivity value is a measure of the amount of information about the resistivity of a model block contained in the measured data set. The higher the sensitivity value, the more reliable is the model resistivity value. In general, the blocks near the surface usually have higher sensitivity values because the sensitivity function has very large values near the electrodes. The blocks at the sides and bottom also have high sensitivity values due to the much larger size of these blocks that are extended to the edges of the finite-difference or finite-element mesh.

Display subsurface sensitivity: It shows a plot of the sensitivity of the subsurface for blocks of equal size. This basically eliminates the effect of changes in the model block size so that it shows more clearly the change of the subsurface sensitivity with depth and location.

Normalize sensitivity values: By default, the calculated sensitivity values are normalized by dividing with the average sensitivity value. In this option, the user can choose not to normalize the sensitivity values.

Generate model blocks: This option generates the model cells by making use of the model sensitivity values.

4.2.6 Displaying Inversion Results

In this option, user can read in a data file or the output file produced by the inversion subroutine and displays the measured and calculated apparent resistivity pseudo-sections and the model section. Within this option, the user can change the contour interval used for

drawing the pseudo and model sections, the vertical scale of the sections, and include topography in the model section. Also the color scheme used by the program is changeable. Figure 4.15 shows the display section window interface of RES2DINV.

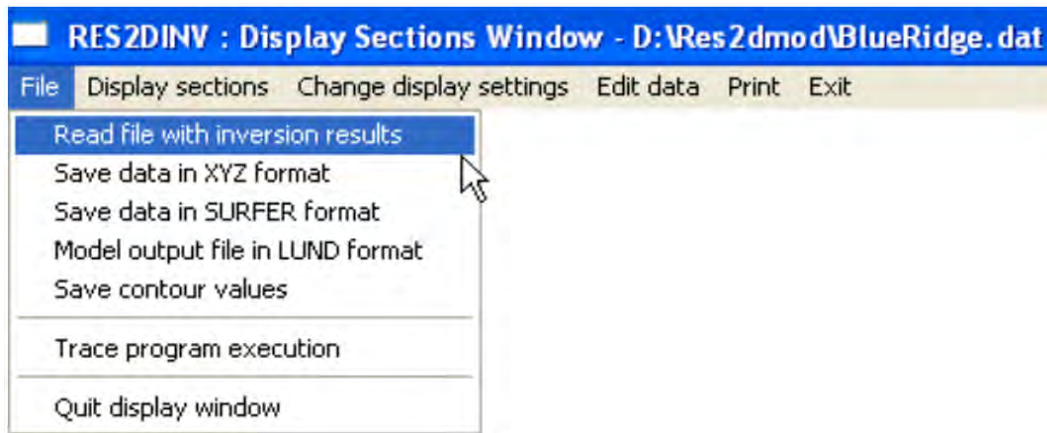


Figure 4.15: Display section window interface of RES2DINV

Read data file with inversion results: Read in the output data file produced by the inversion subroutine or an input data file.

Save data in XYZ format: It is possible to save the inversion results into a disc file with a format used by many contouring programs, such as Geosoft.

Save data in SURFER format: This section helps to save the data and model sections in SURFER format.

4.3 Analysis of ERT Data

Primary data collected from the ERT tests carried out at the Hazaribagh field sites were processed through a 2-D inverse method, using the program RES2DINV. This Section presents the resistivity models based on the three ERT tests, and identifies the locations of contaminated groundwater based on the resistivity models. The relationship between the “apparent” resistivity and the “true” resistivity is a complex relationship. To determine the true subsurface resistivity, an inversion of the measured apparent resistivity values using RES2DINV has been carried out. The validity of these inversion results is supported by the low RMS error.

The RMSE is the square root of the variance of the residuals. It indicates the absolute fit of the model to the data—how close the observed data points are to the model’s predicted values. Whereas R-squared is a relative measure of fit, RMSE is an absolute measure of fit. As the square root of a variance, RMSE can be interpreted as the standard deviation of the unexplained variance, and has the useful property of being in the same units as the response variable. Lower values of RMSE indicate better fit. RMSE is a good measure of how

accurately the model predicts the response, and it is the most important criterion for fit if the main purpose of the model is prediction.

The electrical resistivity of the ground is related to the soils type and its degree of water saturation. Most commonly, resistivity profiling is used to develop a pseudo cross-section of the ground to show the arrangement of strata and groundwater. Where the properties of these change, for example where groundwater becomes contaminated or where strata are faulted against each other, resistivity profiles will reveal the change.

(A) Test Point-01 (ERT1):

Figure 4.16 shows the raw model of, ERT1 test carried out at Hazaribagh generated by using the program RES2DINV.

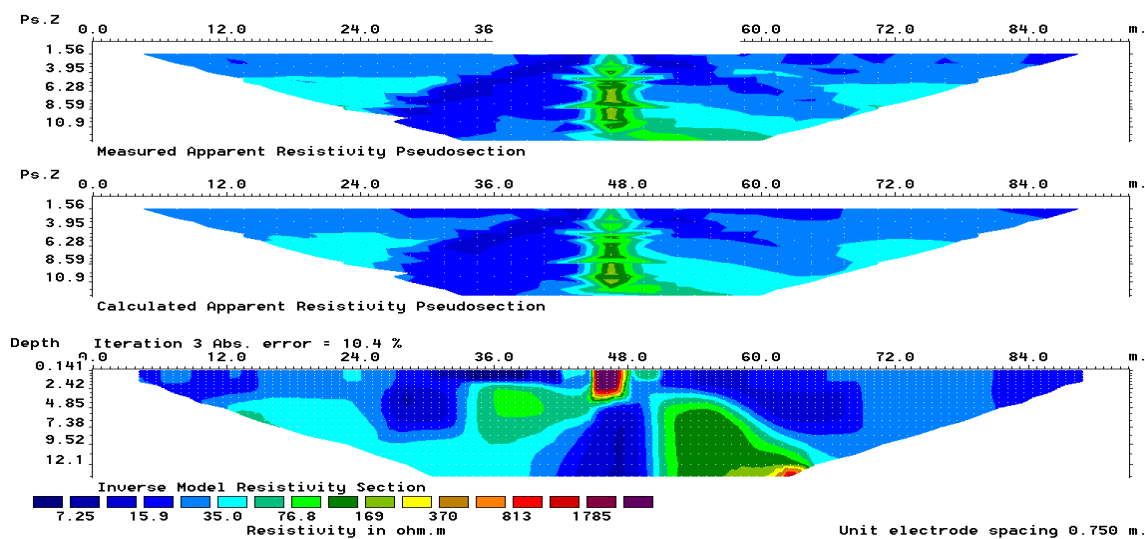


Figure 4.16: Raw resistivity model of ERT1 generated by the program RES2DINV.

The apparent resistivity is the measured electrical resistivity between two points on the Earth's surface, which corresponds to the sensitivity the ground would have if it were homogeneous. In actual occasions, homogeneous soil rarely exists and the result of measurement usually obtained is apparent resistivity. Voltage depends on current and resistance. Depth of current penetration is higher/lower when the lower layer is lower/higher resistivity. Apparent Resistivity is determined from Ohm's law using the potential difference (voltage) between two electrodes for a known current.

Electrical resistivity data is acquired by placing a series of electrodes along the profile of interest. By applying current to successive pairs of electrodes it is possible to generate a profile of data representing the selected depth. Computerized inversion of the data allows a cross-section/ pseudosection model of the ground beneath the profile to be generated. The RES2DINV provides a two-dimensional depth section or modeled pseudosection across a survey area or feature as opposed to a map which is produced by an earth resistance survey.

The apparent resistivity value can be seen as a weighted average of the different resistivity the injected current is flowing through. The area of current penetration is not exactly known since it depends on the underground resistivity distribution, but it is in the general area under the four electrodes. It is the job of the inversion process to calculate the true resistivity distribution under the electrodes as accurately as possible.

Since apparent resistivity isn't actually a physical measurement of a value in a known location, the raw data will look distorted if plotted in a cross-section. Without an inversion software, results are very difficult to evaluate. This is where inversion modeling comes in. The job of an inversion model is to calculate the "true resistivity" distribution from all apparent resistivity. The result is a structured model that best fits raw data. With an inversion model, the usability and ground truth comparison is improved because the result data is "true resistivity". Inversion modeling is based on a statistical data set; one mistake or erroneous data point won't ruin the data. The data is oversampled by design, so any errors are omitted, and the data remains accurate within around 5% to 10% RMS error.

The inversion procedure of ERT1 is as follows:

- From the raw data set, an estimate of what the ground might look like is created based on the apparent resistivity. This is the start model and it is called as "measured apparent resistivity pseudosection".
- Calculates the apparent resistivity data set that would be achieved if a survey was performed on a ground that would look exactly as measured apparent resistivity pseudosection. It may be called as the synthetic data set.
- Adjusted measured apparent resistivity pseudosection model to a new earth model called "calculated apparent resistivity pseudosection" by looking at the difference between the raw data set and Synthetic Data Set-1.
- Calculate the apparent resistivity data set that would be achieved if a survey was performed on a ground which looks exactly as calculated apparent resistivity pseudosection. This data set is called Synthetic Data Set 2.
- Continue to perform steps 3 and 4 until the fit between the raw data set and the synthetic data set is minimal and the generated model is called the "inverse model resistivity section"

Inversion synthetically creates data, tests it against all the different cases of all the different geologic structures in the real data, and examines which of those many thousands of combinations matches the raw data most closely. That's where the term "inversion" comes from making a structure and then "flipping it around" to test it against the raw data.

A more accurate model of the subsurface is a two-dimensional (2-D) model where the resistivity changes in the vertical direction, as well as in the horizontal direction along the survey line. In this case, it is assumed that resistivity does not change in the direction that is

perpendicular to the survey line. However, at the present time, 2-D surveys are the most practical economic compromise between obtaining very accurate results and keeping the survey costs down.

To plot the data from a 2-D imaging survey, the pseudosection contouring method is normally used. In this case, the horizontal location of the point is placed at the mid-point of the set of electrodes used to make that measurement. The vertical location of the plotting point is placed at a distance that is proportional to the separation between the electrodes. The pseudosection gives a very approximate picture of the true subsurface resistivity distribution. The pseudosection is useful as a means to present the measured apparent resistivity values in a pictorial form, and as an initial guide for further quantitative interpretation.

In geophysical inversion, the general target is to find a model that gives a response that is similar to the actual measured values. The model is an idealized mathematical representation of a section of the earth. The model has a set of model parameters that are the physical quantities user wants to estimate from the observed data. The model response is the synthetic data that can be calculated from the mathematical relationships defining the model for a given set of model parameters. All inversion methods essentially try to determine a model for the subsurface whose response agrees with the measured data subject to certain restrictions. In the cell-based method used by the RES2DINV program, the model parameters are the resistivity values of the model cells, while the data is the measured apparent resistivity values. The mathematical link between the model parameters and the model response for the 2-D resistivity model is provided by the finite-difference or finite-element methods. In all optimization methods, an initial model is modified in an iterative manner so that the difference between the model response and the observed data values is reduced.

Figure 4.17 depicts the analyzed inversion result of ERT1, and identifies the locations of contaminated groundwater. Initially after reading the data file in RES2DINV program some inputs have been made as described in the previous section 4.2 (data and model setup for ERT). Then an inversion has been carried out. The program RES2DINV automatically generates the model of figure 4.17. The used resistivity instruments can measure resistivity up to a range of 0-1000 Ωm by penetrating current into the earth during sounding. The scenario of ground water contamination has been find out by comparing the model resistivity to the actual resistivity of various materials and contaminants.

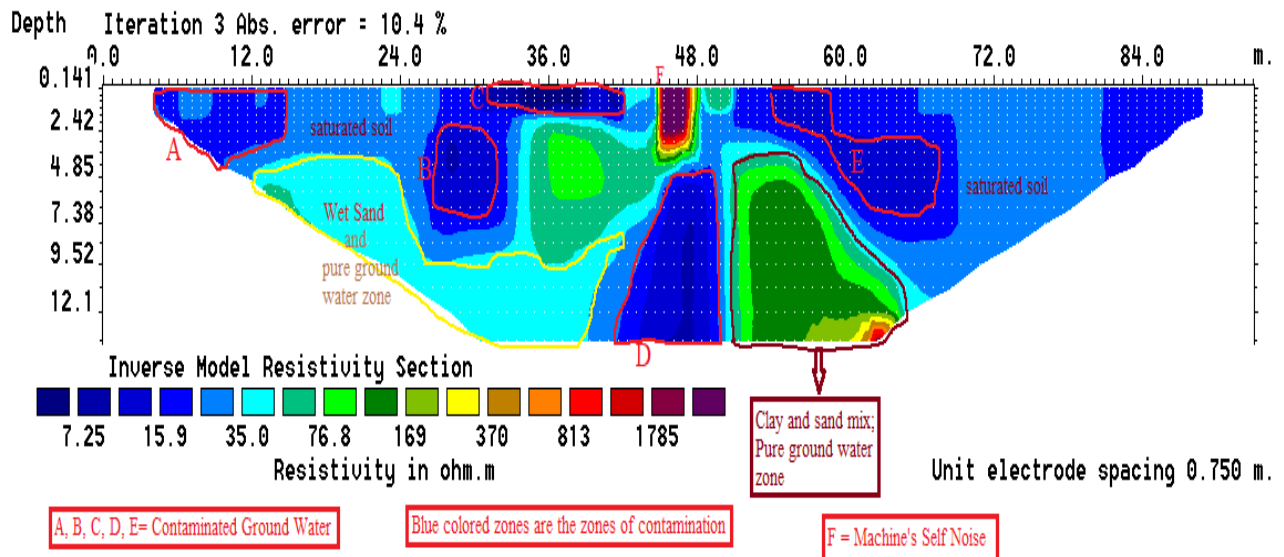


Figure 4.17: Analyzed results of ERT-1 test showing location of contaminated groundwater as well as pure groundwater zones.

Based on the results presented in Figs. 4.16 and 4.17, it appears that the subsurface below the dumpsite at the location of the test ERT-1 is characterized by low resistivity, possibly influenced by contaminants emanating from the dumps. The maximum depth penetrated by the current during the acquisition of data of ERT1 is 14m with resistivity values of contaminated layers below 5 Ωm except few cases of high resistivity in the top layer and isolated high resistivity at depth under some profiles. In the Fig. 4.17, the red marked zones A, B, C, D and E have resistivity lower than 5 Ωm . According to Loke (2004) and Roger et al. (2004), the resistivity of water contaminated with dissolved solids is less 10 Ωm (Salted water- 0.3–0.9 Ωm ; Brackish water-0.9–5 Ωm ; Leachate-0.9–5 Ωm ; 0.01 M Potassium chloride- 0.5-0.8 Ωm ; 0.01 M Sodium chloride- 0.8-1.0 Ωm ; 0.01 M acetic acid-6-7.5 Ωm). A critical look at the resistivity-depth model from ERT-1 profile shows infiltration of leachate containing high concentration of dissolved solids to the subsurface environment. Generally, the result reflects high level of impact of leachate from the decomposed materials from the dumpsite, with resistivity less than 5 Ωm up to 17 Ωm prevalent on the entire traverse. So it is very clear that zones A, B, C, D and E are highly contaminated. Blue color dominates most of the area of ERT1 which is saturated soil and mostly contaminated up to a depth of around 7m. The resistivity of these zones lies around 10 Ωm , which corresponds to the contamination range.

There is a small sky color zone beneath the blue zone which indicates a wet sand and pure ground water zone (wet sand resistivity ranges from 20 Ωm -150 Ωm , Roger et al. (2004), pure water resistivity ranges from 10 Ωm – 150 Ωm) Loke (2004). The deep green colored (resistivity ranges from 4 Ωm -300 Ωm) zone is the zone of clay and sand mix, and a pure ground water zone. The dark deep red in the middle of the surface line caused due to noise of the data acquisition machine itself. During the data acquisition by using two link box (each contains 16 electrodes) starting from both ends to middle sets up the 32 electrodes along a

single line and thus generating a significant noise when running for data acquisitions. ERT1 is very close to Buriganga River ($\approx 500\text{m}$). Water bearing zone is at a depth of approximately 5 m (BWDB) So it appears that the subsurface zone at the location of ERT1 is contaminated up to depth of 15m.

(B) Test Point-02 (ERT2):

Figure 4.18 shows the raw model of ERT2 test carried out at Hazaribagh generated by using the program RES2DINV.

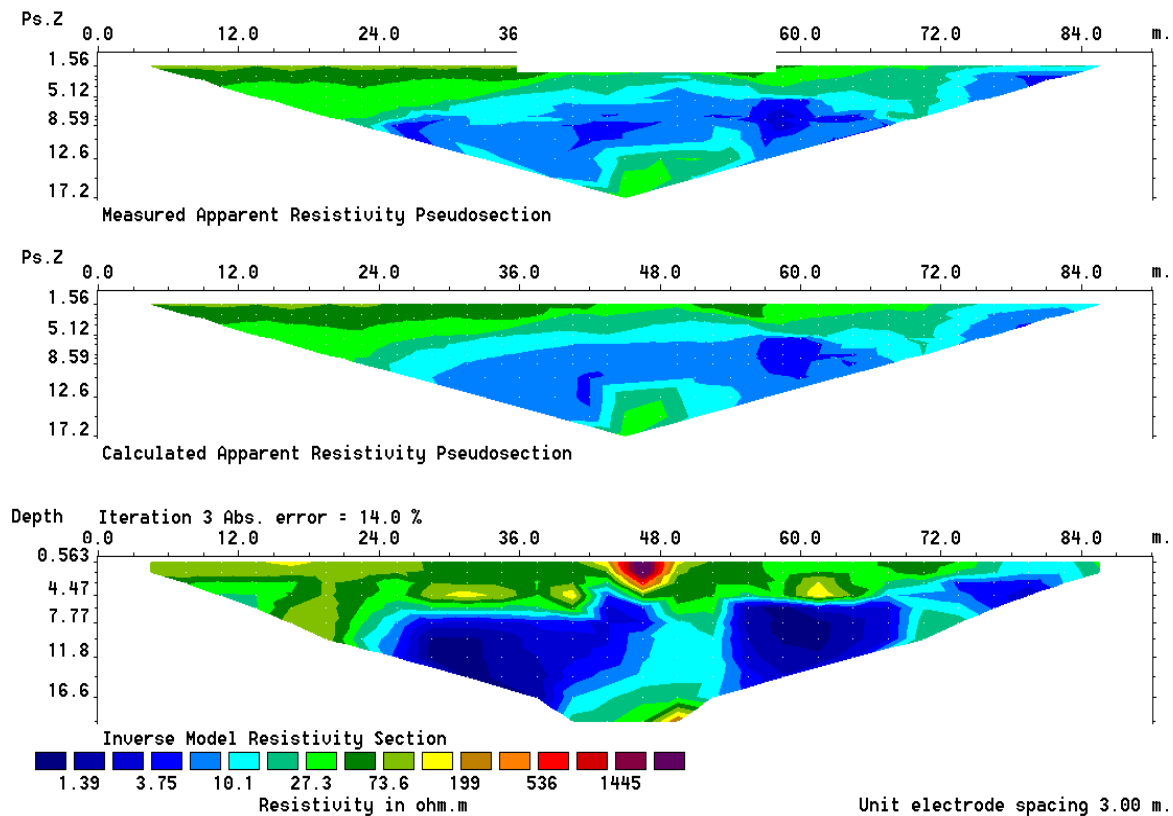


Figure 4.18: Raw resistivity model of ERT2 generated by using the program RES2DINV.

The purpose of electrical surveys is to determine the subsurface resistivity distribution by making measurements on the ground surface. From these measurements, the true resistivity of the subsurface can be estimated. The calculated resistivity value is not the true resistivity of the subsurface, but an “apparent” value that is the resistivity of a homogeneous ground that will give the same resistance value for the same electrode arrangement.

The inversion procedure of ERT2 is as follows:

- From the raw data set, an estimate of what the ground might look like is created based on the apparent resistivity. This is the start model and it is called as “measured apparent resistivity pseudosection”.

- Calculates the apparent resistivity data set that would be achieved if a survey was performed on a ground that would look exactly as measured apparent resistivity pseudosection. It may be called as the synthetic data set.
- Adjusted measured apparent resistivity pseudosection model to a new earth model called “calculated apparent resistivity pseudosection” by looking at the difference between the raw data set and Synthetic Data Set-1.
- Calculate the apparent resistivity data set that would be achieved if a survey was performed on a ground which looks exactly as calculated apparent resistivity pseudosection. This data set is called Synthetic Data Set 2.
- Continue to perform steps 3 and 4 until the fit between the raw data set and the synthetic data set is minimal and the generated model is called the “inverse model resistivity section”.

Figure 4.19 depicts the analyzed result of ERT2 and identifies the locations of contaminated groundwater. Initially after reading the data file in RES2DINV program some inputs have been made as described in the previous section 4.2 (data and model setup for ERT). Then an inversion has been carried out. The program RES2DINV automatically generates the model of figure 4.19. The used resistivity instruments can measure resistivity up to a range of 0-1000 Ωm by penetrating current into the earth during sounding. The scenario of ground water contamination has been find out by comparing the model resistivity to the actual resistivity of various materials and contaminants.

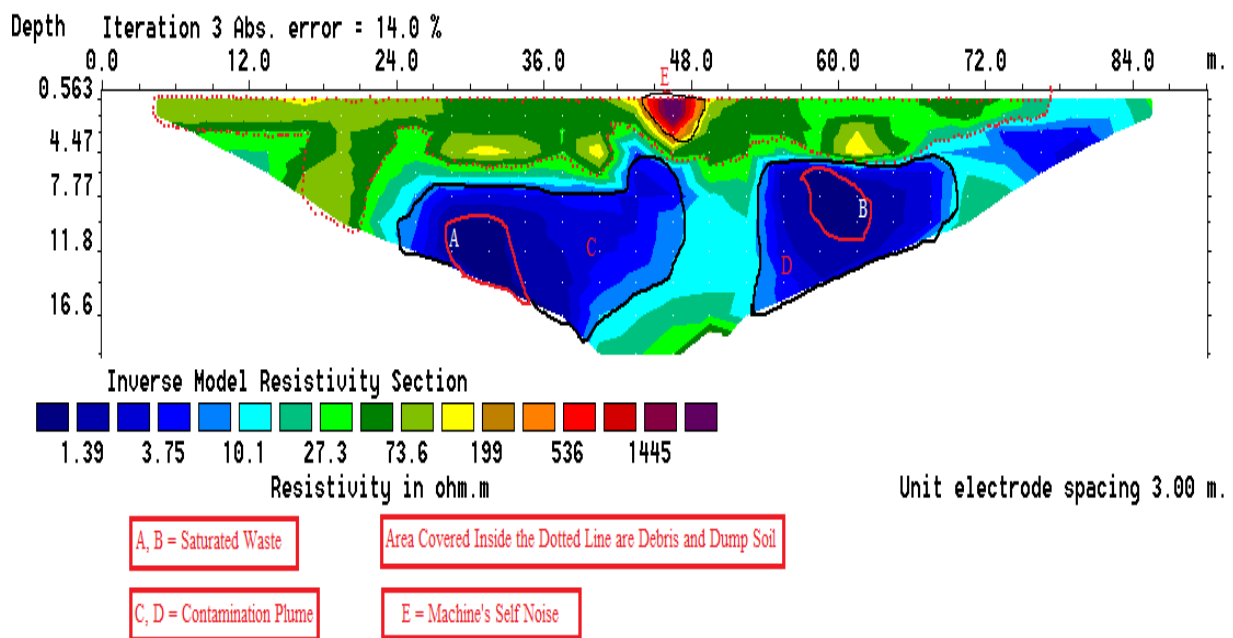


Figure 4.19: Analyzed result of ERT2 test showing location of contaminated groundwater as well as pure groundwater zones

Based on the results presented in Figs. 4.18 and 4.19, it appears that the subsurface below the dumpsite at the location of ERT-2 test is characterized by low resistivity possibly influenced

by contaminants emanating from the dumps. The maximum depth penetrated is 17 m with resistivity values of contaminated layers below 5 Ωm except some few cases of high resistivity in the top layer and isolated high resistivity at depth under some profiles. In the figure 4.19 red marked zones A and B (enclosed by zones C&D) have resistivity lower than 5 Ωm and identified as saturated waste (1-30 Ωm). According to Loke (2004) and Roger et al. (2004), the resistivity of water contaminants is less 10 Ωm (Salted water- 0.3–0.9 Ωm ; Brackish water-0.9–5 Ωm ; Leachate-0.9–5 Ωm ; 0.01 M Potassium chloride- 0.5-0.8 Ωm ; 0.01 M Sodium chloride- 0.8-1.0 Ωm ; 0.01 M acetic acid-6-7.5 Ωm , Iron- $9.074 \times 10^{-8} \Omega\text{m}$). So it is very clear that zones C and D are contamination plume.

There's a small sky color zone in between the zone C and D which indicates a wet sand and pure ground water zone (wet sand resistivity ranges from 20 Ωm -150 Ωm , Roger et al. (2004), pure water resistivity ranges from 10 Ωm – 150 Ωm) Loke (2004). The area enclosed in the dotted lines is debris and dumped soil (resistivity ranges from 200 Ωm -350 Ωm). The dark deep red in the middle of the surface line caused due to noise of the data acquisition machine itself. During the data acquisition by using two link box (each contains 16 electrodes) starting from the both end to middle sets up the 32 electrodes along a single line and thus generating a significant noise when running for data acquisitions. ERT2 is (\approx 600m) away from Buriganga River. Water bearing zone is at a depth of approximately 5 m (BWDB). So it can be concluding that zone of ERT2 has already contaminated up to depth of 17m.

(C)Test Point-03 (ERT3):

Figure 4.20 shows the raw model of ERT3 generated by using the program RES2DINV.

Inversion is the mathematical process of calculating cause from a set of observations. In resistivity work, it is used to calculate the resistivity of different formations in the ground from a set of readings taken at the surface. In geophysics, an electrical resistivity survey is conducted to map the subsurface of the earth. The measurements are performed using four electrodes placed in contact with the earth. Two are for injecting a current, and the other two are for measuring the responding potential. This procedure is repeated in different locations and with different electrode configurations, resulting in a large data set called apparent resistivity values.

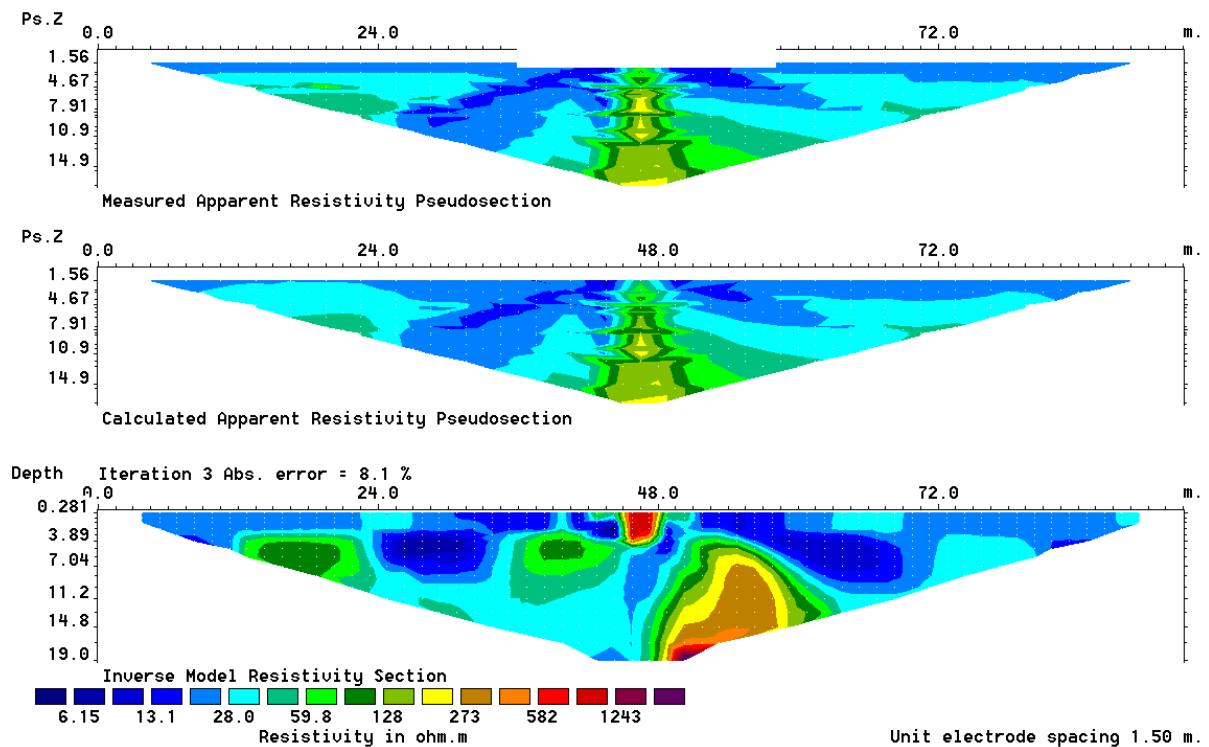


Figure 4.20: Raw resistivity model of ERT3 generated by the program RES2DINV.

The inversion procedure of ERT3 is as follows:

- From the raw data set, an estimate of what the ground might look like is created based on the apparent resistivity. This is the start model and it is called as “measured apparent resistivity pseudosection”.
- Calculates the apparent resistivity data set that would be achieved if a survey was performed on a ground that would look exactly as measured apparent resistivity pseudosection. It may be called as the synthetic data set.
- Adjusted measured apparent resistivity pseudosection model to a new earth model called “calculated apparent resistivity pseudosection” by looking at the difference between the raw data set and Synthetic Data Set-1.
- Calculate the apparent resistivity data set that would be achieved if a survey was performed on a ground which looks exactly as calculated apparent resistivity pseudosection. This data set is called Synthetic Data Set 2.
- Continue to perform steps 3 and 4 until the fit between the raw data set and the synthetic data set is minimal and the generated model is called the “inverse model resistivity section”.

Figure 4.21 below depicts the analyzed result of ERT3 and identifies the locations of contaminated groundwater. Initially after reading the data file in RES2DINV program some inputs have been made as described in the previous section 4.2 (data and model setup for ERT). Then an inversion has been carried out. The program RES2DINV automatically

generates the model of figure 4.21. The used resistivity instruments can measure resistivity up to a range of 0-1000 Ωm by penetrating current into the earth during sounding. The scenario of ground water contamination has been find out by comparing the model resistivity to the actual resistivity of various materials and contaminants.

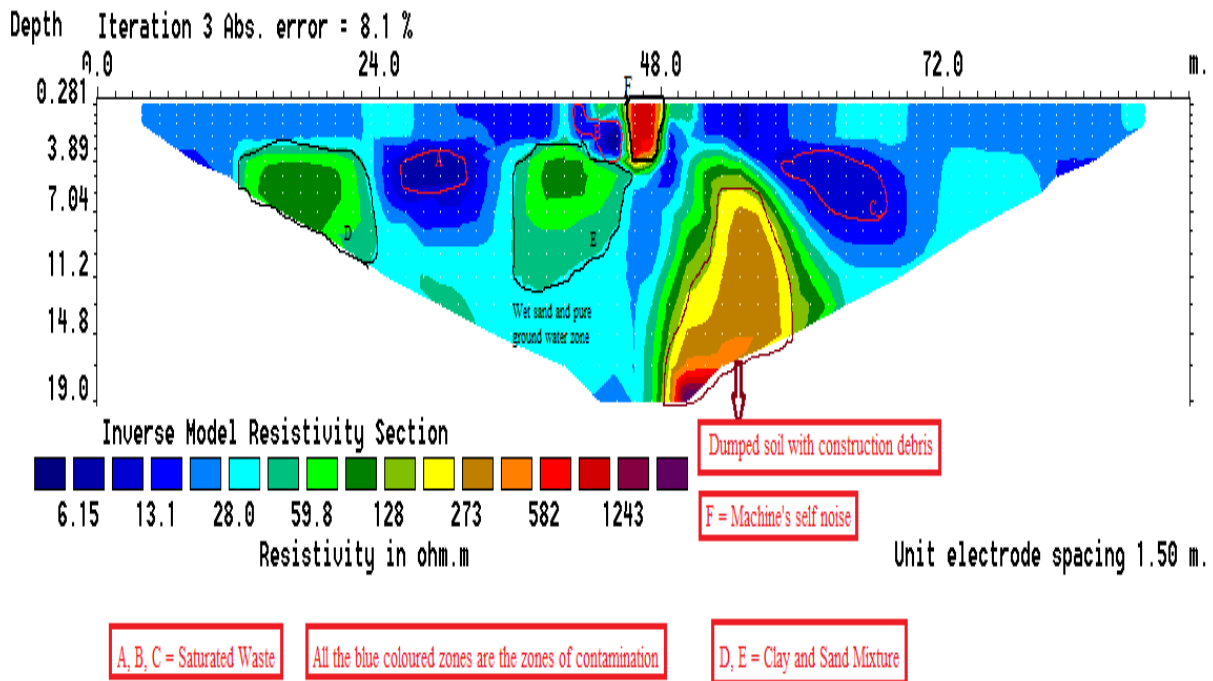


Figure 4.21: Analyzed result of ERT3 test showing location of contaminated groundwater as well as pure groundwater zones

Based on the results presented in Figs. 4.20 and 4.21, it appears that the subsurface below the dumpsite at the location of the test ERT-3 is characterized by low resistivity, possibly influenced by contaminants emanating from the dumps. The maximum depth penetrated by current during the sounding is 19 m with resistivity values of contaminated layers below 5 Ωm . In the Fig. 4.21 red marked zones A, B and C have very low resistivity and identified as saturated waste (12-30 Ωm). According to Loke (2004) and Roger et al. (2004), the resistivity of water contaminants is less 10 Ωm (Salted water- 0.3–0.9 Ωm ; Brackish water-0.9–5 Ωm ; Leachate-0.9–5 Ωm ; 0.01 M Potassium chloride- 0.5-0.8 Ωm ; 0.01 M Sodium chloride- 0.8-1.0 Ωm ; 0.01 M acetic acid-6-7.5 Ωm , Iron- $9.074 \times 10^{-8} \Omega\text{m}$). A critical look at the resistivity-depth model from ERT3 profile shows infiltration of leachate containing high concentration of dissolved solids to the subsurface environment. Generally, the result reflects high level of impact of leachate from the decomposed materials from the dumpsite, with resistivity less than 5 Ωm up to 17 Ωm prevalent on the entire traverse. Blue color dominates most of the area of ERT3 which is saturated soil and mostly contaminated cover up to depth of around 11m. The resistivity of this zone lies around 10 Ωm , which is very marginal to the contamination range.

The sky color zone indicates a wet sand and pure ground water zone (wet sand resistivity ranges from $20\Omega\text{m}$ - $150\Omega\text{m}$, Roger et al. (2004), pure water resistivity ranges from $10\Omega\text{m}$ – $150\Omega\text{m}$) Loke (2004) [19]. The area enclosed by D and E is clay and sand mixture (resistivity ranges from $200\Omega\text{m}$ - $350\Omega\text{m}$). The area covered by yellow circle is the area of dumped soil with construction debris (resistivity ranges from $4\Omega\text{m}$ - $300\Omega\text{m}$). The dark deep red in the middle of the surface line caused due to noise of the data acquisition machine itself. During the data acquisition by using two link box (each contains 16 electrodes) starting from the both end to middle sets up the 32 electrodes along a single line and thus generating a significant noise when running for data acquisitions. ERT3 is ($\approx 700\text{m}$) away from Buriganga River. Water bearing zone is at a depth of approximately 5 m (BWDB). So it can be concluding that zone of ERT3 has already contaminated up to depth of 19m.

4.4 Comparison of Soil Profile from ERT Analysis with Microtremor Analysis

Test Point-01 (ERT1):

Figure 4.22 shows the raw model of ERT1 resistivity model, generated by using the program RES2DINV.

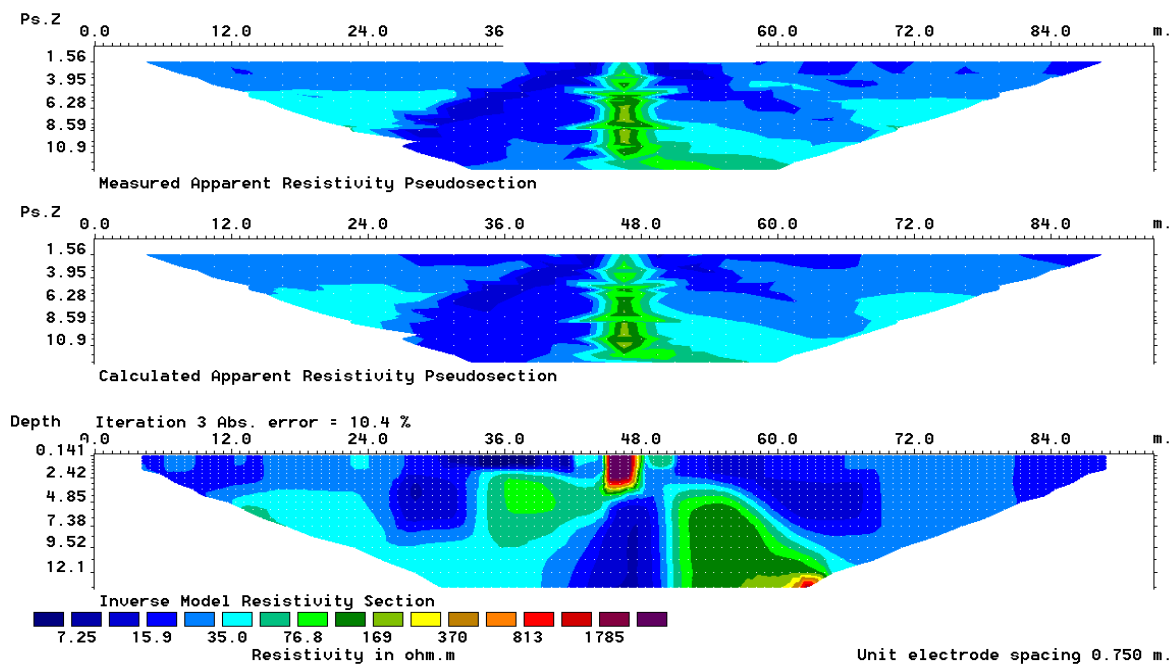


Figure 4.22: Raw resistivity model of ERT1 generated by the program RES2DINV

Based on the reference resistivity a soil profile of the model (Figure 4.22) has been developed, and is shown in the Table 4.1.

Table 4.1: Soil profile of the Test Point-01 (ERT1) based on reference resistivity (Table 3.2)

Depth (meter)	Soil Description	Resistivity ranges (Ω m)
0 to 6	clay	8-70
6 to 14	Clay and Sand Mix	4-300

Test Point-01 (Microtremor):

To characterize the soil profile using the microtremor a plot of Depth versus Shear Velocity (V_s) has been made using the GeoSiG Soft software for microtremor. The soil profile types according to Shear Velocity (V_s) are given below in the Table 4.2. Figure 4.23 presents the analysis of microtremor data to investigate the subsurface.

Table 4.2: The soil profile types according to Shear Velocity (V_s)

Soil Profile type	Shear Velocity (V_s) in m/s	Type of Soil
A	> 1500	Hard rock
B	$760 < V_s \leq 1500$	rock
C	$360 < V_s \leq 7600$	Very dense soil and soft rock
D	$180 < V_s \leq 360$	Clay and Sand Mix
E	< 180	Clay

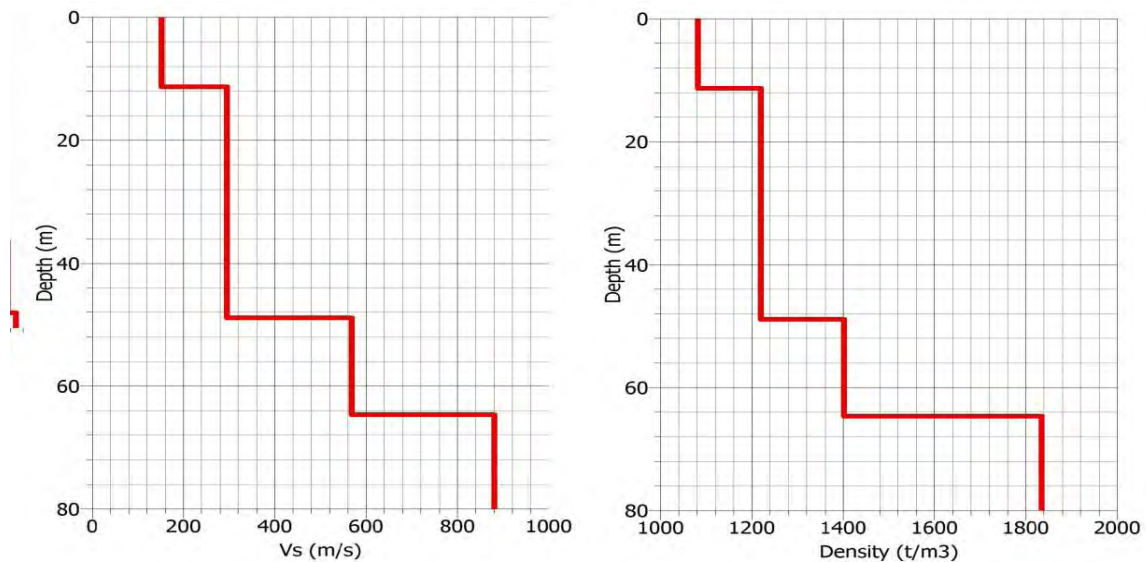


Figure 4.23: Analysis of microtremor data to investigate the subsurface of test point-01

In the Figure 4.23 the Shear Velocity (V_s) increased as the depth increased. The Shear Velocity (V_s) of the first 6m seems less than 180 m/s (Table 4.4). That means first 6m of the profile is clay. The Shear Velocity (V_s) then increased and continues up to depth of 45m. The Shear Velocity (V_s) of this layer is around 270 m/s (Table 4.4) and classified as a Clay and sand mix.

The soil profile generated by ERT inverse model is very similar to the microtremor analyzed soil profile of Test Point-01. Thus, the ERT soil profile and Microtremor soil profile are similar, and thus validates the results.

Test Point-02 (ERT2):

Figure 4.24 shows the raw resistivity model of ERT2, generated by using the program RES2DINV.

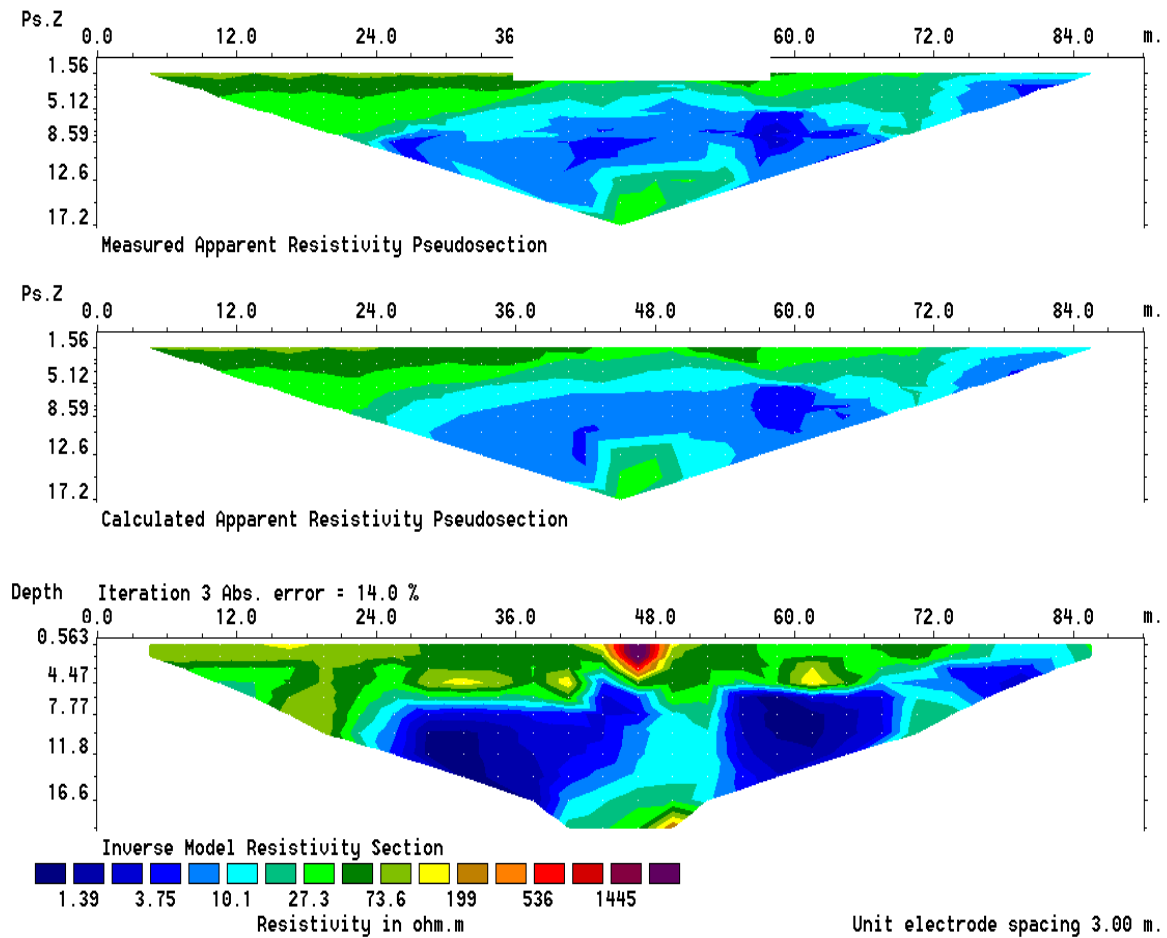


Figure 4.24: Raw resistivity model of ERT2 generated by the program RES2DINV

Based on the reference resistivity a soil profile of the model (Figure 4.24) has been developed, and is shown in the Table 4.3.

Table 4.3: Soil profile of the Test Point-02 (ERT2) based on reference resistivity (Table 3.2)

Depth (meter)	Soil Description	Resistivity ranges (Ω m)
0 to 10	Clay	8-70
10 to 17	Clay and Sand Mix	4-300

Test Point-02 (Microtremor):

To characterize the soil profile using the microtremor a plot of Depth versus Shear Velocity (V_s) has been made using the GeoSiG software for microtremor. The soil profile types according to Shear Velocity (V_s) are given in the Table 4.2. Figure 4.25 presents the analysis of microtremor data to investigate the subsurface.

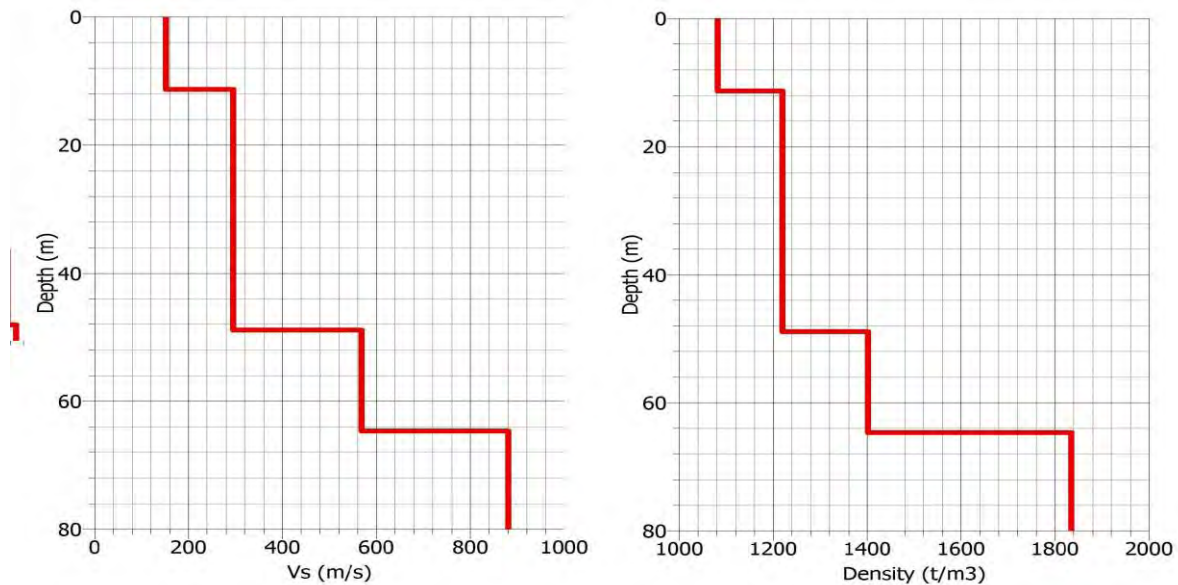


Figure 4.25: Analysis of microtremor data to investigate the subsurface of test point-02

In the Figure 4.25 the Shear Velocity (V_s) increased as the depth increased. The Shear Velocity (V_s) of the first 6m seems less than 180 m/s (Table 4.2). That means first 6m of the profile is clay. The Shear Velocity (V_s) then increased and continues up to a depth of 45m. The Shear Velocity (V_s) of this layer is around 270 m/s (Table 4.2) and classified as a Clay and sand mix.

The soil profile generated by ERT inverse model is very similar to the microtremor analyzed soil profile of Test Point-02 and therefore supports the validity of the methods.

Test Point-03 (ERT3):

Figure 4.26 shows the raw resistivity model of ERT3, generated by using the program RES2DINV. Based on the reference resistivity a soil profile of the model (Figure 4.26) has been developed, and is shown in the Table 4.4

Table 4.4: Soil profile of the Test Point-02 (ERT2) based on reference resistivity (Table 3.2)

Depth (meter)	Soil Description	Resistivity ranges (Ω m)
0 to 10	Clay	8-70
10 to 17	Clay and Sand Mix	4-300

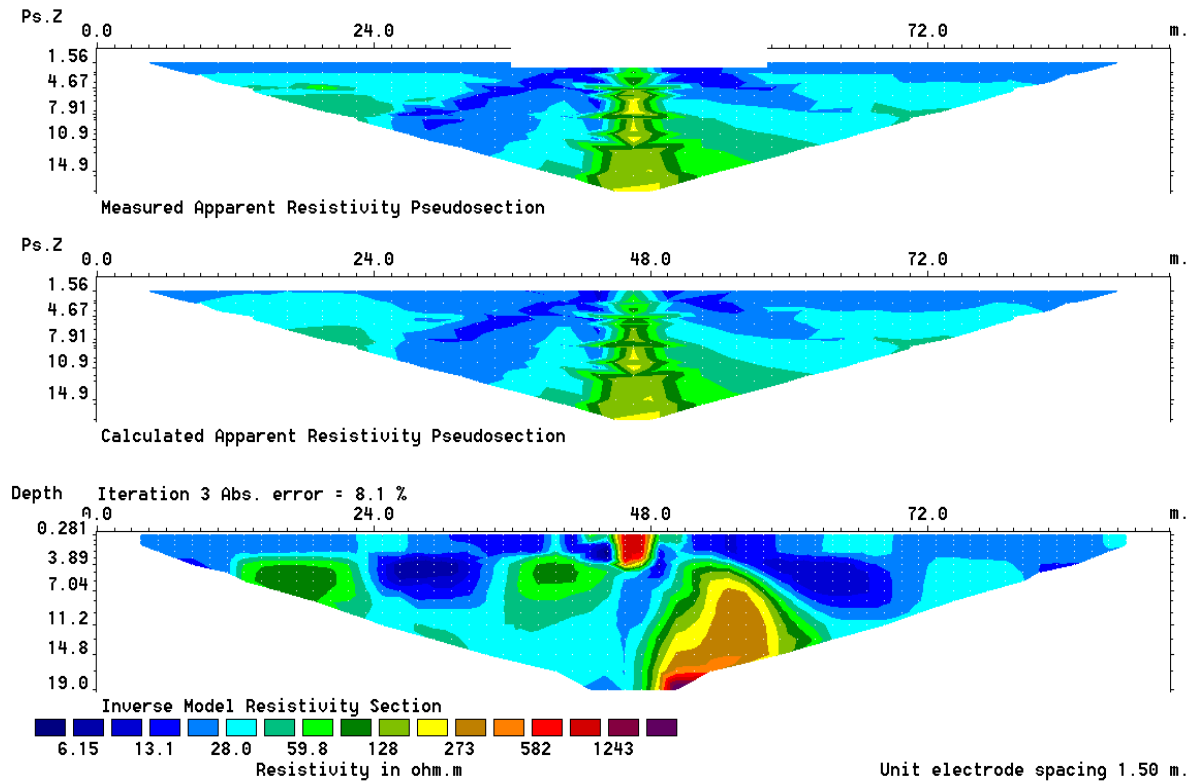


Figure 4.26: Raw resistivity model of ERT3 generated by the program RES2DINV

Test Point-03 (Microtremor):

To characterize the soil profile using the microtremor a plot of Depth versus Shear Velocity (Vs) has been made using the GeoSiG software for microtremor. The soil profile types according to Shear Velocity (Vs) are given in the table 4.2. Figure 4.27 presents the analysis of microtremor data to investigate the subsurface.

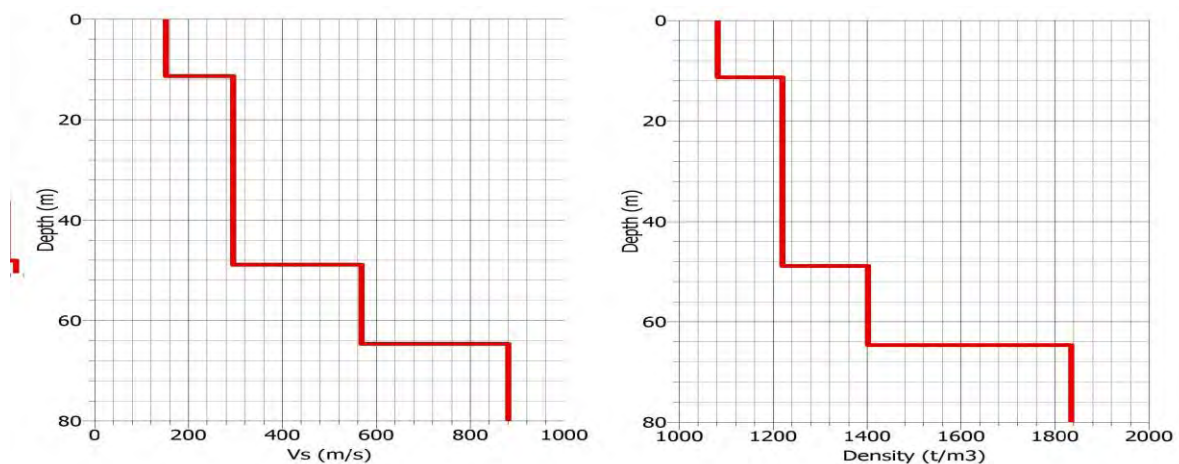


Figure 4.27: Analysis of microtremor data to investigate the subsurface of test point-03

In the Figure 4.27 the Shear Velocity (Vs) increased as the depth increased. The Shear Velocity (Vs) of the first 6m seems less than 180 m/s (Table 4.2). That means first 6m of the

profile is clay. The Shear Velocity (V_s) then increased and continues up to depth of 45m. The Shear Velocity (V_s) of this layer is around 270 m/s (Table 4.2) and classified as a Clay and sand mix.

The soil profile generated by ERT inverse model is very similar to the microtremor analyzed soil profile of Test Point-03, and therefore supports the validity of the ERT method.

4.5 Comparison between ERT1 Model and EC of Ground Water Samples

In order to check the resistivity model generated from ERT data, Electrical Conductivity (EC) of ground water samples were compared with the resistivity model for the Test Point-01. Three boreholes (5m, 10, 15m) were made to collect the ground water samples. Then the samples were tested for the Electrical Conductivity (EC) values. Table 4.5 shows the electrical conductivity (EC) values of analyzed water samples. These EC values have been compared with the resistivity values of the inverse resistivity pseudosection of ERT1. Figure 4.28 presents the analyzed inverse resistivity pseudosection of ERT1.

Table 4.5: Electrical Conductivity (EC) Values of Analyzed Water Samples

Sl. No.	Borehole Depth (m)	Electrical Conductivity (EC) in ($\mu\text{S}/\text{cm}$)	Electrical Conductivity (EC) in (S/m)
01	5m	904	0.0904
02	10m	890	0.0890
03	15m	732	0.0732

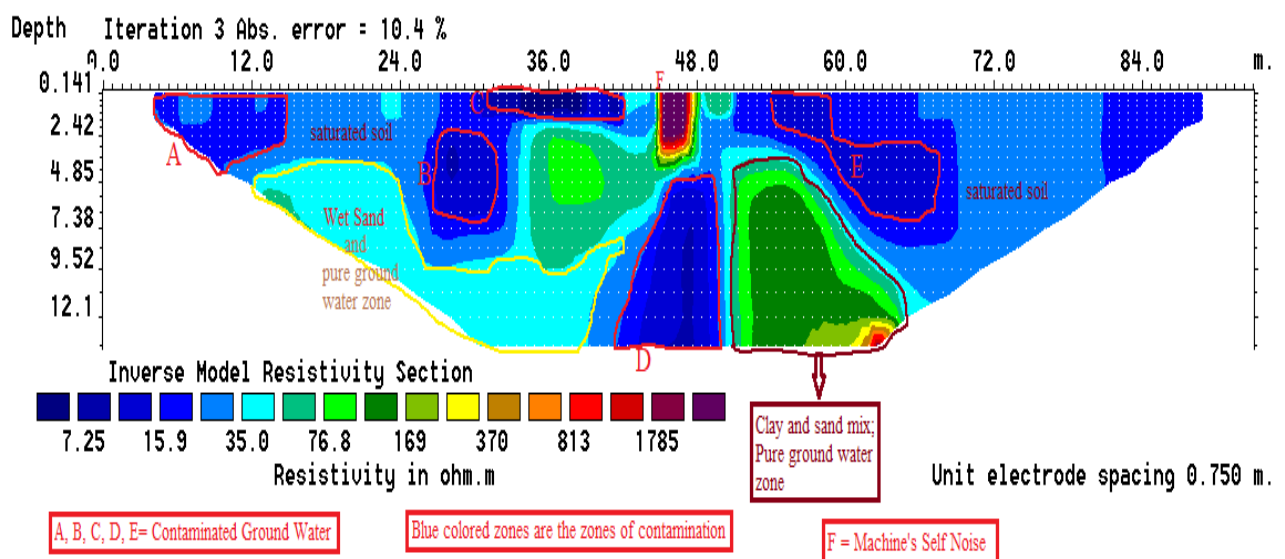


Figure 4.28: Analyzed results of ERT-1 test showing location of contaminated groundwater as well as pure groundwater zones.

Based on the results presented in Figs. 4.16 and 4.17, it appears that the subsurface below the dumpsite at the location of the test ERT-1 is characterized by low resistivity, possibly influenced by contaminants emanating from the dumps. In the Fig. 4.28, the red marked zones A, B, C, D and E have resistivity lower than 5 Ωm . According to Loke (2004) and Roger et al. (2004), the resistivity of water contaminated with dissolved solids is less 10 Ωm (Salted water- 0.3–0.9 Ωm ; Brackish water-0.9–5 Ωm ; Leachate-0.9–5 Ωm ; 0.01 M Potassium chloride- 0.5-0.8 Ωm ; 0.01 M Sodium chloride- 0.8-1.0 Ωm ; 0.01 M acetic acid-6-7.5 Ωm). A critical look at the resistivity-depth model from ERT-1 profile shows possible infiltration of leachate containing high concentration of dissolved solids to the subsurface environment. Generally, the result reflects high level of impact of leachate from the decomposed materials from the dumpsite, with resistivity less than 5 Ωm up to 17 Ωm prevalent on the entire traverse.

The Electrical Conductivity (EC) values presented in Table 4.6 indicates that the total model area is highly conductive, similar to the analyzed ERT1 results. The Electrical Conductivity (EC) values of 5m, 10 and 15m depths are 0.0904, 0.0890 and 0.0732 S/cm, respectively. Resistivity is the inverse of conductivity. If the inverse of the Electrical Conductivity (EC) is done the results resistivity values for 5m, 10 and 15m depths are 11.06, 11.23 and 13.66 Ωm respectively, which clearly indicates pollution in the analyzed pseudosection of ERT1 (Figure 4.28).

Chapter 5

CONCLUSIONS

5.1 Introduction

The main objective of this study was to assess the probable groundwater contamination at a waste dump site in Hazaribagh, Dhaka using Electrical Resistivity Tomography (ERT). To achieve this objective, 3 ERT tests were carried out in Hazaribagh, and the ERT data were analyzed using the software RES2DINV to generate a resistivity model of the test site. The resistivity model was used to identify possible groundwater pollution through comparison with reference resistivity values of materials. In addition, the soil profiles at the test sites generated by the resistivity models were compared with soil profile generated by microtremor analysis. The resistivity model of a test site was also compared with electrical conductivity of ground water samples collected from the site, in order to assess the validity of the ERT method for identification of ground water contamination. This Chapter presents the major conclusions from this study and presents recommendation for future studies.

5.2 Conclusions

The major conclusions from the present study are as follows:

- (1) The 2D electrical resistivity model generated from the ERT measurements successfully delineated the soil profile, and lateral and vertical extent of possible contaminated zones in the subsurface, through identification of low resistivity zones.
- (2) The result revealed that the groundwater within and around the dump sites at Hazaribagh have become contaminated up to a depth of about 15 m with leachate containing high concentration of dissolved salts.
- (3) It appears that the results of 2D resistivity imaging could help characterize the subsurface underneath a dumpsite, such as dumpsite geometry and leachate plumes.
- (4) The soil profiles developed by the resistivity model and microtremor analysis have been found to be similar, suggesting applicability of the ERT method.
- (5) Good comparison of resistivity model with the measured EC values of ground water at a dump site also supports the applicability of the non-destructive ERT method in identification of ground water contamination.

5.3 Recommendation for Future Work

The followings are suggested for future study:

- (1) The present study has been done to assess applicability of ERT method to identify probable groundwater contamination at waste dumpsites. A comparison between the ERT tests at waste dumpsites and fresh uncontaminated sites would be useful for assessing the applicability of ERT in characterization of ground water.

- (2) Ground water samples have been collected and analyzed for one test point. Collection and analysis of ground water samples from all test points would be more useful to make comparison with ERT results.
- (3) This study has been carried out during post rainy season only. Study for seasonal variation of subsurface characteristics should be carried out.

REFERENCES

- Abu-Hassanein, Z.S., Benson, C.H., Blotz, L.R., “Electrical resistivity of compacted clays”. *J. Geotech. Eng.* 122 (5), 397–406, 1996.
- Aki, K., “Space and time spectra of stationary stochastic waves with special reference to microtremors”. *Bull. Earthq. Res. Inst. Tokyo University*, 35, pp.415-456, 1957.
- Allen, A. R., Dillon, A., and O’Brien, M., “Approaches to landfill site selection in Ireland,” in *Engineering Geology and the Environment*, P. G. Marinos, G. C. Koukis, G. C. Tsiambaos, and G. C. Stournaras, Eds., pp. 1569–1574, Rotterdam, The Netherlands, 1997.
- Ansal, A., “Recent advances in earthquake geotechnical engineering and microzonation”. *Kluwer Academic Publishers, Dordrecht*, 354 pp., 2004.
- Arai, H., and Tokimatsu, K., “S-wave velocity profiling by inversion of microtremor H/V spectrum”. *Bulletine of the Seismological Society of America*, Vol. 94, No. 1, pp. .53-63, 2004.
- Archie, G. E., “The electrical resistivity log as an aid in determining some reservoir characteristics.” *Trans. Am. Inst. Min., Metall. Pet. Eng.*,146(99), 54 –67, 1942.
- Aristodemou, E., and Thomas-Betts, A., “DC resistivity and induced polarization investigations at a waste disposal site and its environments, “*Journal of Applied Geophysics*, vol.44, no.2-3, pp. 275–302, 2000.
- Bard, P. Y., “Microtremor measurements: a tool for site effect estimation” and “The Effects of Surface Geology on Seismic Motion”. *Rotterdam*, 1251–1279, 1999.
- Barker R. D., White C. C., and Houston J. F. T., “Borehole siting in an African accelerated drought relief project in: Wright EP, Burgess”. *WGE (eds) Hydrogeology of crystalline basement aquifers in Africa*, Geological Society Special Publication, No. 66, London, 183–201, 1992.
- Bengtsson, L., Bendz, D., Hogland, W., Rosqvist, H., and Akesson, M., “Water balance for landfills of different age,” *Journal of Hydrology*, vol.158, no.3-4, pp.203–217, 1994.
- Bernstone, C., Dahlin, T., Ohlsson, T., and Hogland, W., “DC-resistivity mapping of internal landfill structures: two pre-excavation surveys,” *Environmental Geology*, vol.39, no.3-4, pp. 360–371, 2000.
- Cahyna, F., “Monitoring of artificial infiltration using geoelectrical methods”. In: Ward SH (ed) *Geotechnical and Environmental Geophysics*. Vol II. *SocExpl Geophysicists*, 101–106, 1990.
- Capon, J., “High-Resolution frequency-wavenumber spectrum analysis”. *Proc. Of the IEEE*, Vol.57, No.8, pp.1408-1418, 1969.

Carpenter, P. J., Kaufmann R. S., and Price B., “Use of resistivity soundings to determine landfill structure”. *Ground Water*, 28, 569–575, 1990.

Carpenter, P. J., Calkin, S. F., Kaufmann, R. S., “Assessing a fractured landfill cover using electrical resistivity and seismic refraction techniques”. *Geophysics* 56 (11), 1896–1904, 1991.

Carruthers R. M., and Smith I. F., “The use of ground electrical survey methods for siting water-supply boreholes in shallow crystalline basement terrains”. In: Wright EP, Burgess WGE (eds) *Hydrogeology of crystalline basement aquifers in Africa*. Geological Society Special Publication, No. 66, London, 203–220, 1992.

Clement, R., Descloitres, M., Gunther, T., Oxarango, L., Morra, C., Laurent, J.P., Gourc, J., “Improvement of electrical resistivity tomography for leachate injection monitoring”. *Waste Manage.* 30 (3), 452–464, 2010.

Dahlin, T., “2D resistivity surveying for environmental and engineering applications”. *First Break*, 14, 275-284, 1996.

Dahlin, T., “The development of DC resistivity imaging techniques”. *Computer & Geosciences* 27, pp. 1019 – 1029, 2001.

deGroot-Hedlin, C., and Constable, S., “Occam's inversion to generate smooth, two-dimensional models from magneto telluric data,” *Geophysics*, 55, 1613-1624, 1990.

Daniel, D.E., Benson, C.H., “Water content-density criteria for compacted soil liners”. *J. Geotech. Eng.* 116 (12), 1811–1830, 1990.

Dawson, C. B., Lane, J. W., White, E. A., and Belaval, M., “Integrated geophysical characterization of the Winthrop land-fill southern flow path, Winthrop, Maine,” in *Proceedings of the Symposium on the Application of Geophysics to Engineering and Environmental Problems*, p. 22, Environmental and Engineering Geophysical Society, Las Vegas, Nev, USA, February 2002.

Genelle, F., Sirieix, C., Naudet, V., Riss, J., Naessens, F., Rénié, S., Dabas, M., “Geophysical methods applied to characterize landfill covers with geo-composite”. GSP 211. In: *Proceedings of Geo-Frontiers 2011“Advances in Geotechnical Engineering*, pp. 1951–1960, 2011.

Georgaki, I., Soupios, P., Sakkas, N., et al., “Evaluating the use of electrical resistivity imaging technique for improving CH₄ and CO₂ emission rate estimations in landfills,” *Science of the Total Environment*, vol.389, no.2-3, pp.522–531, 2008.

Green, A., Lanz, E., Maurer, H., and Boerner, D. “Template for geophysical investigations of small landfills,” *Leading Edge*, vol. 18, no. 2, pp. 248–254, 1999.

Grellier, S., Bouye, J., Guerin, R., Robain, H., and Skhiri, N., “Electrical resistivity tomography (ERT) applied to moisture measurements in bioreactor: principles, in situ measurements and results.” Proc., Int. Workshop Hydro-Physico-Mechanics of Landfills, Grenoble, France, 2005.

Grellier, S., Guerin, R., Robain, H., Bobachev, A., Vermeersch, F., and Tabbagh, A., “Monitoring of leachate recirculation in a bioreactor landfill by 2-D electrical resistivity imaging.” *J. Environ. Eng. Geophys.*, 13(4), 351–359, 2008.

Grellier, S., Reddy, K. R., Gangathulasi, J., Adib, R., and Peters, C. C., “Correlation between electrical resistivity and moisture content of municipal solid waste in bioreactor landfill.” Geotechnical Special Publication No.163, ASCE, Reston, VA, 2007.

Griffiths D. H., and Barker R. D., “Two-dimensional resistivity imaging and modelling in areas of complex geology”. *Journal of Applied Geophysics*, 29, 211-226, 1993.

Hakonson, T.E., “Capping as an alternative for landfill closures-perspectives and approaches”. In: Proceedings Environmental Science and Research Foundation., *Landfill Capping in the Semi-Arid West: Problems, Perspectives, and Solutions*, Grand Teton National Park, Wyoming. May 21–22. ESRF-019, pp. 1–18, 1997.

Heitfeld, K. H., and Heitfeld, M., “Siting and planning of waste disposal facilities in difficult hydrogeological conditions,” in *Engineering Geology and the Environment.*, Eds., pp.1623–1628, Rotterdam, The Netherlands, 1997.

Horike., M., “Inversion of phase velocity of long-period microtremors to the S-wave-velocity structure down to the basement in urbanized area”. *Journal of Phys. Earth* 33, pp. 59-96, 1985.

Imhoff, P. T., “Review of state of the art methods for measuring water in landfills.” *Waste Manage.*, 27(6), 729–745, 2007.

Khan, M.S., Hossain, M.S., Hossain, J., Kibria, G., “Determining unknown bridge foundation depth by resistivity imaging method”. In: *GeoCongress 2012*, pp. 275–284, 2012.

Kalinski, R. J., Kelly, W., “Estimating water content of soils from electrical resistivity”. *J. Geotech. Eng.* 120 (2), 451–457, 1994.

Kalinski, R.J., “Surface geoelectrics for characterizing ground water protective layers and compacted soil liners”. Ph.D. Dissertation, University of Nebraska at Lincoln, NE, 1992.

Lanz, E., Jemmi, E., Muller, R., Green, A., Pugin, A., and Huggen-berger, P., “Integrated studies of Swiss waste disposal sites: results from geo radar and other geophysical surveys,” in *Proceedings of the 5th International Conference on Ground Penetrating Radar (GPR ‘94)*, pp.1261–1274, 1994.

Loke, M. H., “Electrical imaging surveys for environmental and engineering studies. User’s Manual for Res2dinv”. Electronic version [<http://www.geometrics.com>], 1999

Loke, M. H., “Tutorial, “2-D and 3-D electrical imaging surveys”, pp. 13, 2004.

Loke M. H., and Barker R.D., “Rapid least-squares inversion of apparent resistivity pseudo-sections using a quasi-Newton method,” *Geophysical Prospecting*, 44, 131-152, 1996.

Loke, M.H., “Tutorial: 2-D and 3-D electrical imaging surveys”. Geotomo Software Sdn Bhd, Malaysia. (Available for download from www.geotomosoft.com), 2018.

Loke, M.H.,. Topographic modelling in resistivity imaging inversion. 62nd EAGE Conference & Technical Exhibition Extended Abstracts, D-2, 2000.

Mather, J. D., “Preventing groundwater pollution from landfilled waste-is engineered containment an acceptable solution?” in *Groundwater Quality*, H. Nashand G. J. H. McCall, Eds., pp. 191–195, Chapman & Hall, London, UK, 1995.

McCarter, W., “The Electrical Resistivity Characteristics of Compacted Clays”. *Geotechnique* 34 (2), 263–267, 1984.

Nakamura, Y., and Ueno, M., “A simple estimation method of dynamic characteristics of subsoil”. *Proc. the 7th Japan Earthq. Engrg. Symp.*, pp265-270 (in Japanese), 1986.

Nguyen, F., and Garambois, S., “Image processing of 2D resistivity data for imaging faults”. *Journal of Applied Geophysics* 57, pp. 260 –277, 2005.

Orlando, L., and Marchesi, E., “Georadar as a tool to identify and characterize solid waste dump deposits,” *Journal of Applied Geophysics*, vol.48, no.3, pp. 163–174, 2001.

Parkhomenko, E. I., “Electrical Properties of Rocks”. Plenum Press, pp. 121, 1967.

Pastor, J., and Hernández, A. J., “Heavy Metals, Salts and Organic Residues in Old Solid Surface Waters in Their Discharge Areas: Determinants for Restoring Their Impact”. *Journal of Environmental Management*, Vol. 98, 2012, pp. S42-S49, 2012.

Pitchford, A. M., Mazzella, A. T., and Scarbrough, K. R., “Soil-Gas and Geophysical Techniques for Detection of Subsurface Organic Contamination”. Final Report, Air Force Engineering and Services Center Report, ESL-TR-87-67, 172 p, 1989.

Reynolds, J. M., *An introduction to applied and environmental geophysics*, Wiley, New York, 1997.

Roger, G., Marie, L. M., Christophe, A., Claire, L., Mustapha, H., Eric, D., Solenne, G., “Leachate recirculation: moisture content assessment by means of a geophysical technique”. *Elsevier, Waste Management* 24, 785–794, 2004.

Ross H. P., Mackelprang C. E., and Wright P. M., “Dipole–dipole electrical resistivity surveys at waste disposal study sites”. In: Ward SH (ed) Geotechnical and environmental geophysics, vol II. SocExpl Geophysicists, 145–152, 1990.

Saltas, V., Vallianatos, F., Soupios, P., Makris, J. P., and Triantis, D., “Application of dielectric spectroscopy to the detection of contamination in sandstone,” in Proceedings of the International Workshop in Geo-environment and Geotechnics, pp. 269–274, Milos Island, Greece, September 2005.

Tokimatsu, K., and Miyadera, Y., “Characteristics of Rayleigh waves in microtremors and their relation to underground structures”. Journal of Struct. Constr. Engng, AIJ, No.439, pp81-87 (in Japanese), 1992.

Trochobanogous, G., Thisen, H., and Vigil, S., “Integrated Solid Waste Management”. McGraw Hill, New York, NY, USA, 1993.

Ward, S. H., “Resistivity and induced polarization methods.” Geotech. Environ. Geophys, 1, 147 –190, 2000.